PILED RAFT FOUNDATIONS SUBJECTED TO SEISMIC LOADING

Pastsakorn Kitiyodom
Research Associate, Kanazawa University

Tatsunori Matsumoto
Professor, Kanazawa University

PILED RAFT FOUNDATIONS SUBJECTED TO SEISMIC LOADING

REFERENCES

Horikoshi, K., Matsumoto, T., Hashizume, Y. and Watanabe, T. (2003): Performance of piled raft foundations subjected to dynamic loading, *Int. Journal of Physical Modelling in Geotechnics* 2: 51-62.

Matsumoto, T., Fukumura, K., Kitiyodom, P., Oki, A. and Horikoshi, K. (2004): Experimental and analytical study on behaviour of model piled rafts in sand subjected to horizontal and moment loading, *Int. Journal of Physical Modelling in Geotechnics* 4(3): 1-19.

Matsumoto, T., Fukumura, K., Oki, A. and Horikoshi, K. (2004): Shaking table tests on model piled rafts in sand considering influence of superstructures, *Int. Journal of Physical Modelling in Geotechnics* 4(3): 20-37.

Kitiyodom, P., Sonoda, R. and Matsumoto, T. (2005): Simplified dynamic analysis of piled raft foundation subjected to earthquake load, *Proc. 2nd Sino-Japanese Symposium on Geotechnical Engineering*. 568-573.

Matsumoto, T., Kitiyodom, P., Oki, A. and Tachibana, T. (2006): Influence of flexible superstructure on behaviour of piled rafts during shaking table test, *Proc. 6th Int. Conf. on Physical Modelling in Geotechnics*. 1021-1027.

Background

- Piled raft foundations have been widely recognized as one of the most economical foundation systems.

- In piled raft foundations, piles are extensively used to reduce the settlement of foundations to an acceptable level, rather than to support the weight of superstructures.

- The establishment of a seismic design concept for piled raft foundations is necessary especially in highly seismic areas such as Japan.

- Although piled raft foundations have already been applied to actual structures in Japan, most seismic designs seem to treat piled rafts as rafts alone by ignoring the existence of piles.

Contents of Today Presentation

Part I: Performance of piled raft foundations subjected to dynamic loading

Part II: Influence of superstructure on behaviour of model piled rafts in sand under shaking tests

Part III: Analysis of piled raft subjected to dynamic loading

Performance of piled raft foundations subjected to dynamic loading

Focus

The effects of the rigidity of the pile head connection on the dynamic response. The contribution of the raft base contact with the soil surface. Comparisons between the results of dynamic loading tests with those obtained from the static horizontal loading tests.

Horikoshi, K., Matsumoto, T., Hashizume, Y. and Watanabe, T. (2003): Performance of piled raft foundations subjected to dynamic loading, *Int. Journal of Physical Modelling in Geotechnics* 2: 51-62.

Schematic figure of centrifuge package

Laminar box was used.

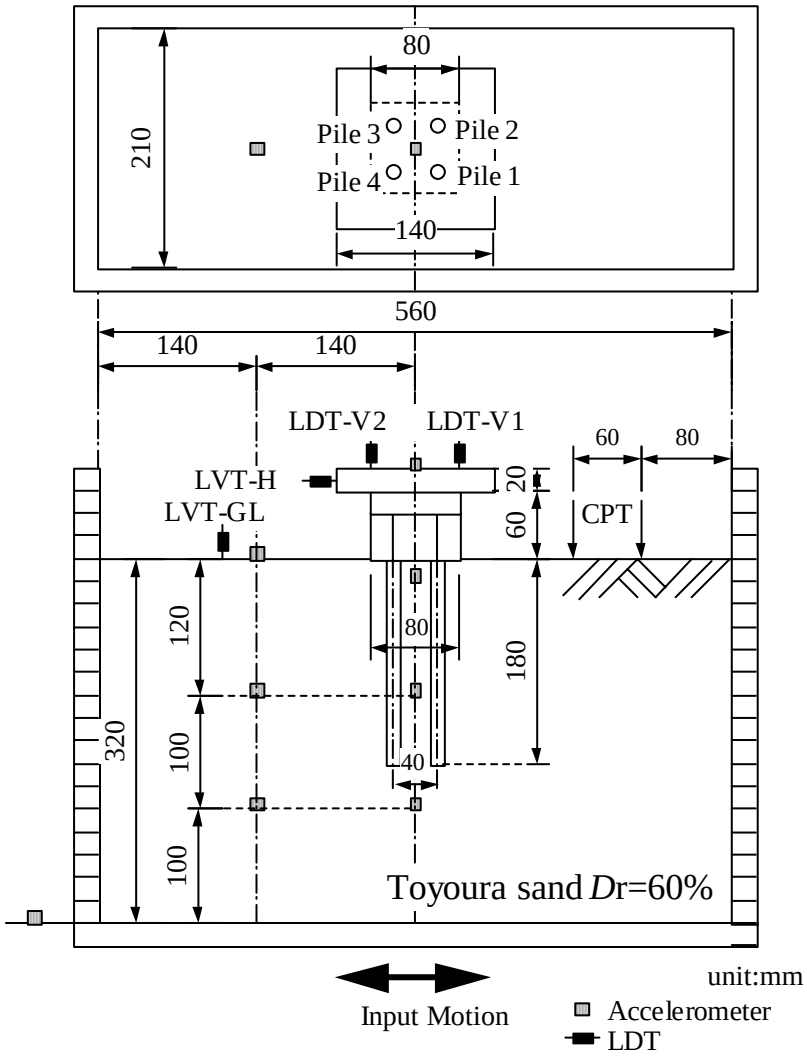

Piled raft model

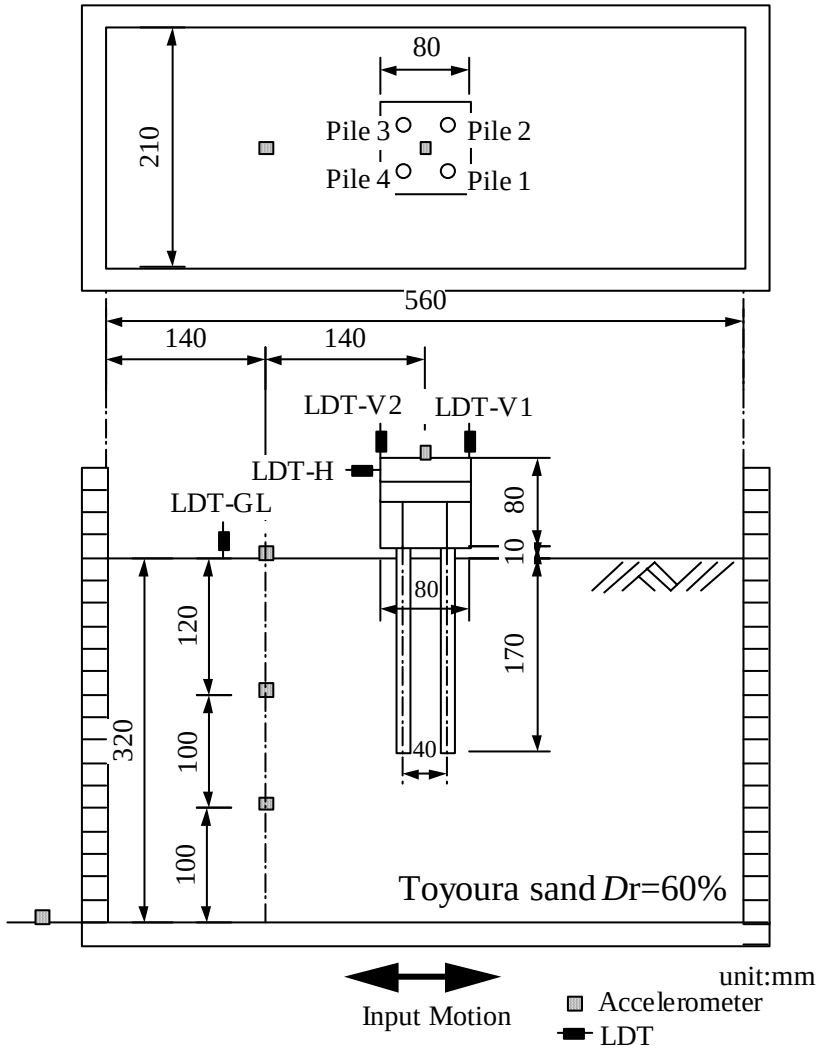

Pile group model

Properties of the model pile and the corresponding prototype pile

Properties	Centrifuge model	Prototype
Material	Aluminum	Concrete
Diameter	10 mm	500 mm
Wall thickness	1 mm	Solid
Pile length, L_p	180 mm	9.0 m
Young's modulus, E_p	71 GN/m^2	41.7GN/m^2
Cross-sectional rigidity, E_pA_p	2.0×10^{-3} GN	5.0 GN
Bending rigidity, E_pI_p	2.0×10^{-8}GNm^2	0.13 GNm^2

Properties of Toyoura sand

Properties	Value
Density of soil particle, ρ_s (t/m^3)	2.661
Mean grain size, D_{50} (mm)	0.162
Maximum dry density, ρ_{dmax} (t/m^3)	1.654
Minimum dry density, ρ_{dmin} (t/m^3)	1.349

Experimental cases and their conditions

Model Type	Loading direction		
	Vertical loading (see Horikoshi et al. 2003)	Horizontal loading (see Horikoshi et al. 2003)	Dynamic loading (present study)
Single Pile	L_p = 250mm L_d = 120, 170, 200 mm h = 505 mm	L_p = 250mm L_d = 170 mm h = 440 mm	
Raft (alone)	B = 80, 120 mm M_r = 0.36 kg h = 470 mm	B = 80 mm M_r = 4.69 kg h = 460 mm	
Piled Raft	L_p = 170 mm B = 80 mm, 120 mm M_r = 0.90 kg h = 470 mm	L_p = 180 mm B = 80 mm M_r = 4.69 kg h = 460 mm Rigid or hinged pile head conditions	L_p = 180 mm B = 80 mm M_r = 4.69 kg h = 320 mm Rigid or hinged pile head conditions
Free-standing Pile group			L_p = 180 mm L_d = 170 mm B = 80 mm M_r = 2.35 kg h = 320 mm Rigid pile head conditions

L_p: Pile length, L_d: Embedment length, B: Square raft width, M_r: Mass of raft, h: Soil thickness

Design of model raft for rigid pile head connection

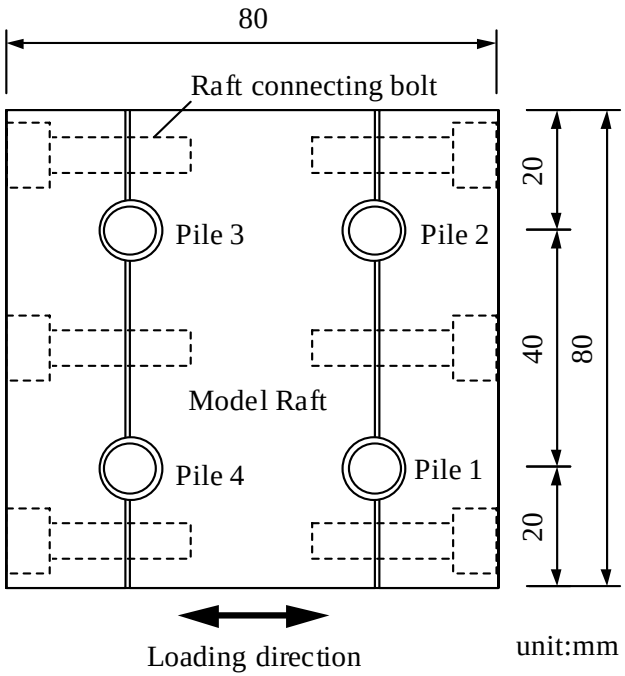

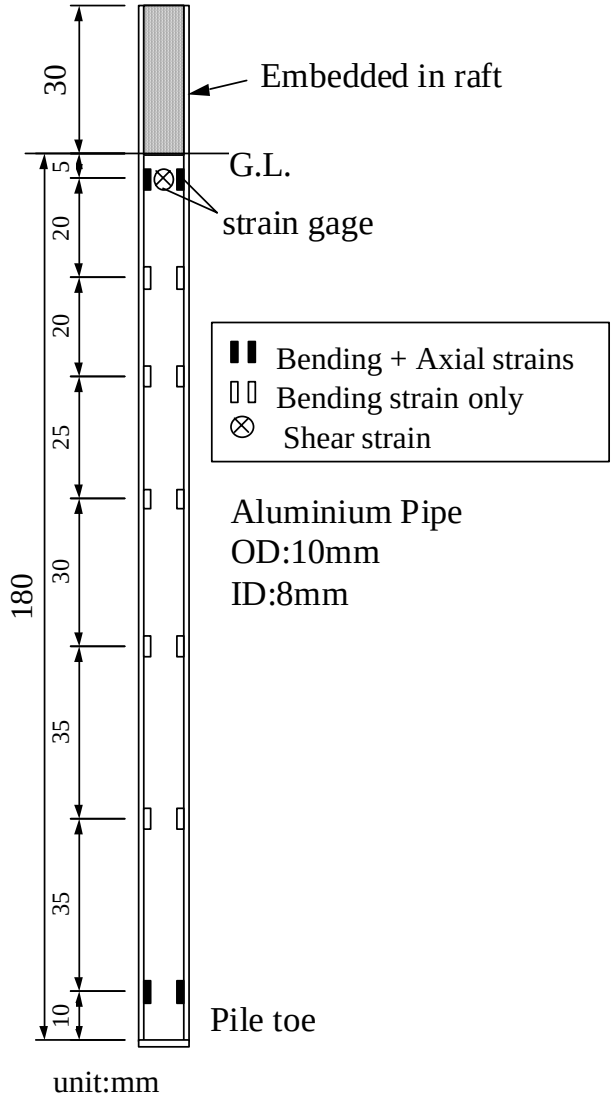

Design of model raft for hinged pile head connection

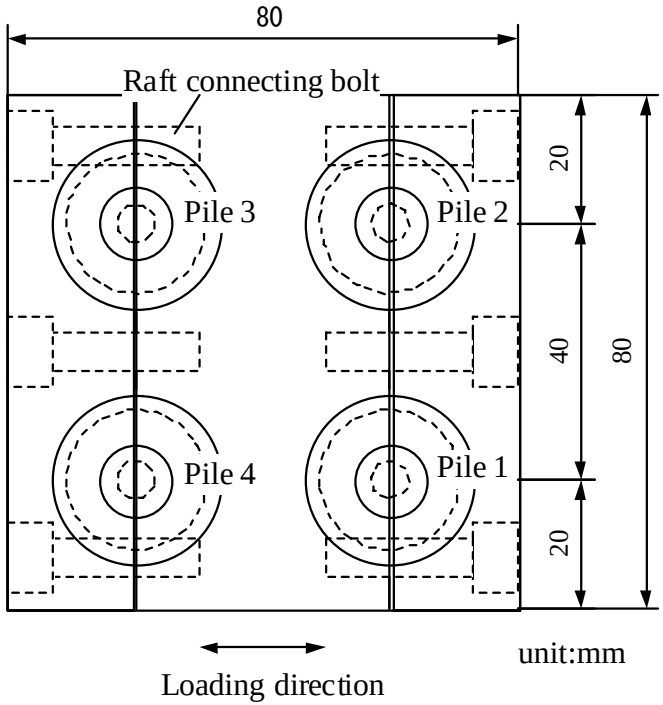

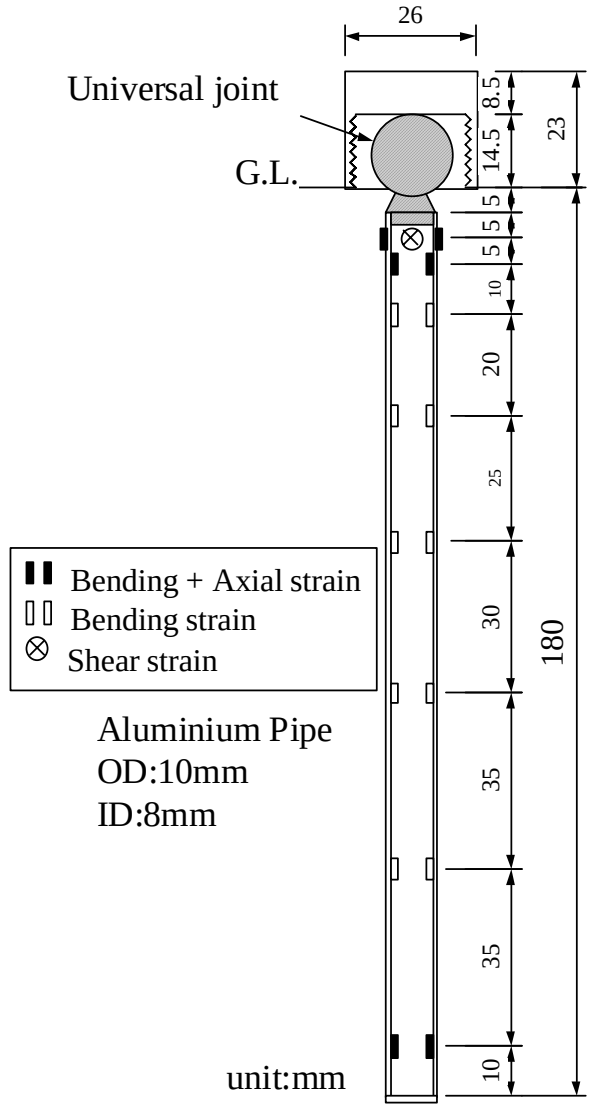

Universal joint used for hinged pile head connection model

Profiles of cone tip resistance

Penetration rate 1.0 mm/s

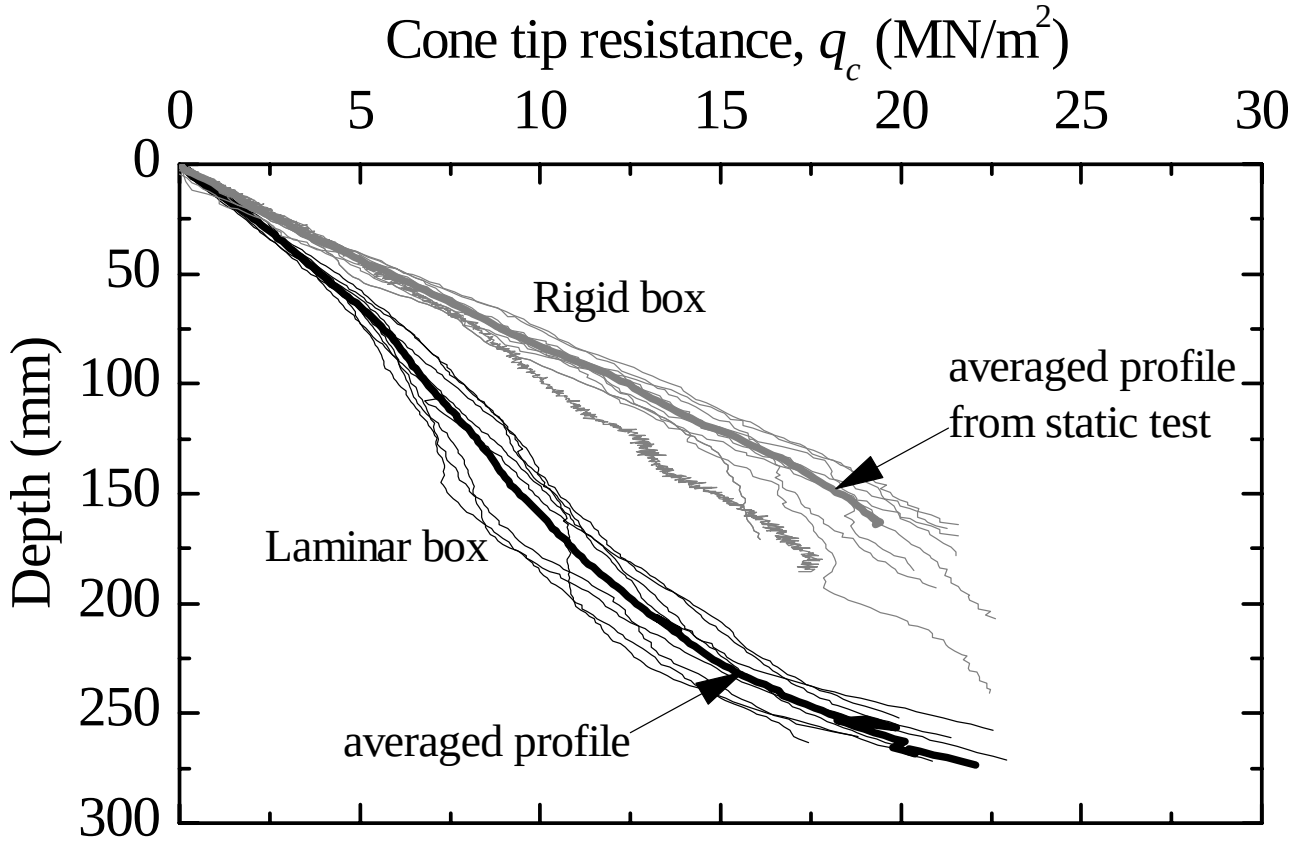

The cone resistances at a deeper soil were much smaller compared with those measured in the rigid box used for static loading tests. However the q_c values at upper soils, which are important in the horizontal resistance of the piles, were closer to those observed in the static models.

Profiles of vertical load carried by each component during increase in g level to 50 g

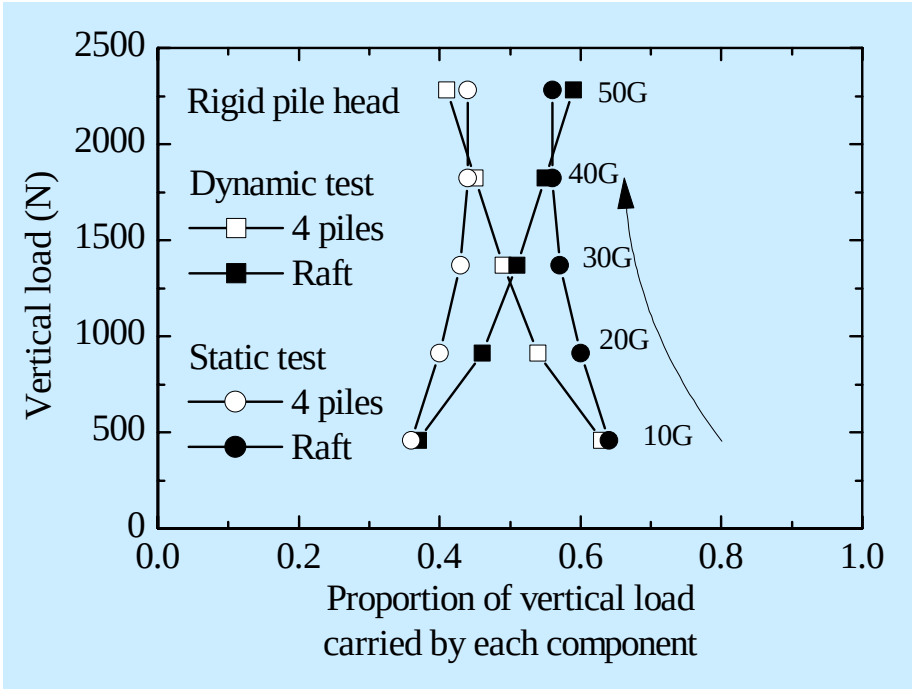

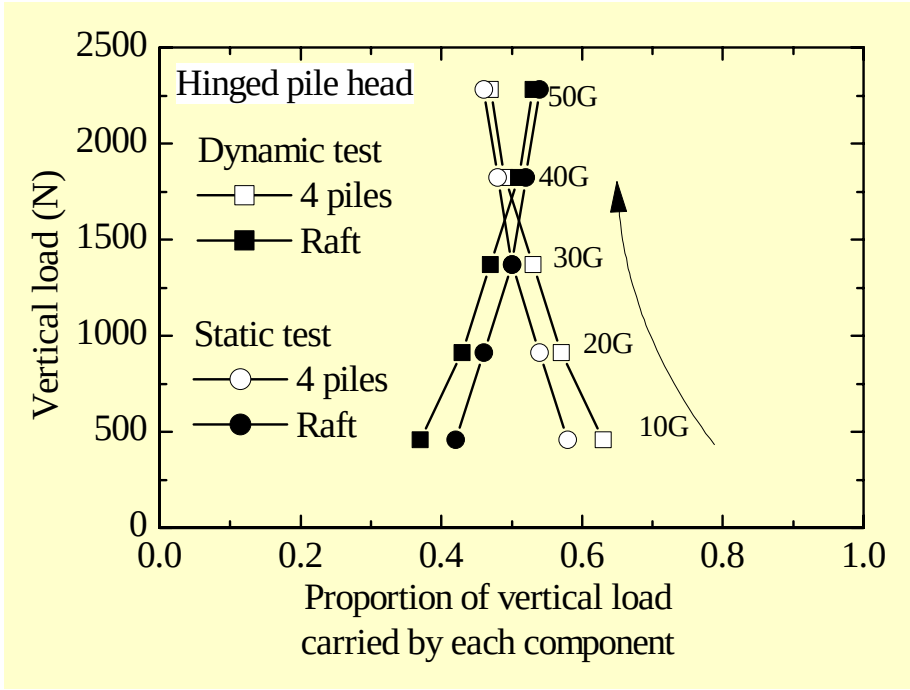

Rigid pile head connection

Hinged pile head connection

At 50 g, the piles carried 40% and 45% of the total load for the rigid connection model and the hinged connection model, respectively, which were almost the same as observed in the static models.

Time history of input acceleration

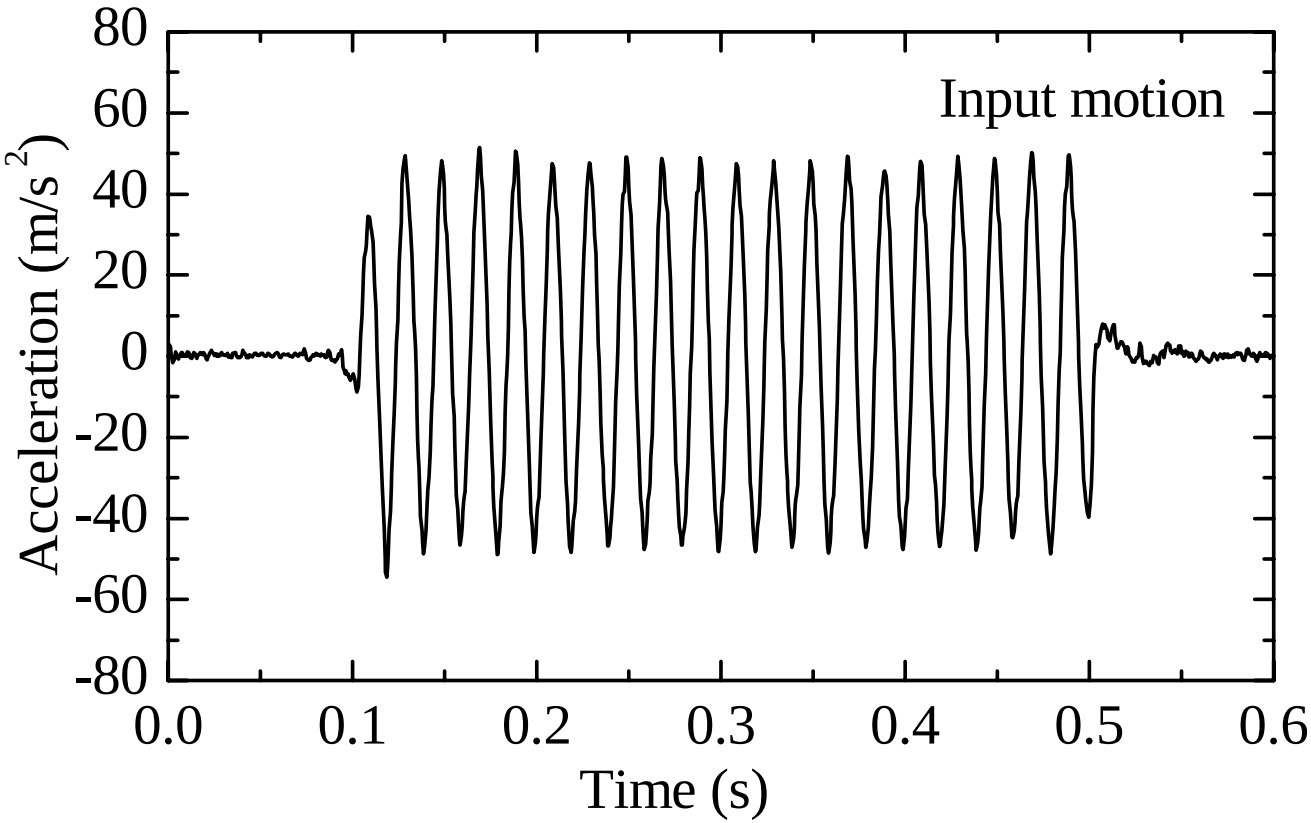

50 Hz, 50 m/s^2（model） ⇒

1 Hz, 100 gal（prototype with a scale ratio λ =50）

Acceleration response measured on piled raft model

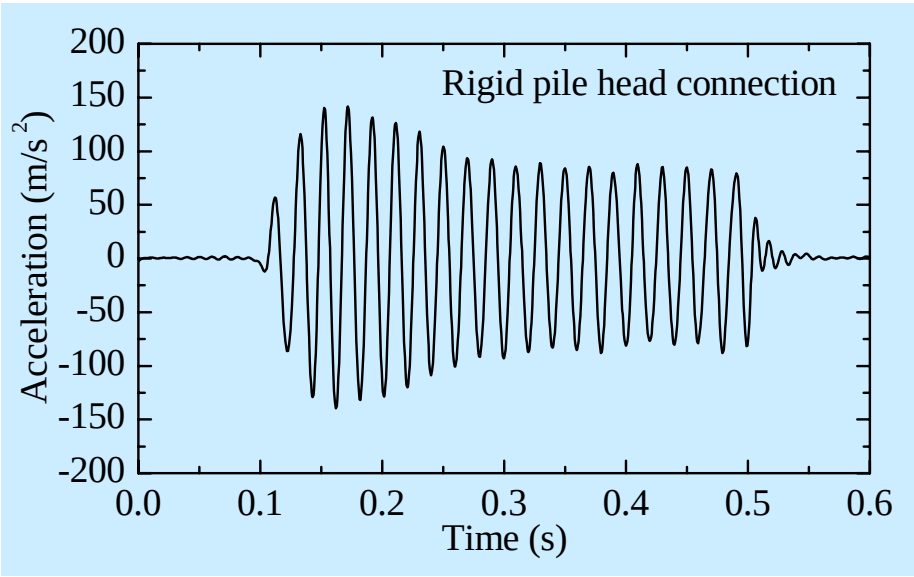

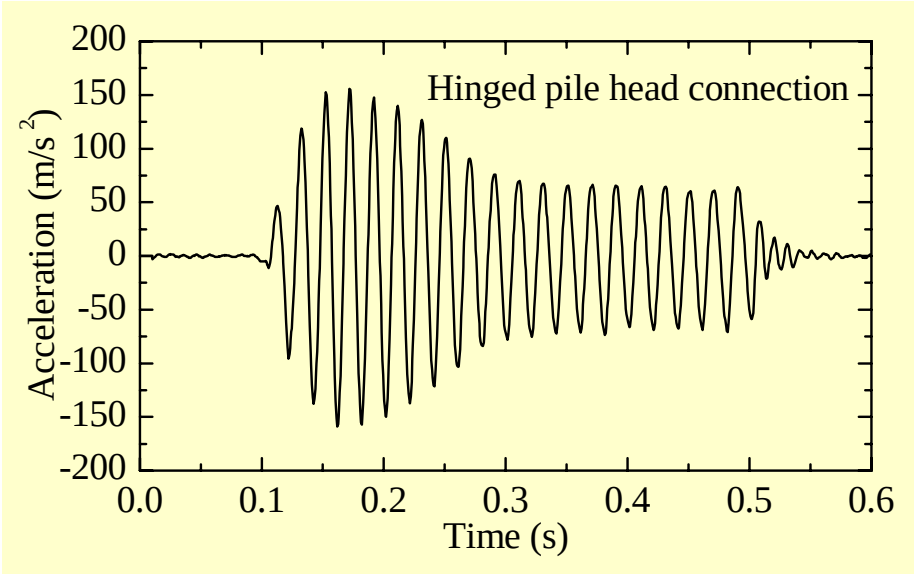

Rigid pile head connection

Hinged pile head connection

The maximum acceleration was a little bit of higher in the hinged pile head connection model.

Attenuation of the acceleration occurred in both models.

The rate of the attenuation of acceleration was higher in the hinged pile head connection model.

Horizontal displacement of piled raft during shaking period

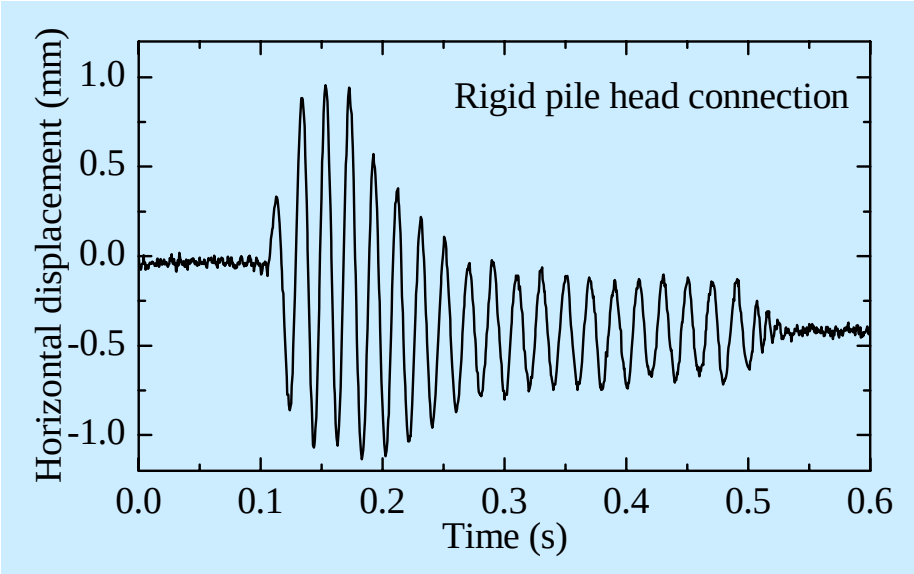

Rigid pile head connection

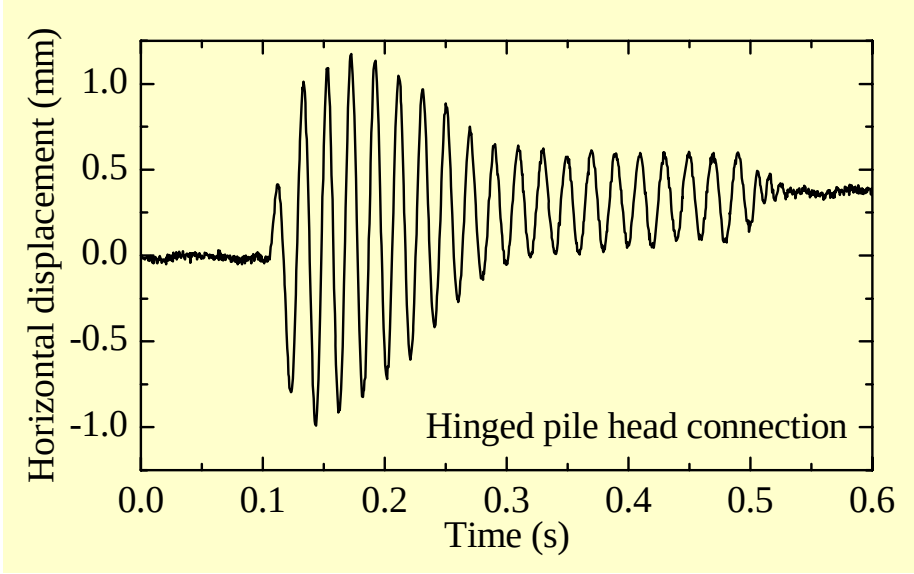

Hinged pile head connection

The maximum horizontal displacement was a little bit of higher in the hinged pile head connection model.

Attenuation of the horizontal displacement occurred in both models.

The rate of the attenuation of displacement was higher in the hinged pile head connection model.

Settlement of piled raft and ground surface

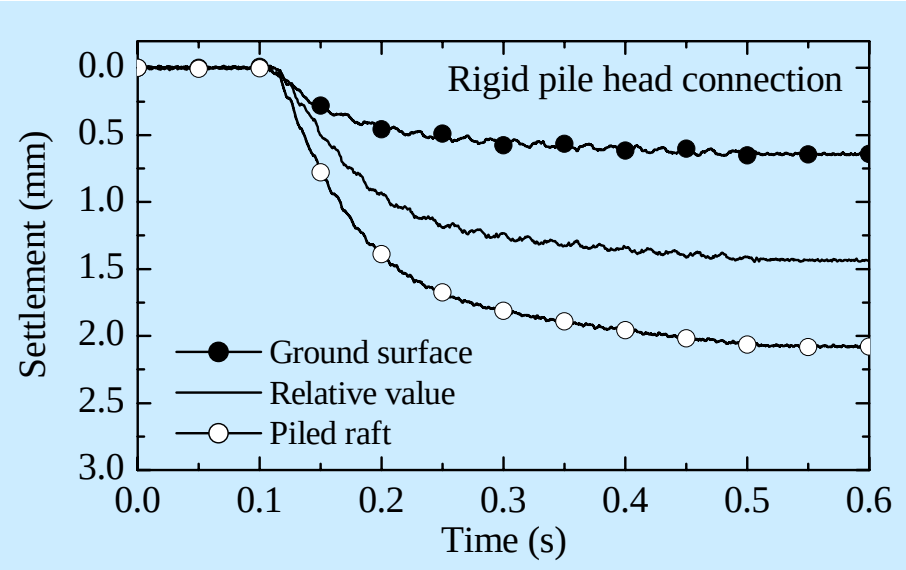

Rigid pile head connection

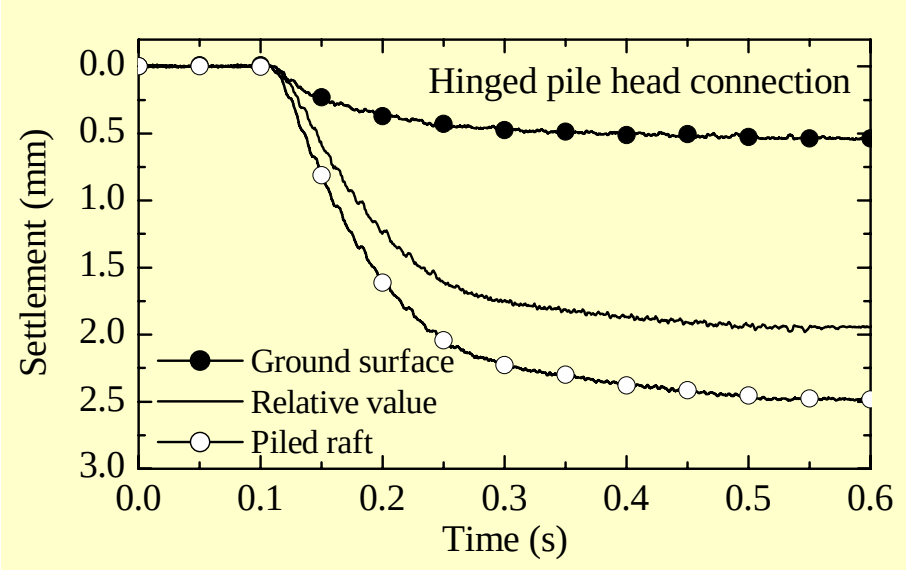

Hinged pile head connection

The settlements of the ground surface in both tests were consistent.

Higher relative displacement (penetration of the raft into the ground) occurred in the hinged pile head connection model.

Amplitude of horizontal displacement in comparison with relative settlement of piled raft

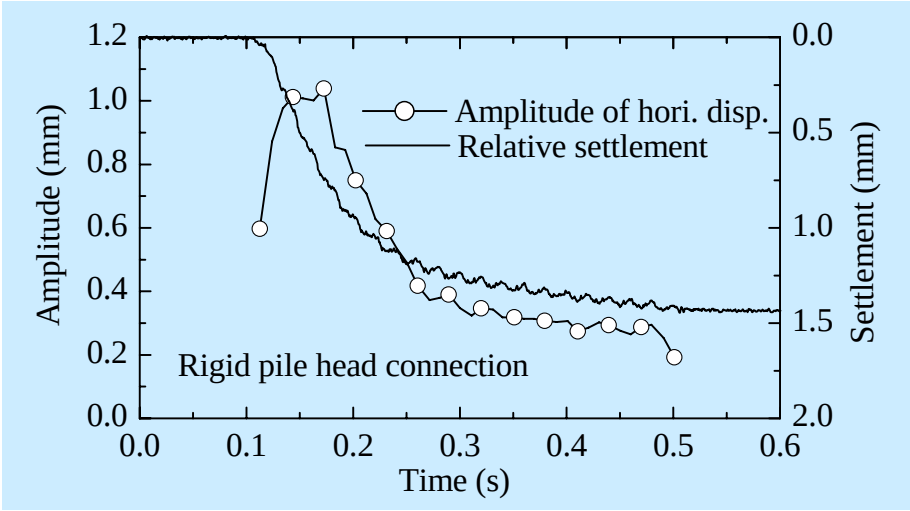

Rigid pile head connection

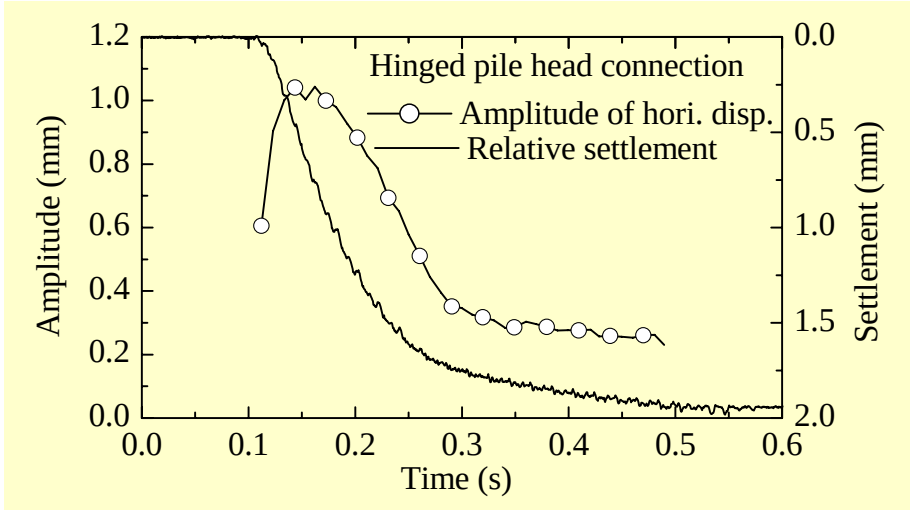

Hinged pile head connection

The relative settlements clearly correspond to the amplitudes of the horizontal displacements.

The attenuation of the horizontal displacement was caused by the increase in the relative settlement.

Horizontal load displacement relationship of piled raft compared with static test result

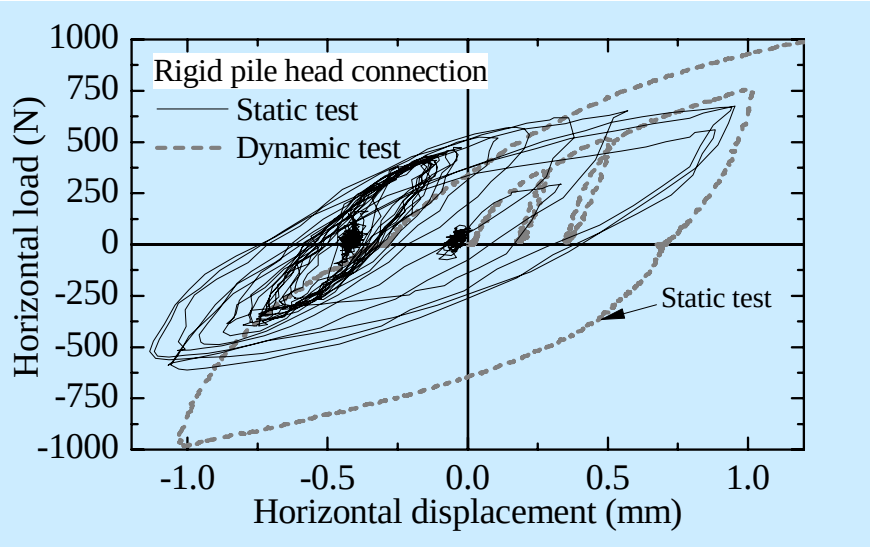

Rigid pile head connection

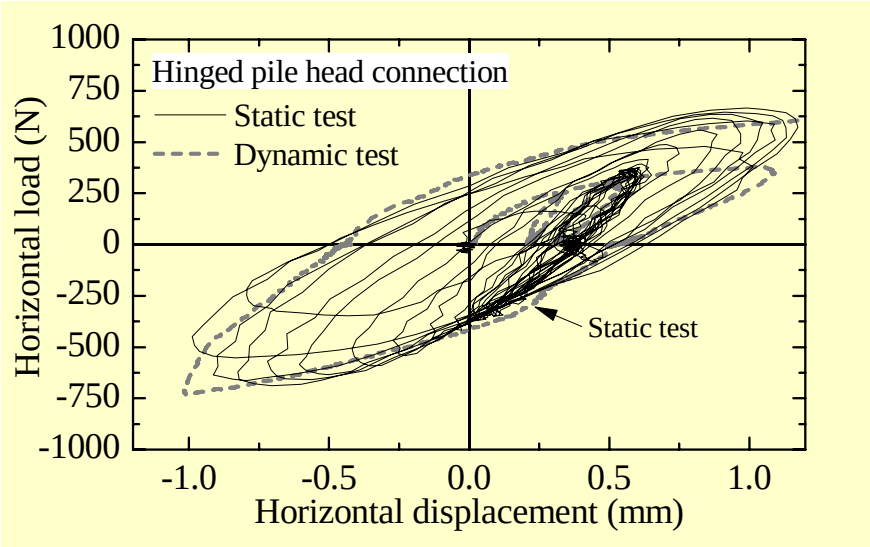

Hinged pile head connection

The overall load-displacement behaviour was consistent between the static and the dynamic tests, although the loading-unloading hysteresis curves shifted gradually in the dynamic tests due to the occurrence of the residual displacements.

Inclination of piled raft during shaking period

Clock-wise inclination → Positive

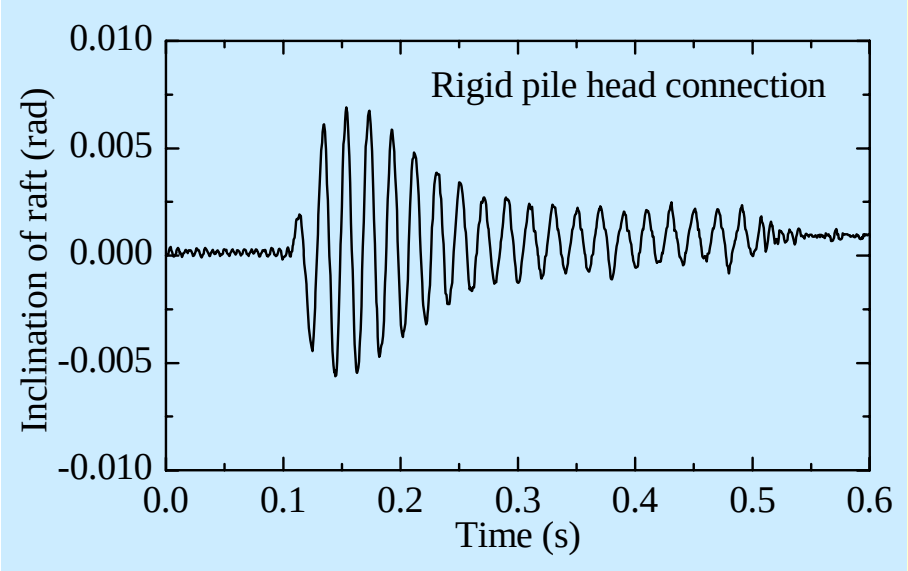

Rigid pile head connection

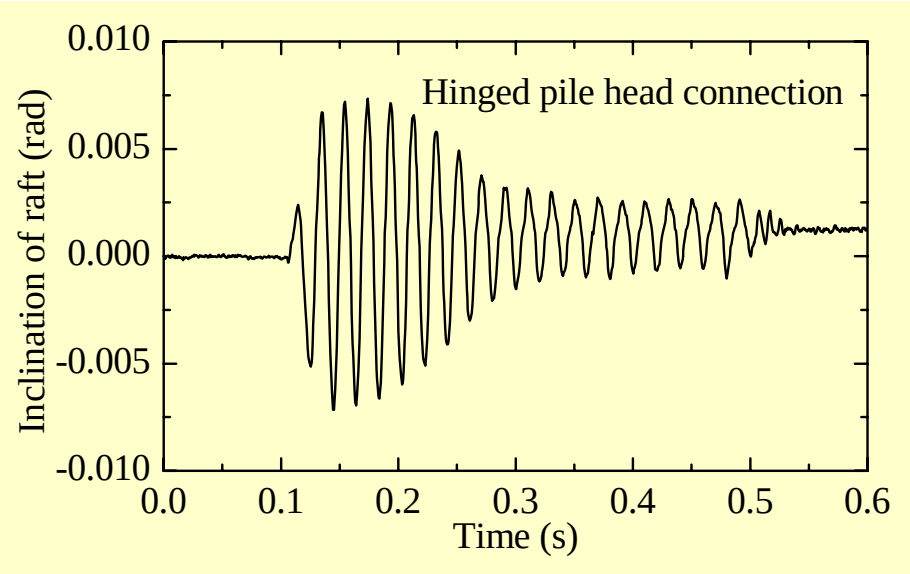

Hinged pile head connection

The amplitude of the inclination in each cycle attenuated with time as was seen in the horizontal acceleration and the displacement responses.

Relationship between inclination and horizontal displacement

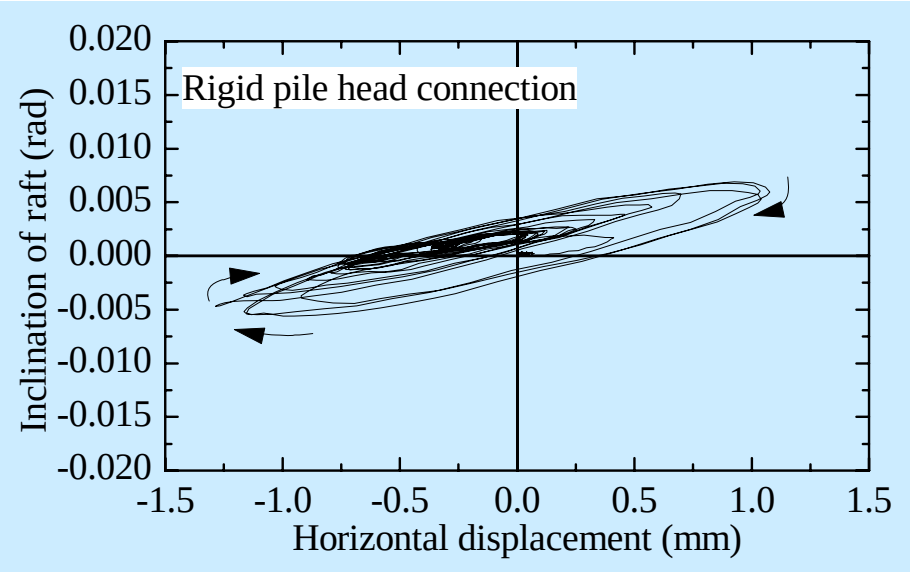

Rigid pile head connection

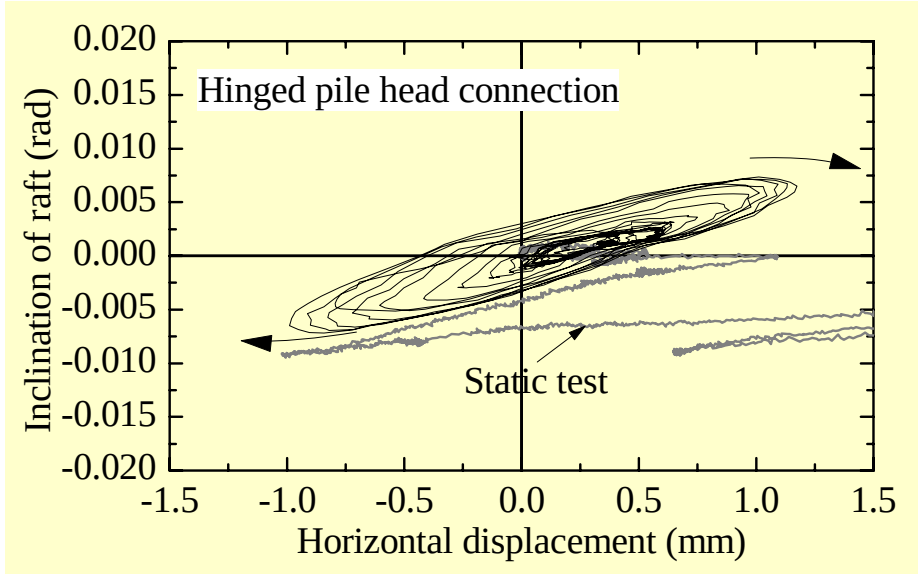

Hinged pile head connection

The point at a peak horizontal displacement coincides to the point at the peak raft inclination in the rigid pile head connection model, whereas both did not coincide in the hinged connection model.

Proportion of horizontal load carried by 4 piles

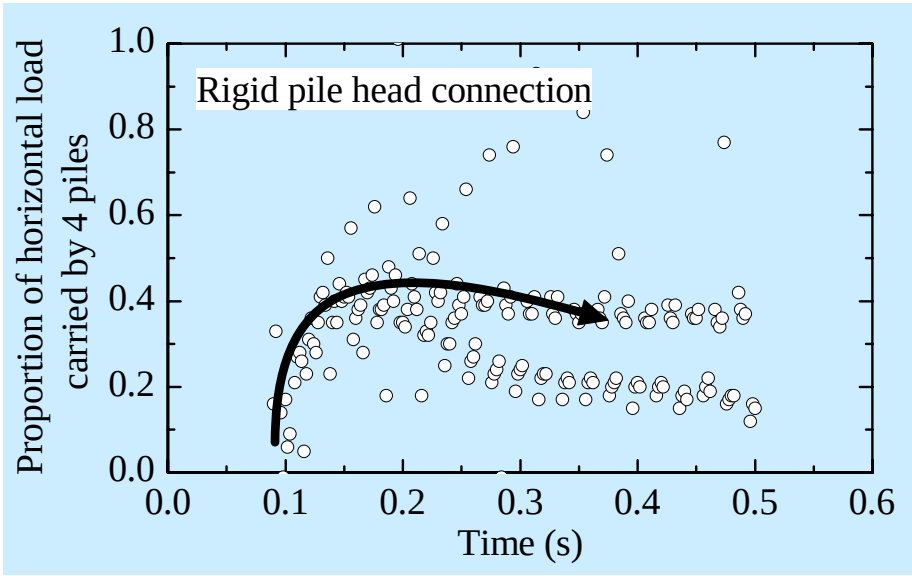

Rigid pile head connection

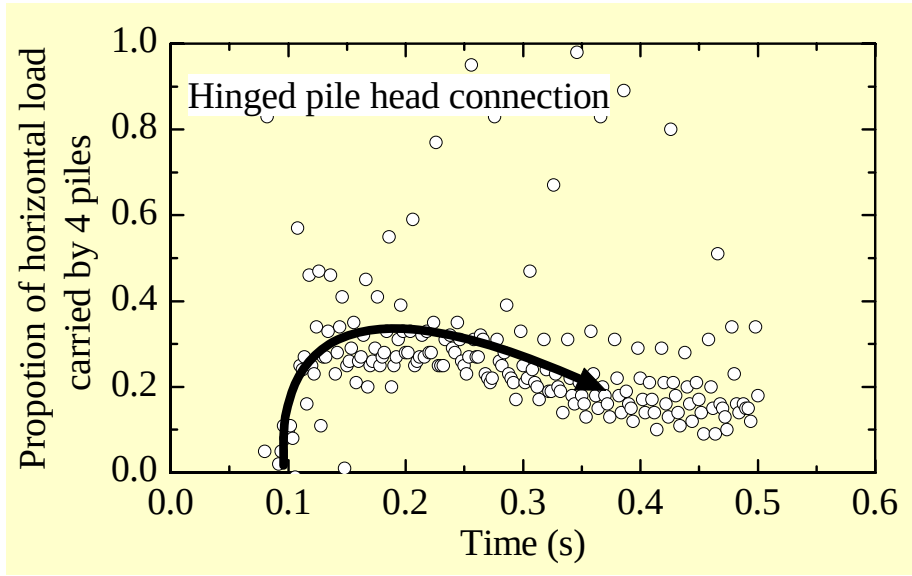

Hinged pile head connection

The proportion is higher in the rigid connection model.

A rapid increase in the load carried by the piles was observed in both piled rafts during the initial stage of shaking.

Proportion of horizontal load carried by 4 piles during shaking period in comparison with static test result

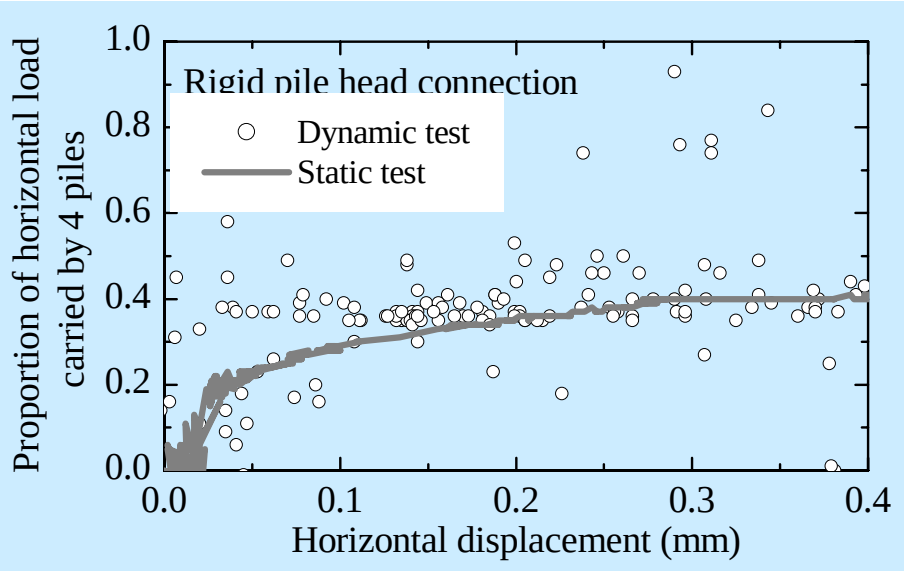

Rigid pile head connection

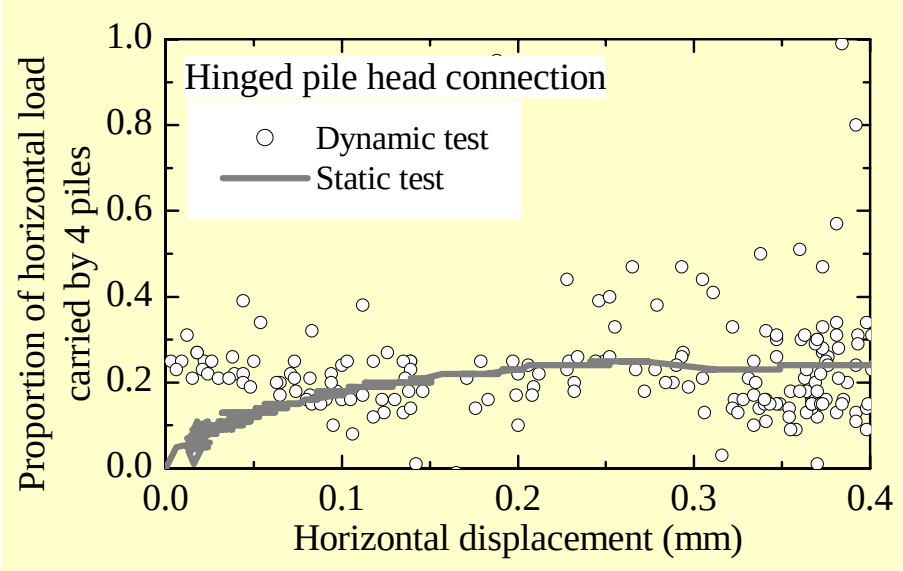

Hinged pile head connection

The results from the dynamic tests and the static loading tests were consistent in both piled rafts.

Distributions of bending moment along pile shaft

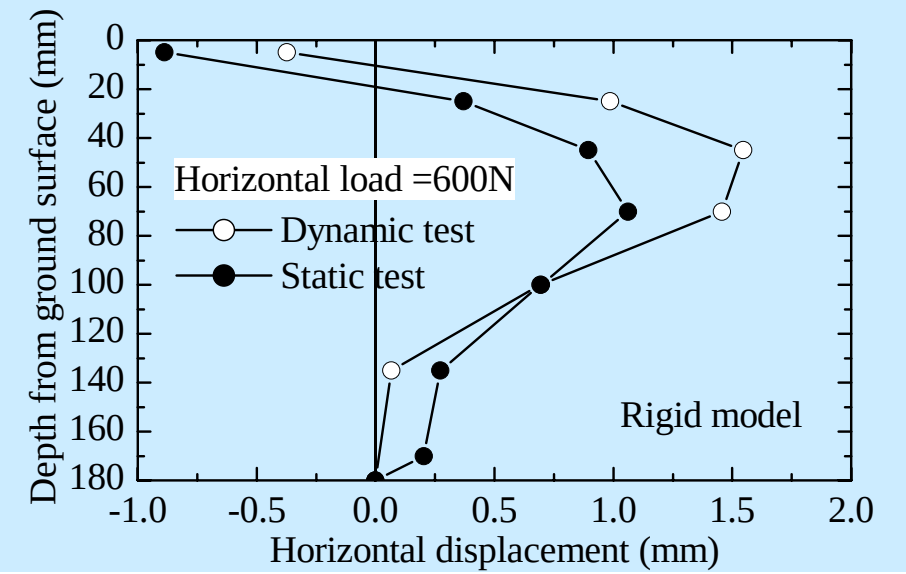

Rigid pile head connection

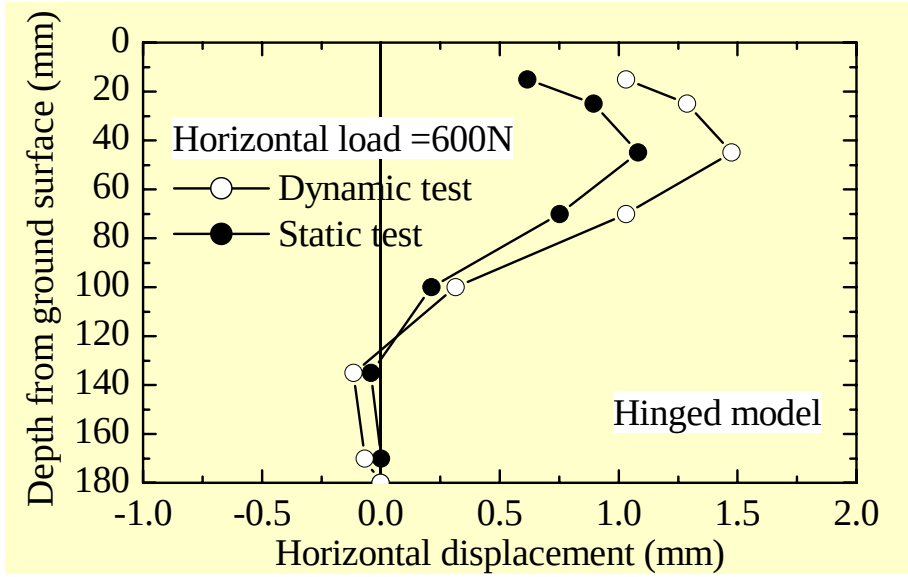

Hinged pile head connection

Since the mass of the raft model was relatively large, inertia effects seemed to be much dominant compared with the kinematic effects, thus the dynamic responses were similar to the static responses.

Proportion of vertical load carried by 4 piles

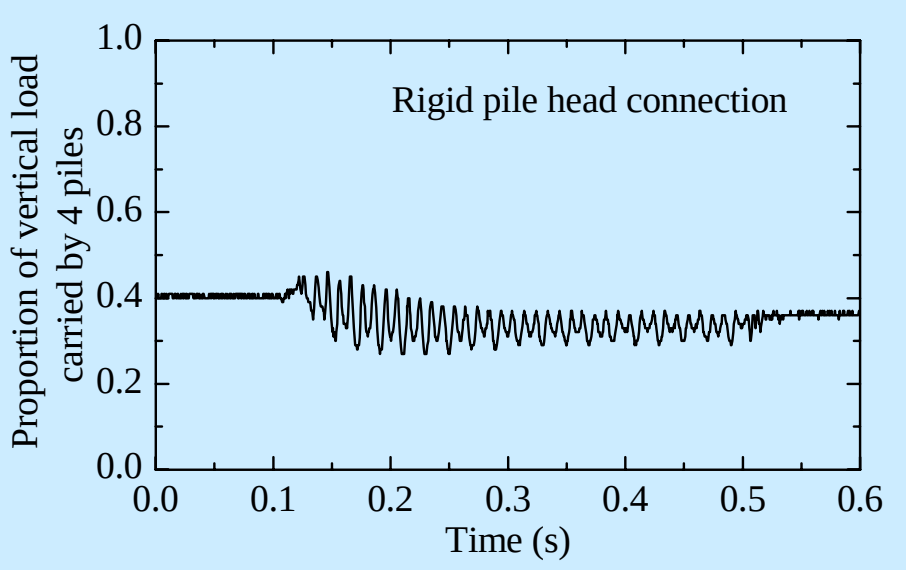

Rigid pile head connection

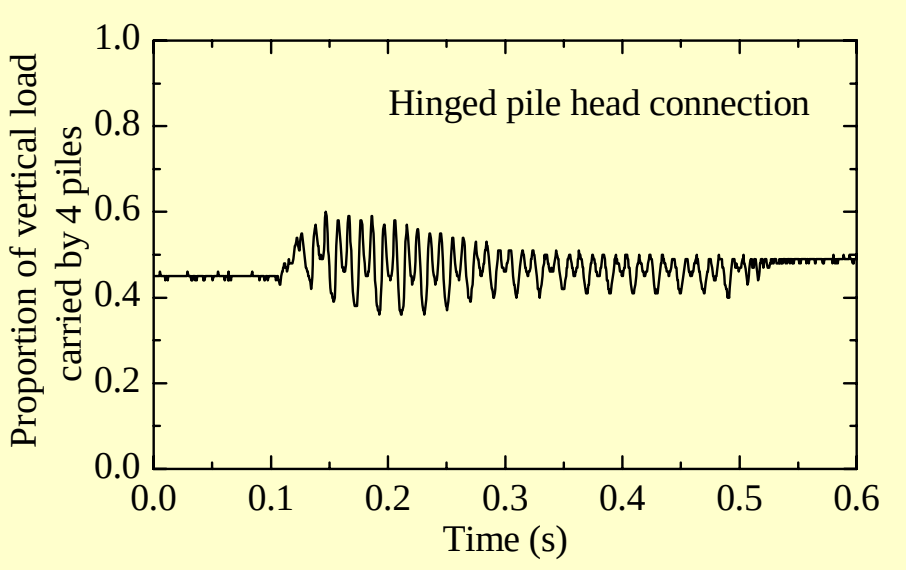

Hinged pile head connection

The load carried by the piles did not change significantly before and after shaking.

Proportion of vertical load carried by 4 piles in comparison with static test result

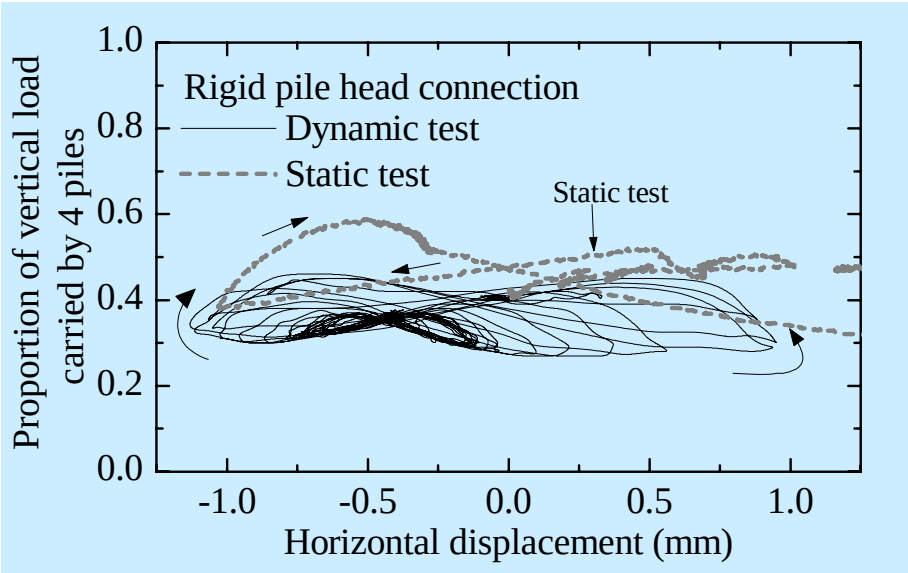

Rigid pile head connection

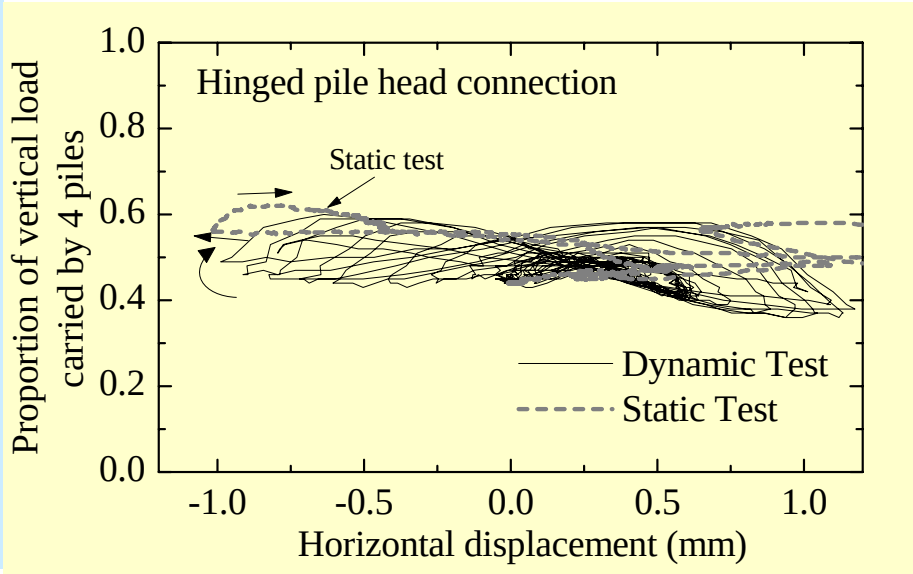

Hinged pile head connection

The consistent trend between the dynamic and static loading tests is shown.

Proportion of vertical load carried by piles at different pile positions

The degree of change in the axial load was more significant in the rigid connection model.

The piles in the hinged connection model tended to carry more uniform vertical load within the group.

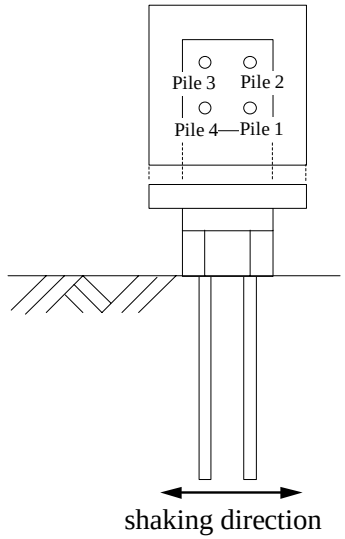

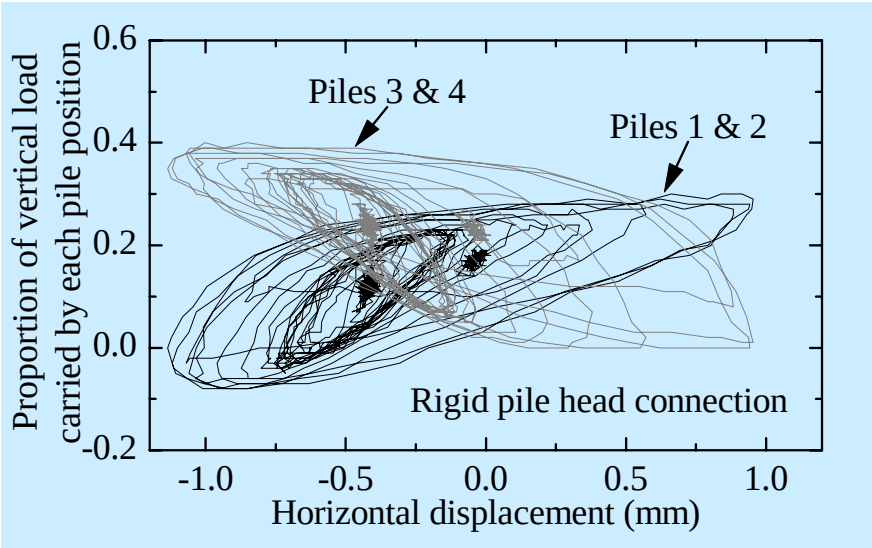

Rigid pile head connection

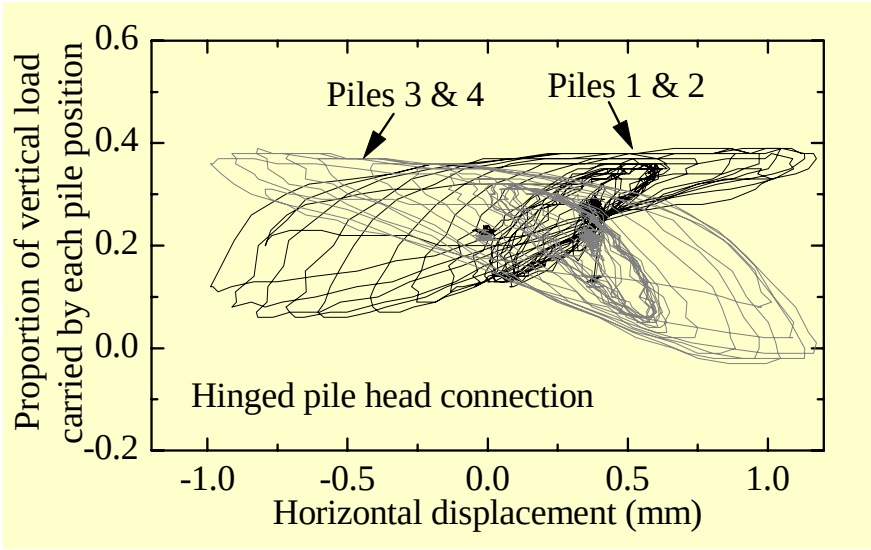

Hinged pile head connection

Proportion of vertical load carried by 4 piles for higher input motion

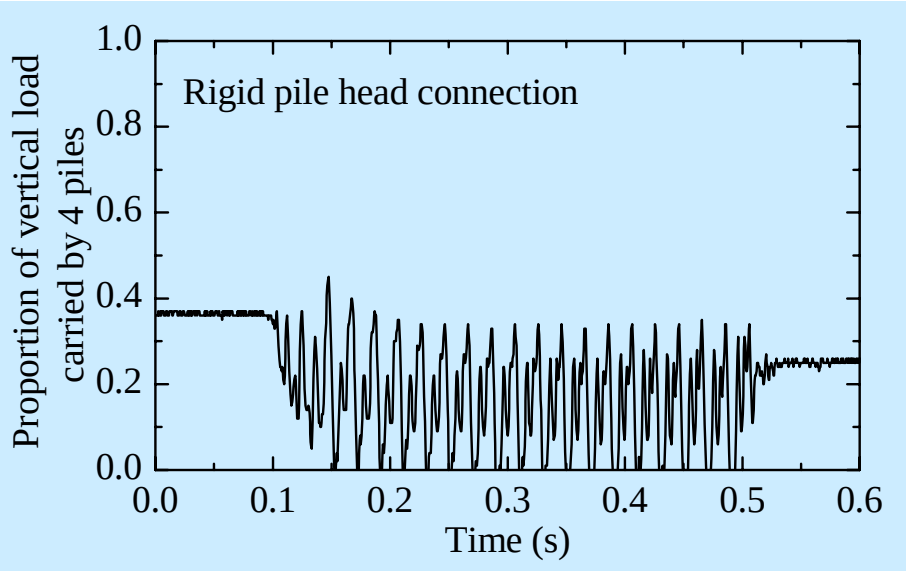

Rigid pile head connection

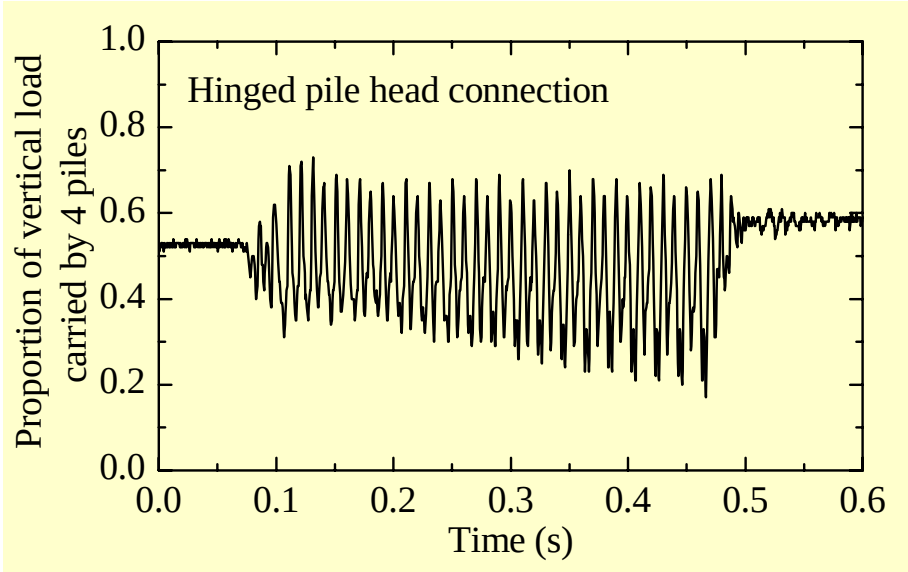

Hinged pile head connection

The change in the proportion of the vertical load carried by the piles before and after the shaking was still relatively small, although the amplitude of the proportion during shaking period became larger.

Schematic figure of centrifuge package

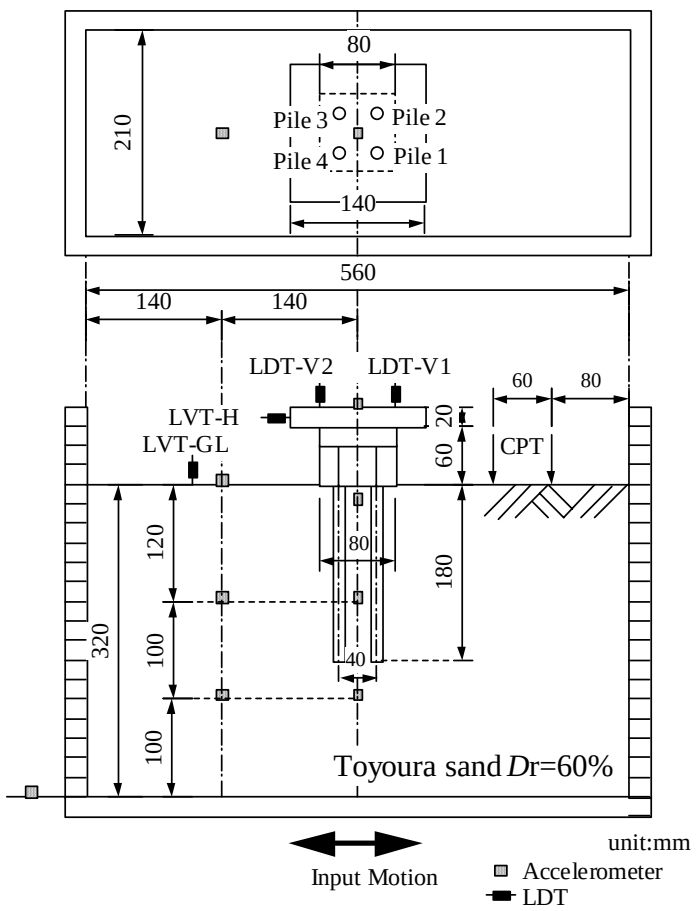

Piled raft model

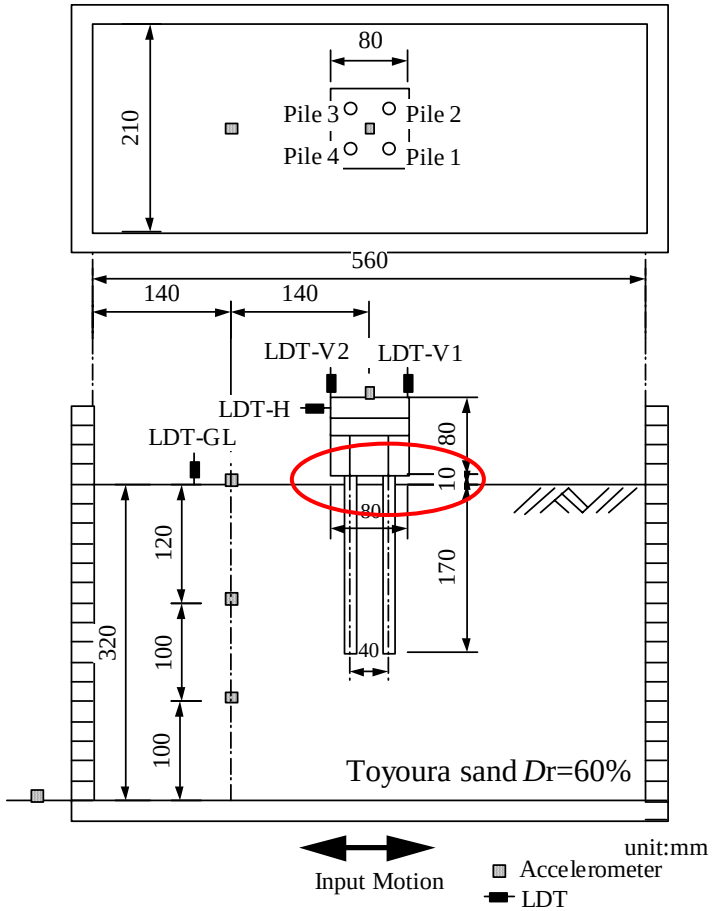

Pile group model

In the test of a free-standing pile group, the piled raft model with the rigid head connection was used by allowing a gap of 10 mm between the raft base and the soil.

Acceleration response measured on free-standing pile group model

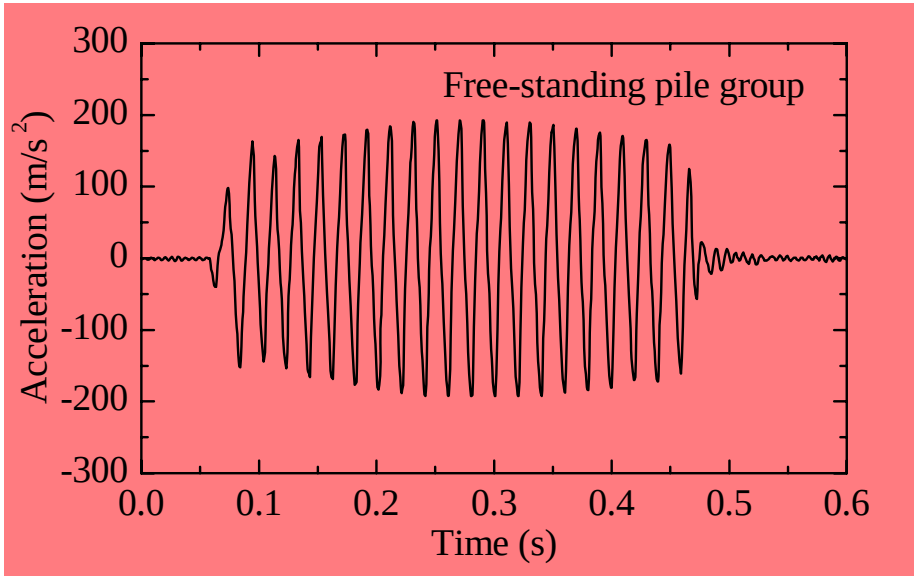

Free-standing pile group

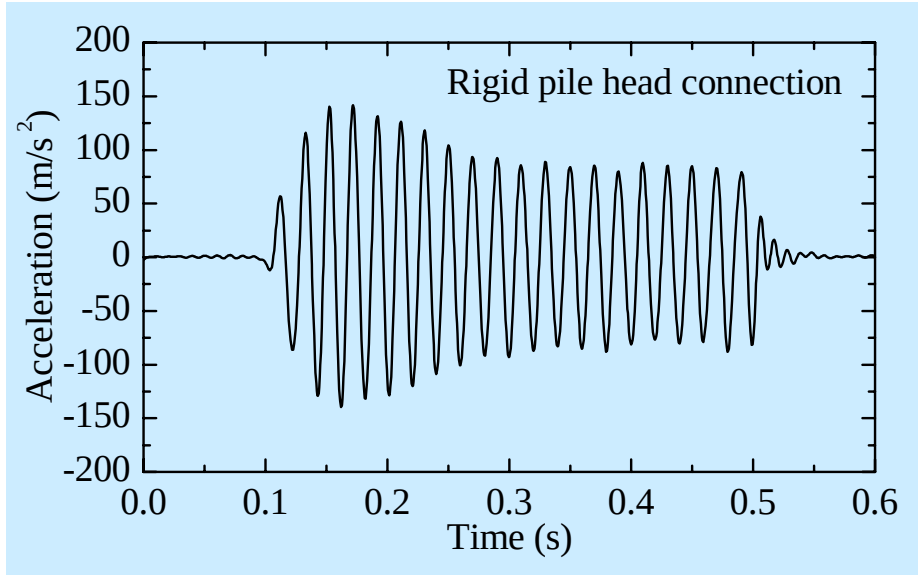

Piled raft

No attenuation was observed in the response of pile group.

Even though the mass of the raft was about half, the acceleration response was much higher in the pile group model.

Settlement and inclination of pile group during shaking period

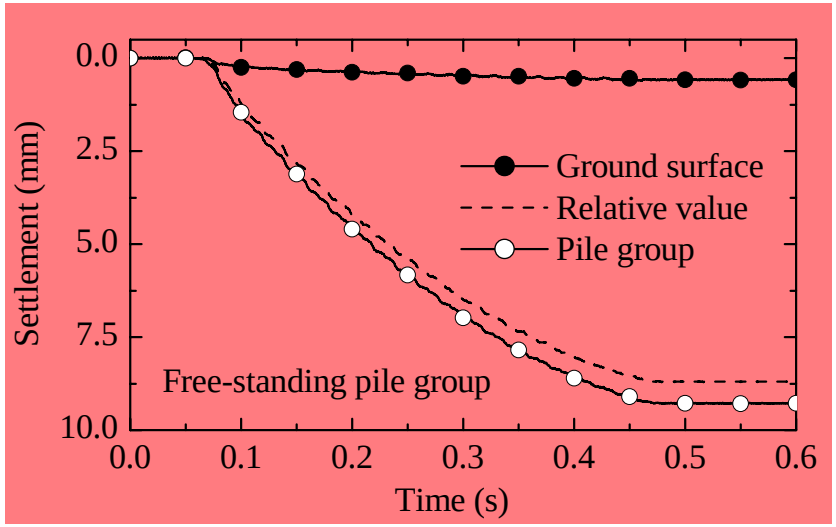

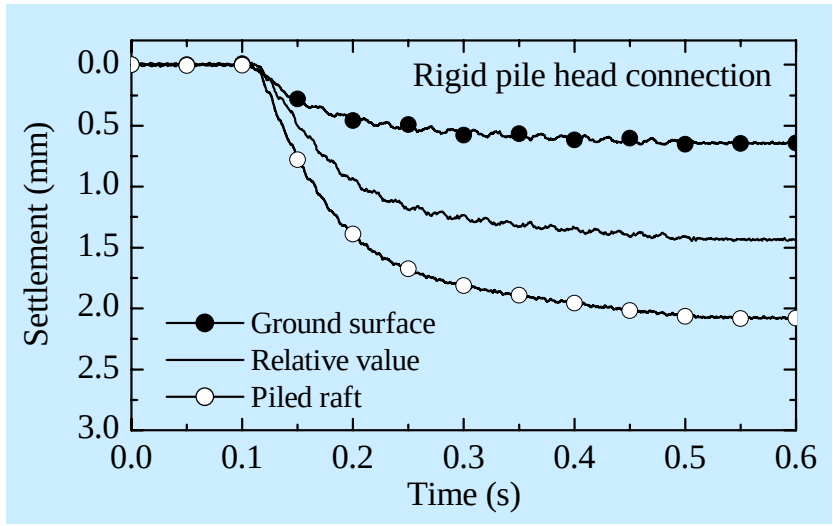

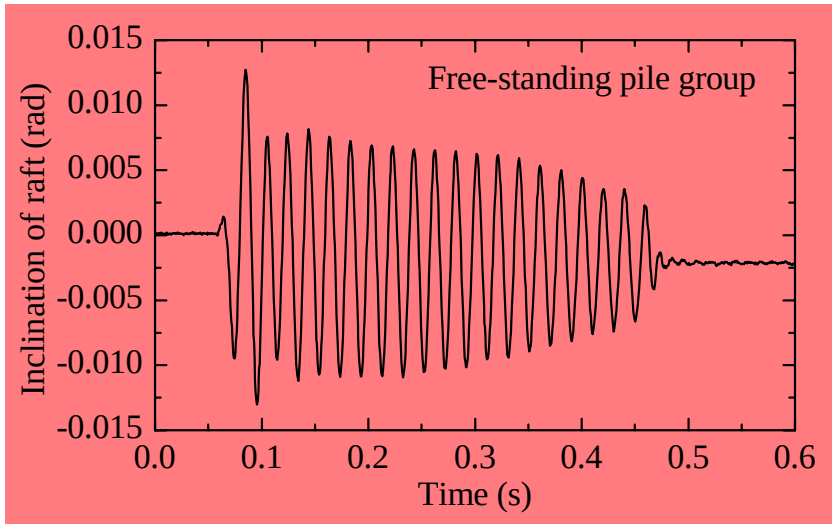

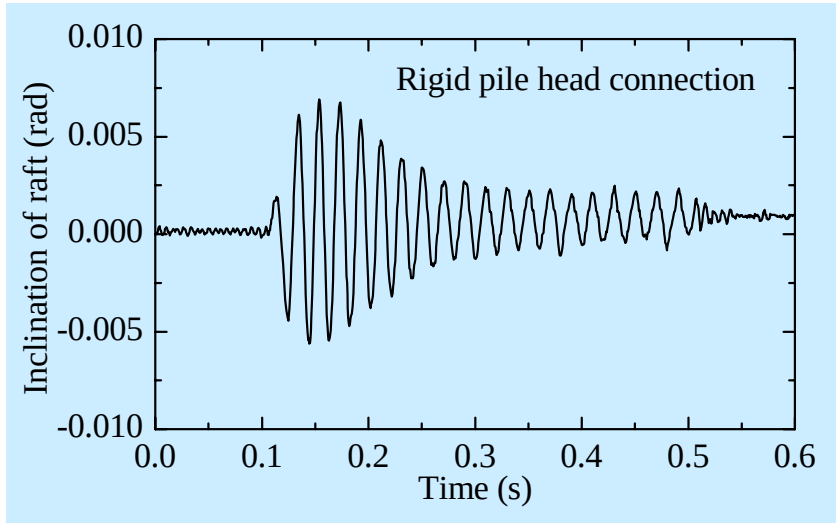

Free-standing pile group

Piled raft

Distributions of bending moments along pile shaft

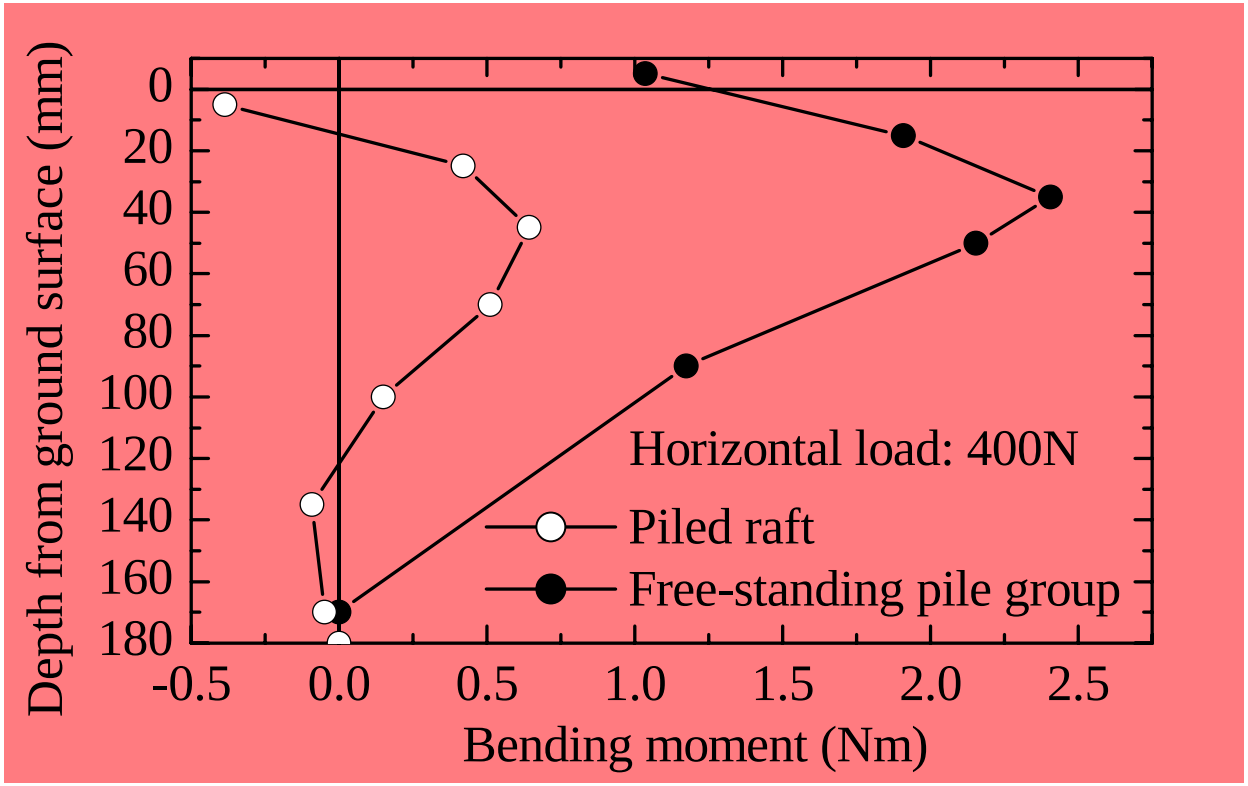

The maximum bending moment of the pile in the piled raft was significantly reduced to about one fourth of that in the pile group, indicating a large contribution of the raft also in reducing the bending moments in the pile.

Conclusion (1)

In the piled raft designs, evaluation of the displacement (settlement, horizontal displacement, and inclination) and the proportion of the load carried by the components are highly important factors. The dynamic responses of the above factors were intensively examined in this paper.

As was also shown in the static modeling by the authors, the dynamic tests also indicate that the proportion of the horizontal load carried by each component is highly non-linear, and dependent on the horizontal displacement of the piled raft system. The evaluation of horizontal displacement is therefore important in the seismic design of piled rafts.

The change in the vertical load sharing between the piles and the raft base was relatively small compared with the horizontal load, even when the piled rafts were subjected to relatively strong input motion.

Conclusion (2)

As far as the model conditions in the present study are concerned, the rigid pile head connection gave higher horizontal stiffness than the hinged pile head connection. The acceleration response and the inclination of the model were also smaller in the rigid pile head connection model.

The proportion of the horizontal load carried by the piles was smaller in the hinged pile head connection model, indicating the role of piles in the horizontal resistance of the piled raft was smaller in the hinged connection model.

The contact of raft base with the soil surface played highly important roles in reducing horizontal acceleration, inclination, and bending moments of the piles.

Influence of superstructure on behaviour of model piled rafts in sand under shaking tests

Focus

1 g field

Influence of the height of the gravity centre of the superstructure on the dynamic behaviour of the whole structure consisting of the superstructure and the piled raft foundation during shaking.

Matsumoto, T., Fukumura, K., Kitiyodom, P., Oki, A. and Horikoshi, K. (2004): Experimental and analytical study on behaviour of model piled rafts in sand subjected to horizontal and moment loading, *Int. Journal of Physical Modelling in Geotechnics* 4(3): 1-19.

Matsumoto, T., Fukumura, K., Oki, A. and Horikoshi, K. (2004): Shaking table tests on model piled rafts in sand considering influence of superstructures, *Int. Journal of Physical Modelling in Geotechnics* 4(3): 20-37.

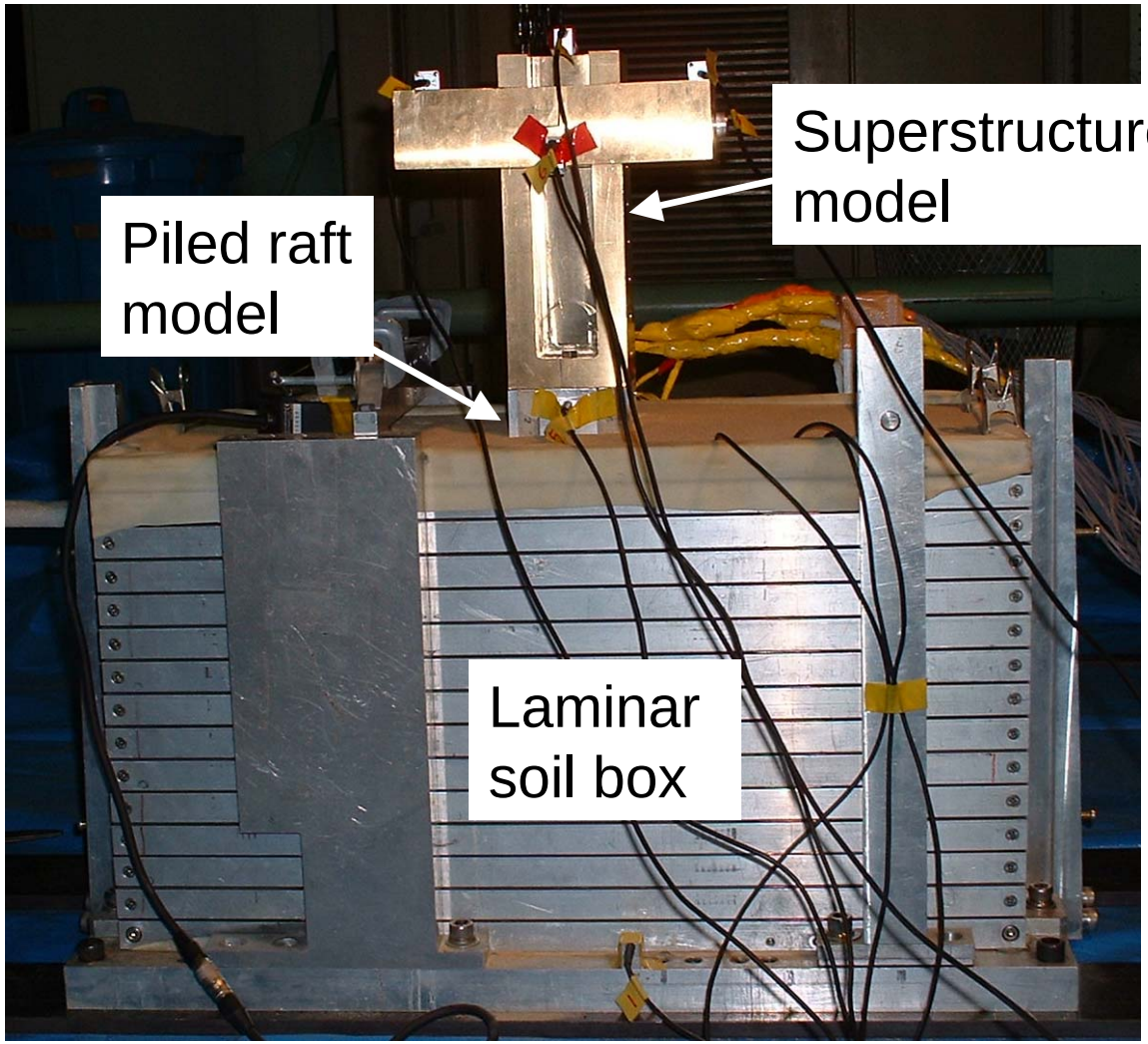

Model ground:

dry Toyoura sand

$D_r = 95\ \%$

Test set-up for shaking table test on combined model of superstructure and piled raft

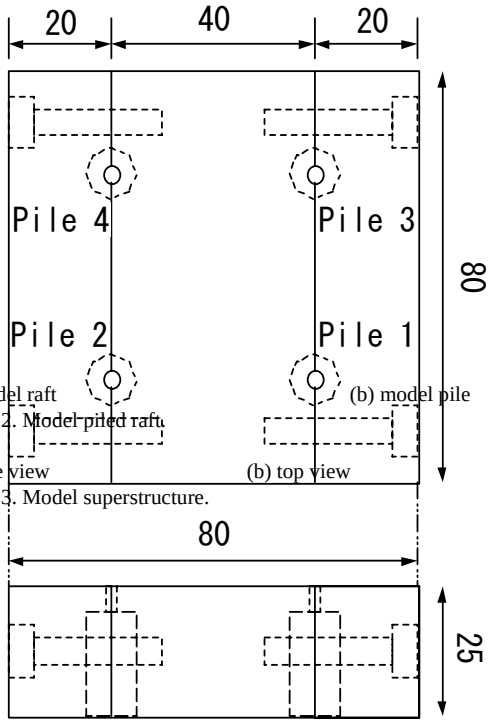

(a) model raft (b) model pile

Figure 2. Model piled raft

(a) side view (b) top view

Figure 3. Model superstructure.

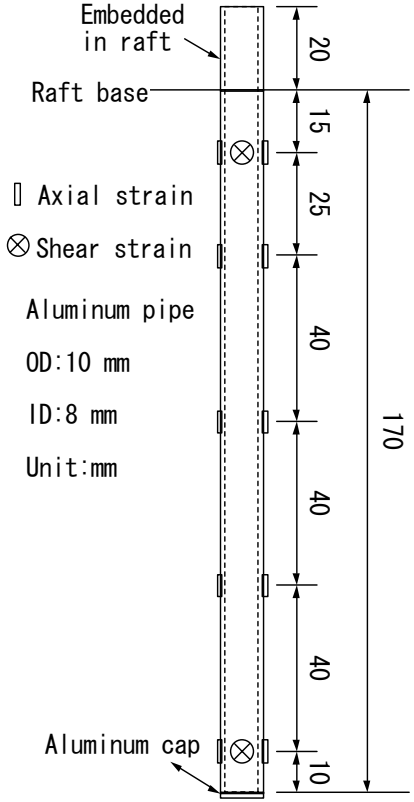

Geometrical and mechanical properties of the model pile

	Model	Prototype (λ=50)
Outer diameter, r_o (mm)	10	500
Wall thickness, t_w (mm)	1	50
Length, L (mm)	170	8500
Cross section area, A (mm^2)	28.3	70685.8
Young's modulus, E_p (GPa)	67.1	3354
Poisson's ratio, ν_p	0.345	0.345
Longitudinal rigidity, E_pA (GN)	1.90×10^{-3}	33.53
Bending rigidity, E_pI (GNm^2)	19.4×10^{-8}	0.859

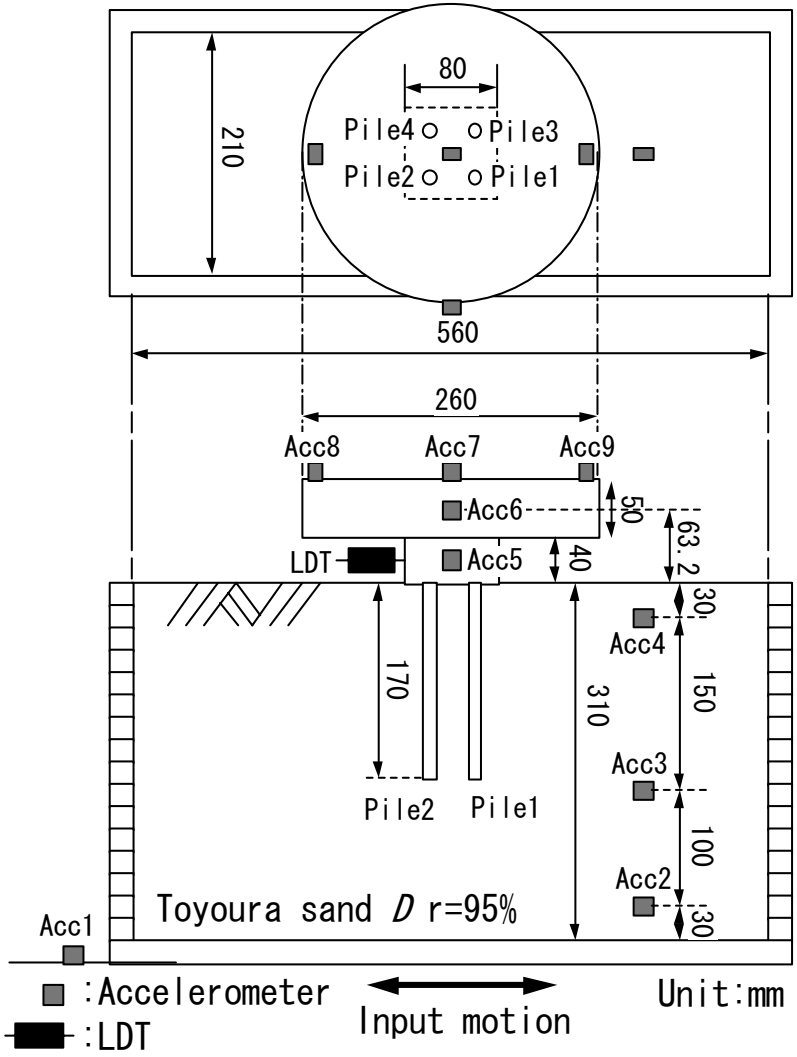

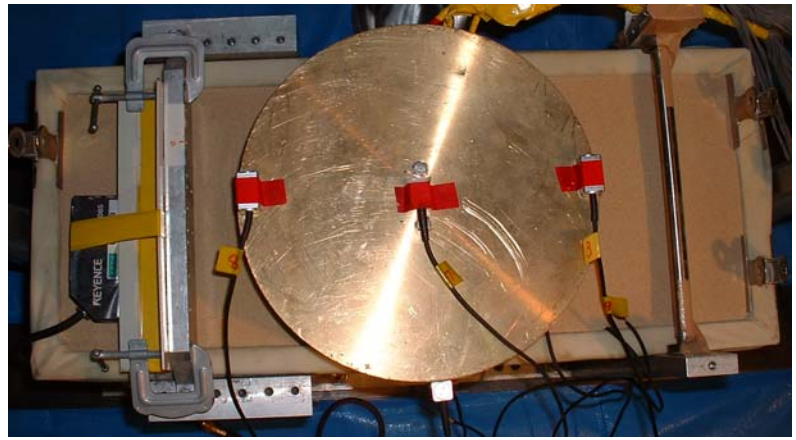

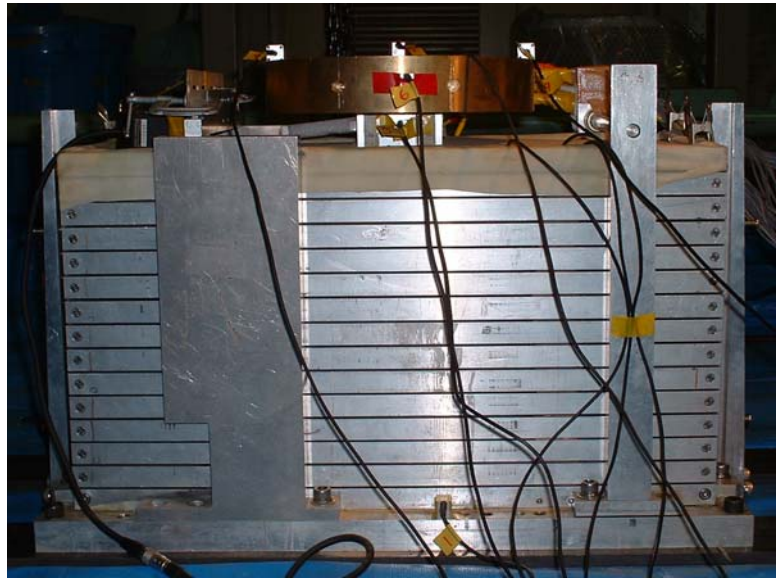

Test set-up for shaking table test on combined model of superstructure and piled raft

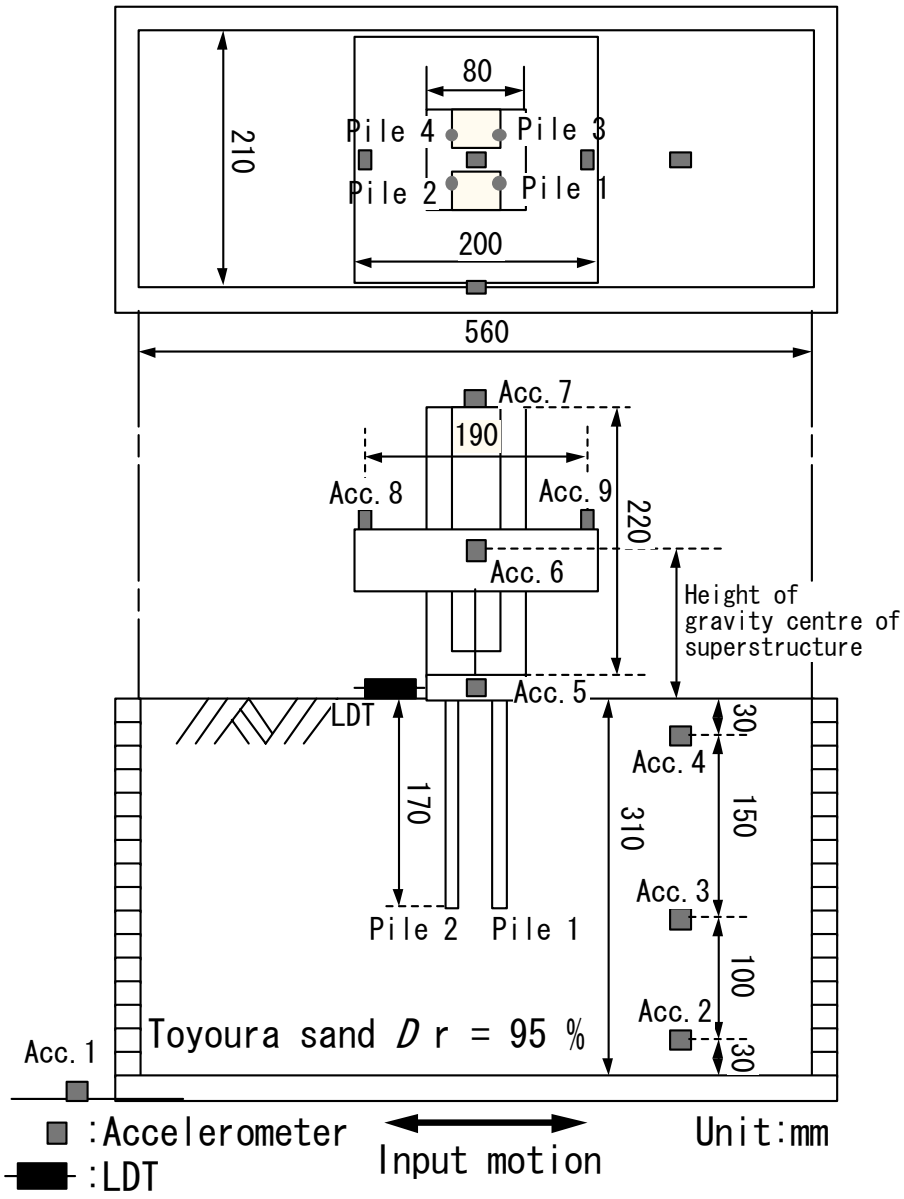

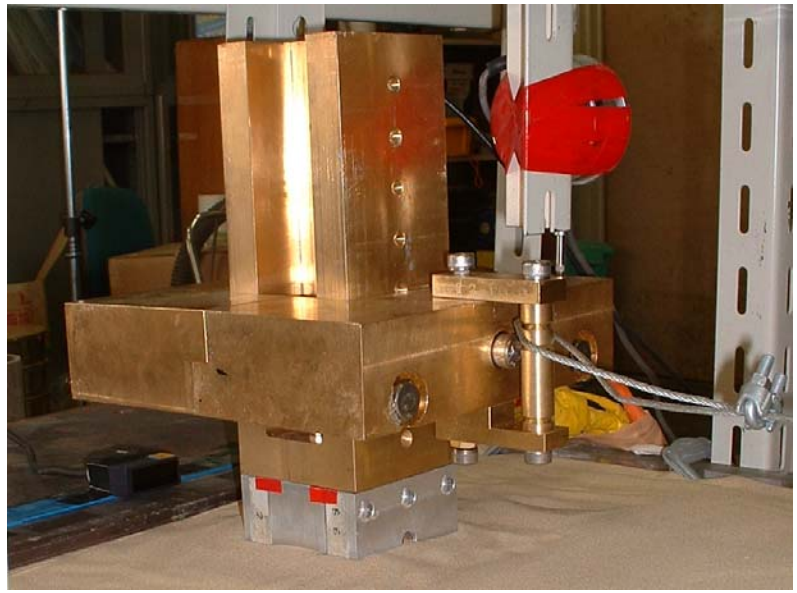

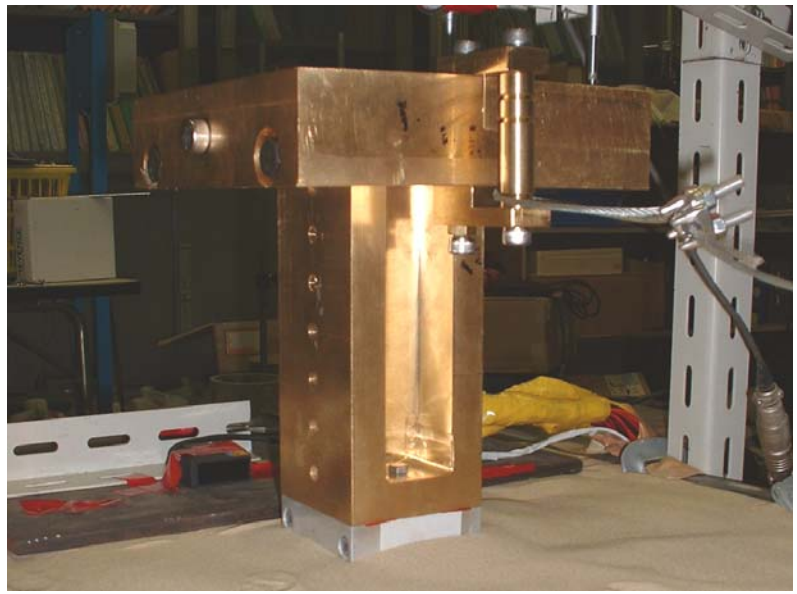

Superstructure models

Model ground: dry Toyoura sand, D_r = 95 %

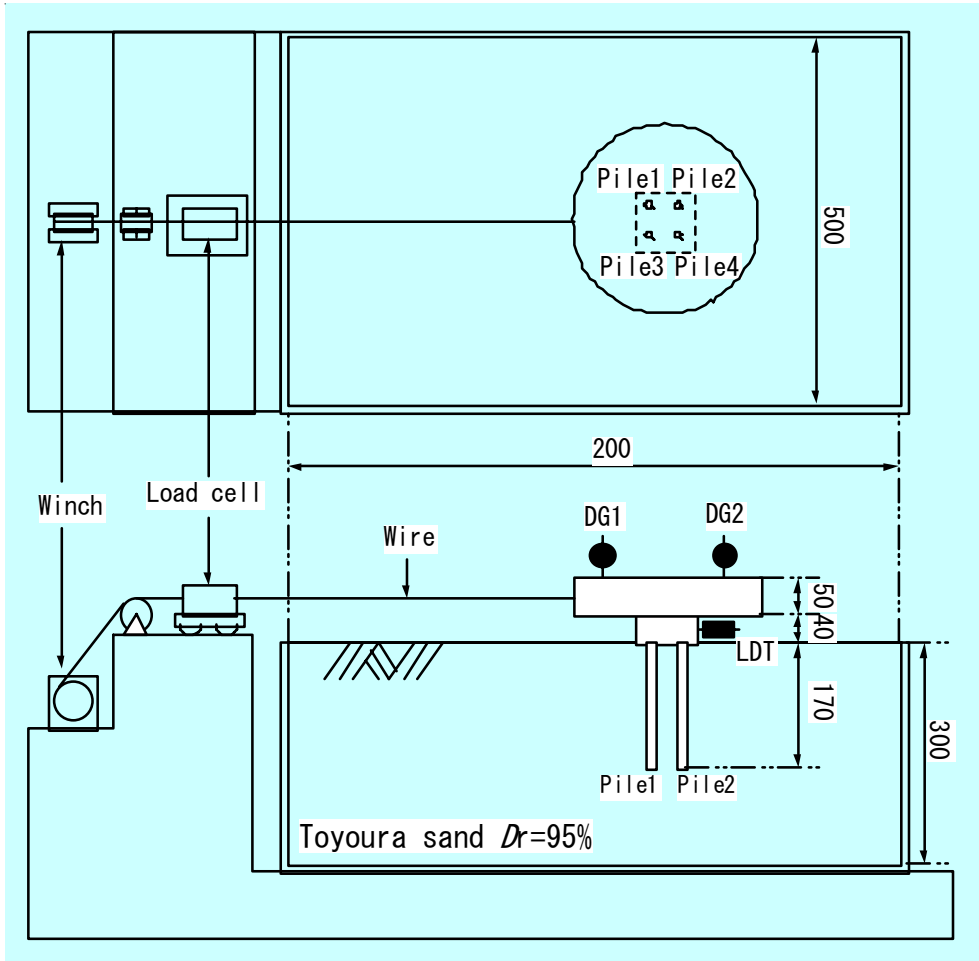

Test set-up for static horizontal load test

Horizontal load was applied to the gravity centre level of the superstructure in the static load test.

Density at test	ρ_t	1.635 t/m^3
Relative density at test	D_r	95 %
Internal friction angle	ϕ'	44 deg.
Mean grain size	D_{50}	0.162 mm
Density of soil particle	ρ_s	2.661 t/m^3
Maximum density	$\rho_{d\max}$	1.654 t/m^3
Minimum density	$\rho_{d\min}$	1.349 t/m^3

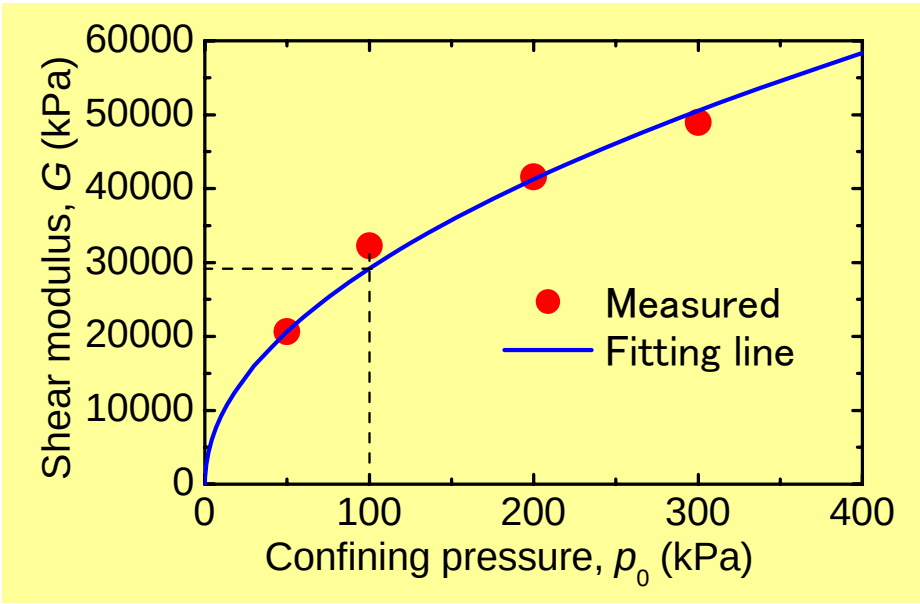

$$G = G_0 \left(p / p_0 \right)^n$$

n =0.5 , p_0=100 kPa, G_0=29163 kPa

Similarity for model tests at 1-g field (Iai, 1989)

Items	prototype / model
Length (Size)	λ
Density	1
Stress	λ
Strain	$\lambda^{1/2}$
Time	$\lambda^{3/4}$
Frequency	$1/\lambda^{3/4}$
Displacement	$\lambda^{3/2}$
Velocity	$\lambda^{3/4}$
Acceleration	1
Bending rigidity of pile	$\lambda^{7/2}$
Longitudinal rigidity of pile	$\lambda^{3/2}$

Middle gravity centre model

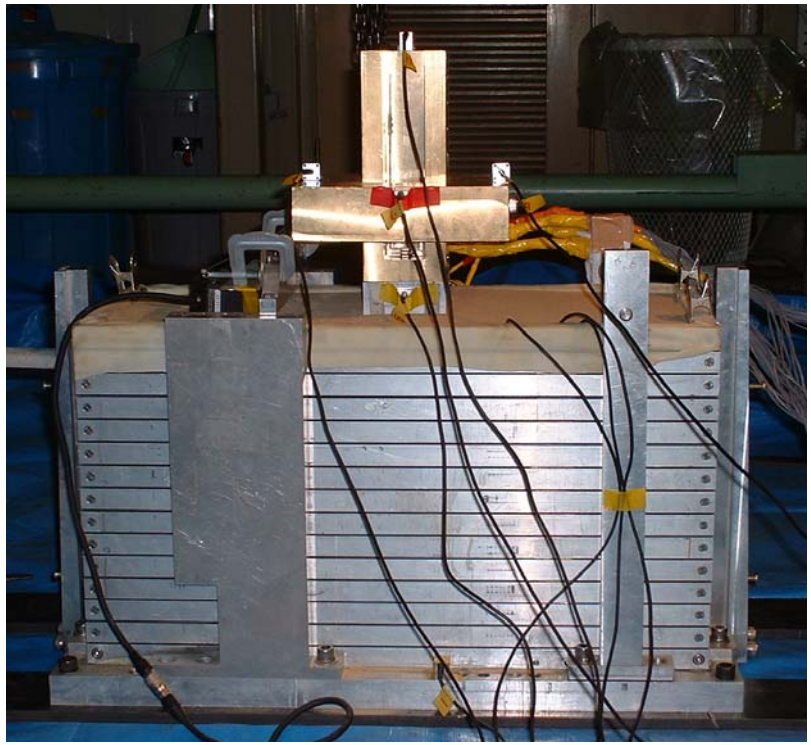

Low gravity centre model

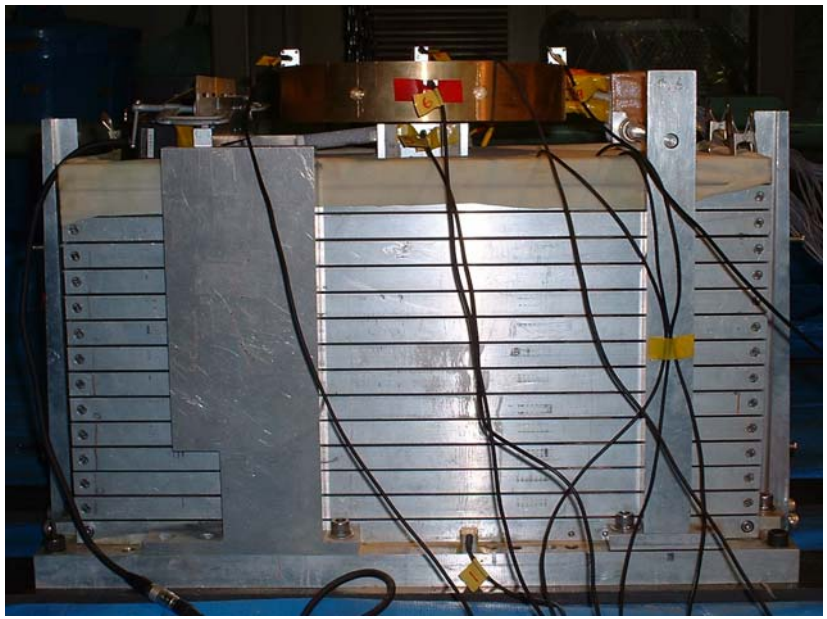

Test name and test conditions

Test name	Height of gravity centre from G.L.	Type of loading	Proportion of vertical load carried by piles before load test (%)
DRL	Low (49.3mm)	Dynamic	72.6
DRM	Middle (123.4mm)	Dynamic	73.4
SRL	Low (49.3mm)	Static	79.6
SRM	Middle (123.4mm)	Static	78.5

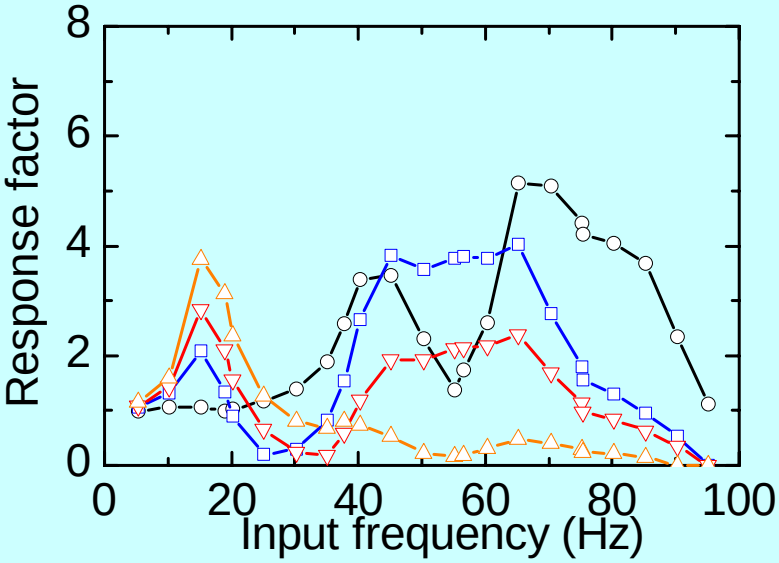

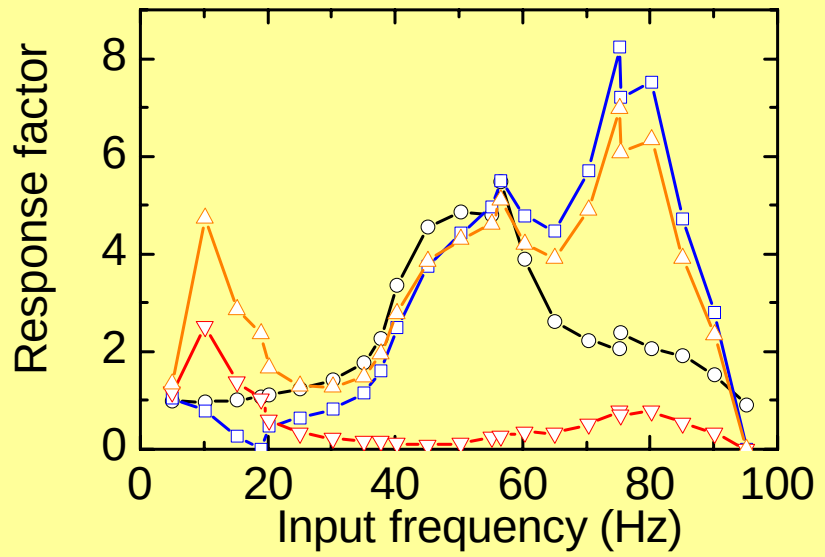

(a) DRM

Transf eleration

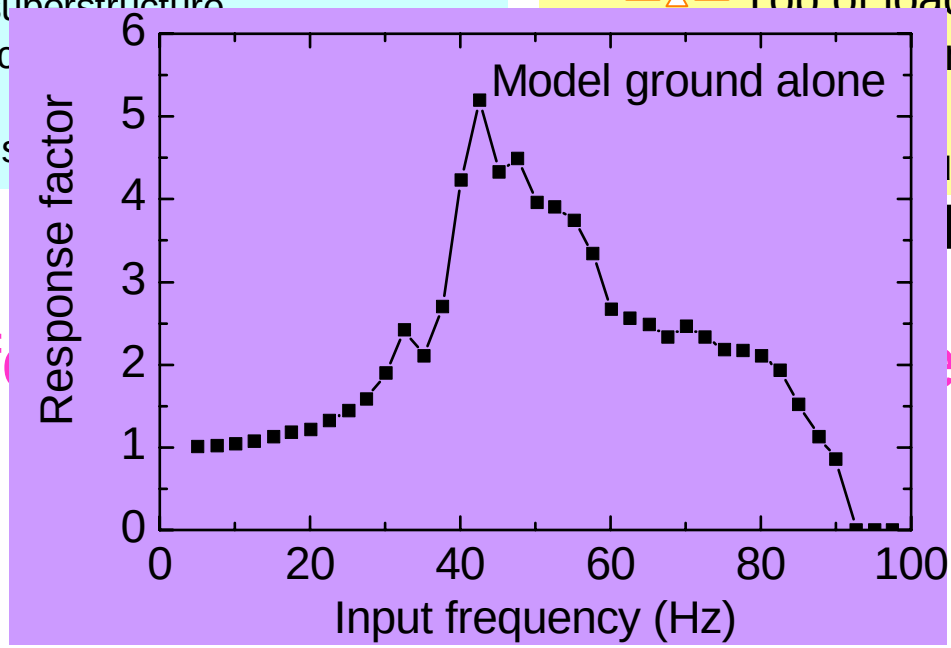

DRL (5Hz)

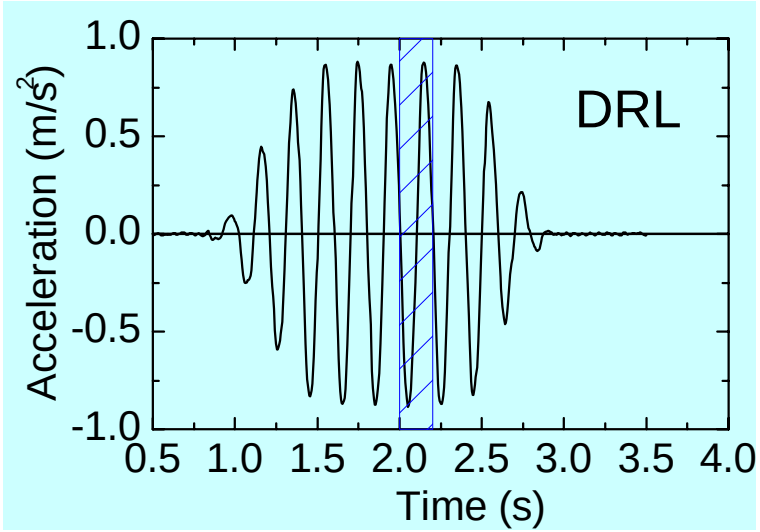

DRM (5Hz)

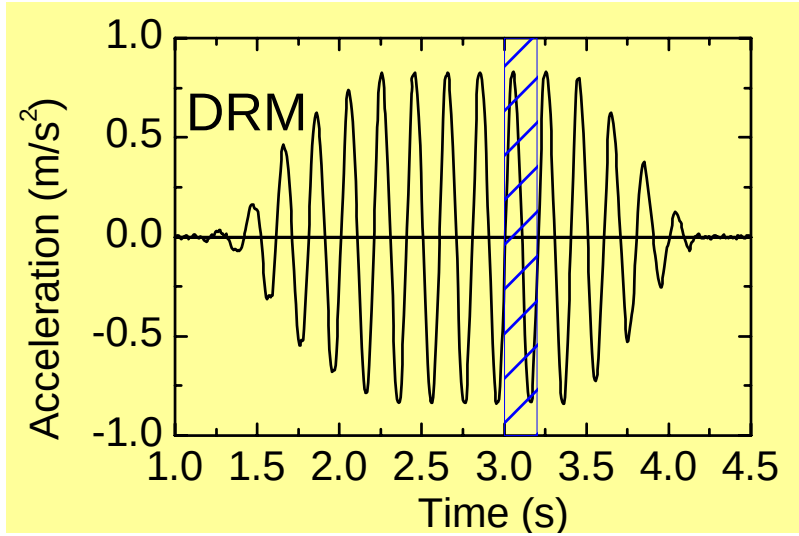

Input acceleration at the ground base (5 Hz)

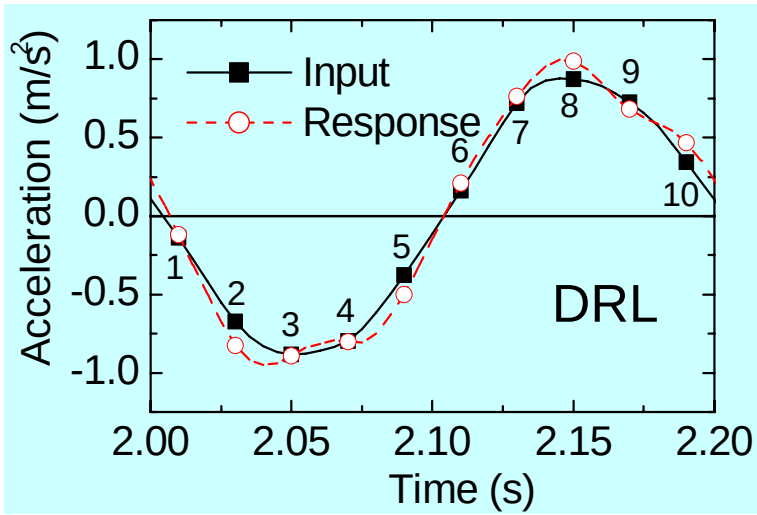

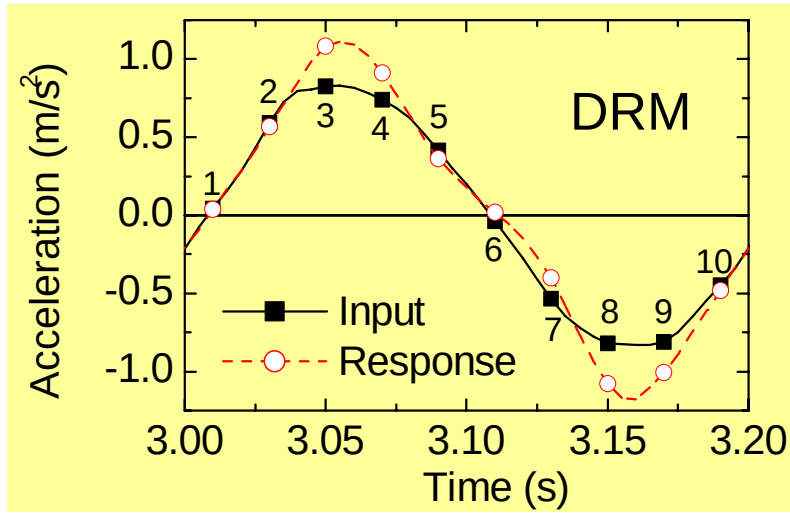

Response horizontal acceleration at the gravity centre (5 Hz)

DRL (5Hz)

DRM (5Hz)

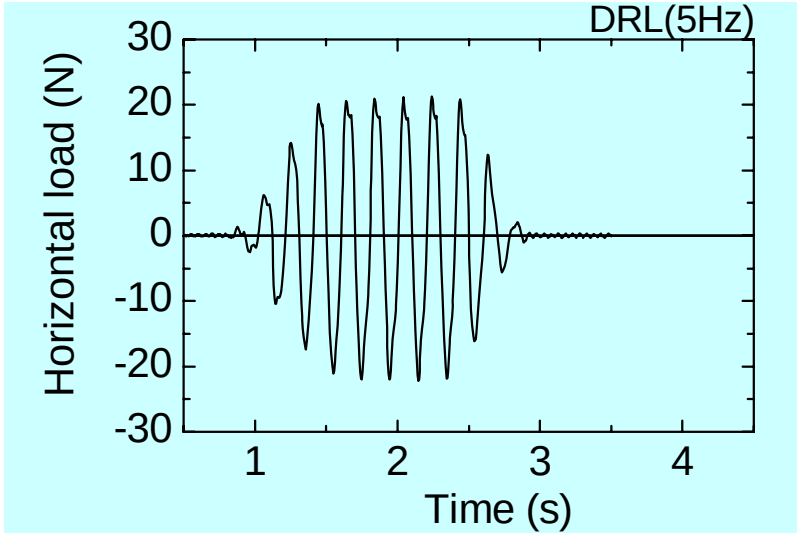

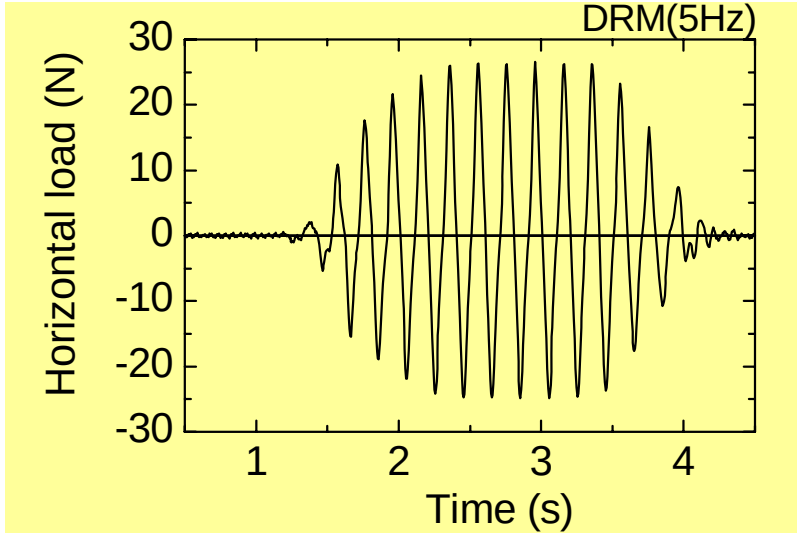

Horizontal loads acting on superstructure

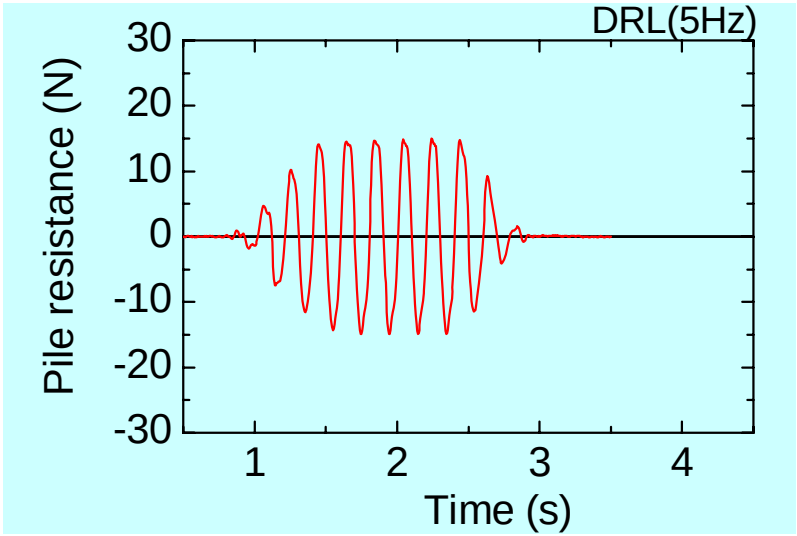

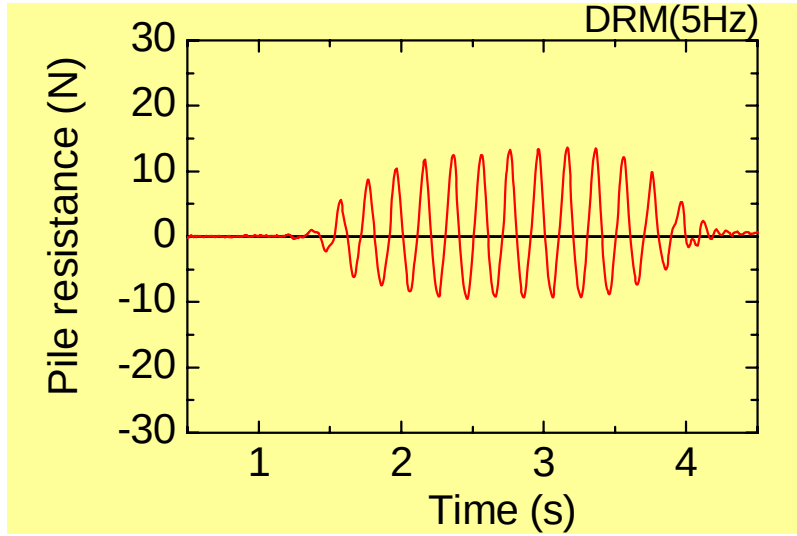

Pile resistance

DRL (5Hz)

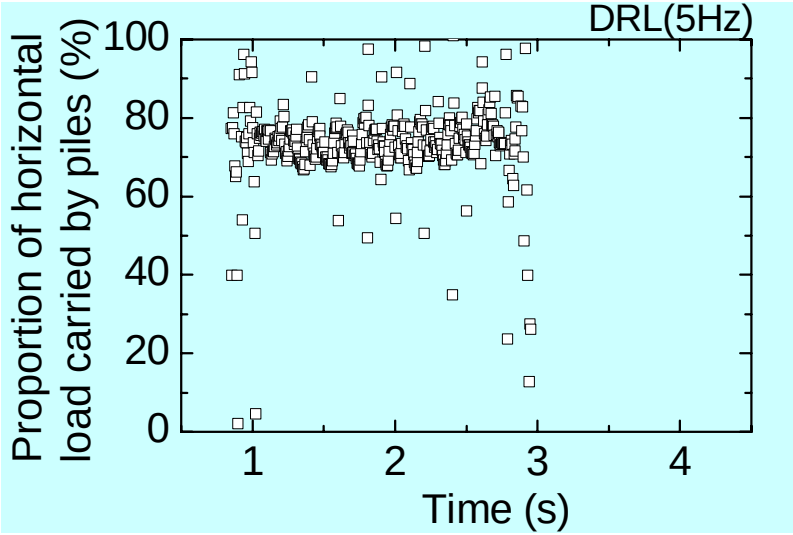

DRM (5Hz)

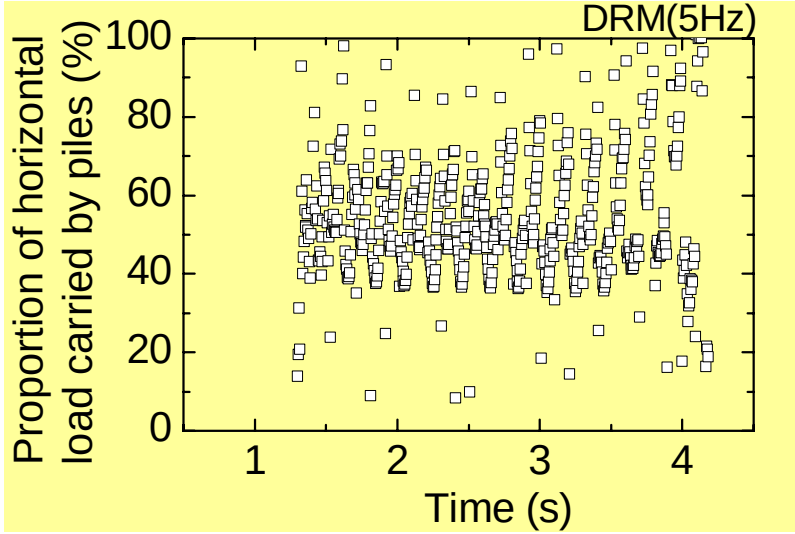

Proportions of horizontal load carried by piles

The proportion carried by the piles concentrated in a range from 70 to 80 % in DRL and 40 to 70 % in DRM.

Obviously the horizontal load proportion decreased with the increase in height of centre of gravity.

DRL (5Hz)

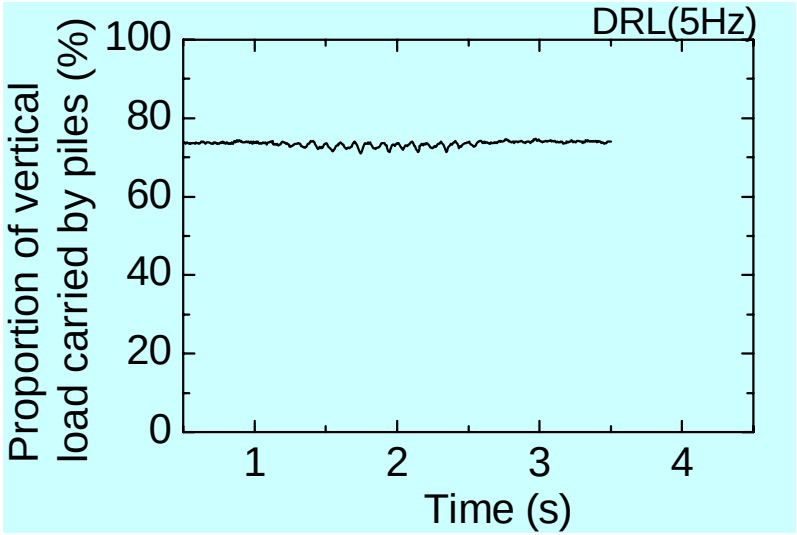

DRM (5Hz)

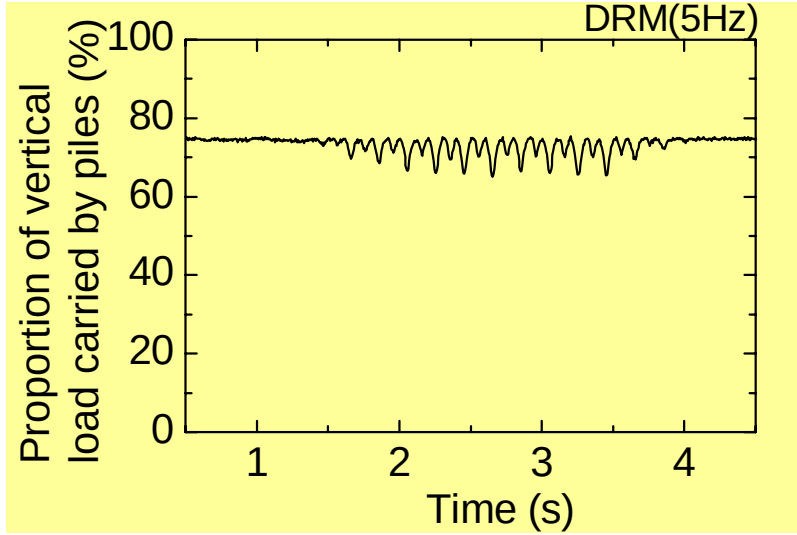

Proportions of vertical load carried by piles

Although the vertical load proportion carried by the piles fluctuated, it almost returned to the initial value in all the tests.

DRL (5 Hz) & SRL

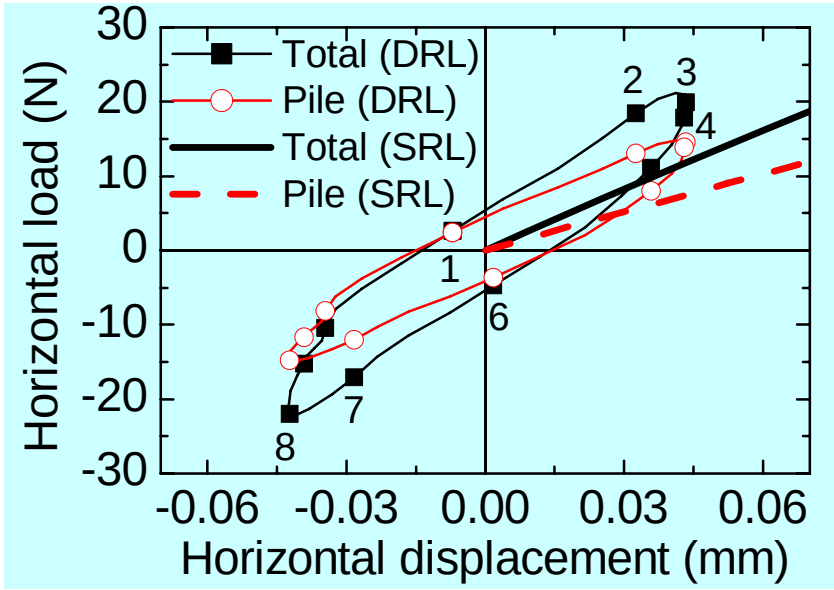

DRM (5 Hz) & SRM

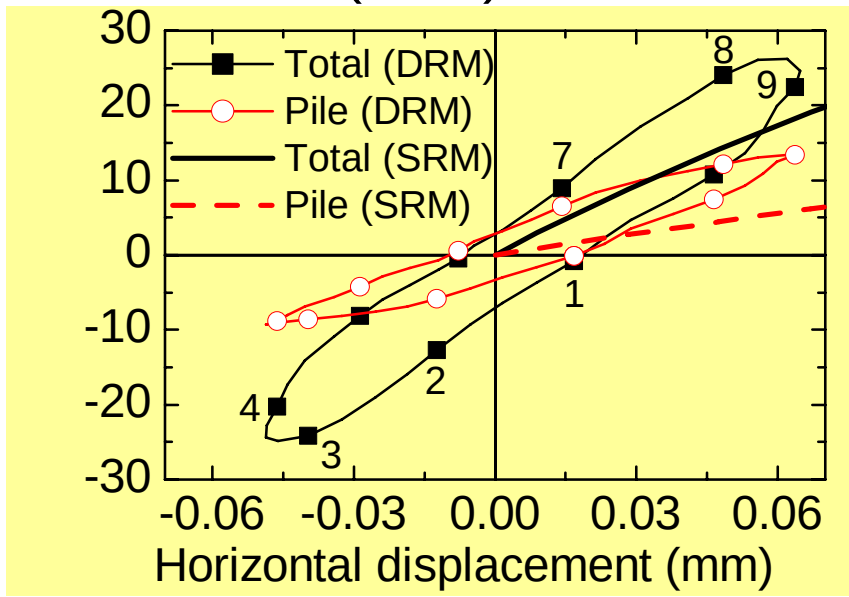

Horizontal load versus horizontal displacement of raft

The raft base resistance was effectively mobilised during both dynamic and static loading tests.

Contribution of the raft base resistance increased as the height of gravity of the superstructure increased.

DRL (5 Hz) & SRL

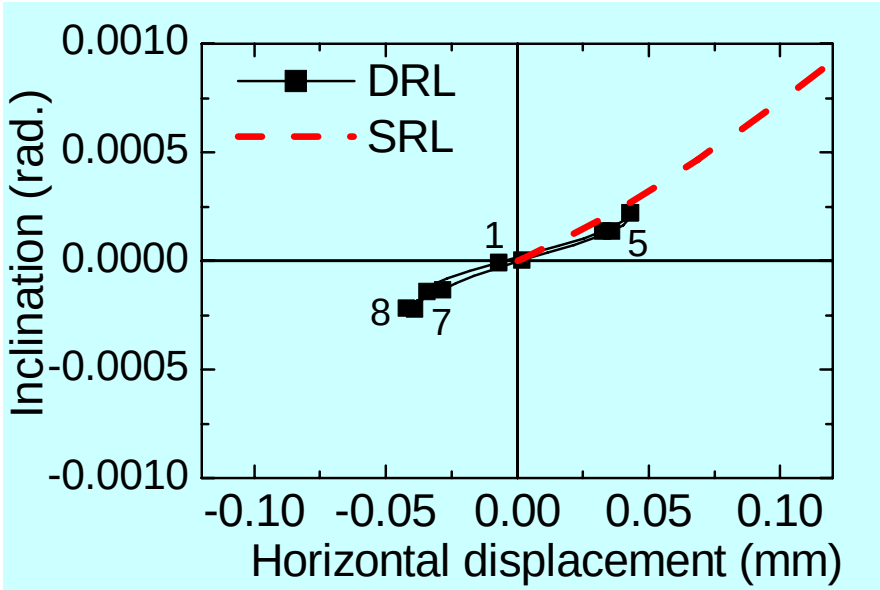

DRM (5 Hz) & SRM

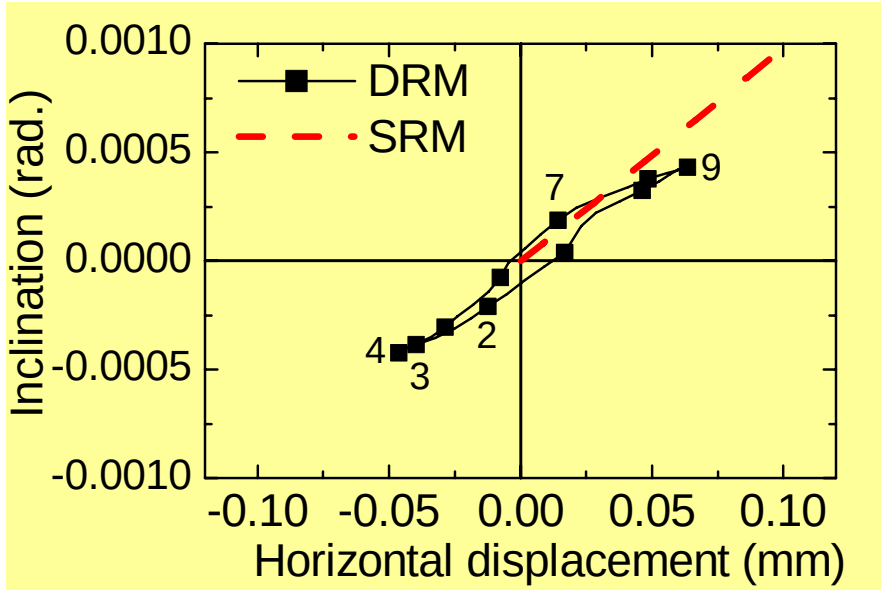

Horizontal displacement vs inclination

The relationship from the static load test was reasonably similar to that in the shaking table test.

The inclination of the raft at a given horizontal displacement tended to increase with increase in the height of centre of gravity.

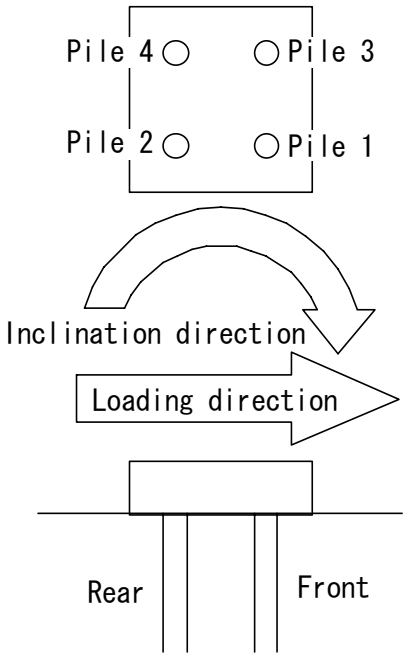

DRL (5Hz)

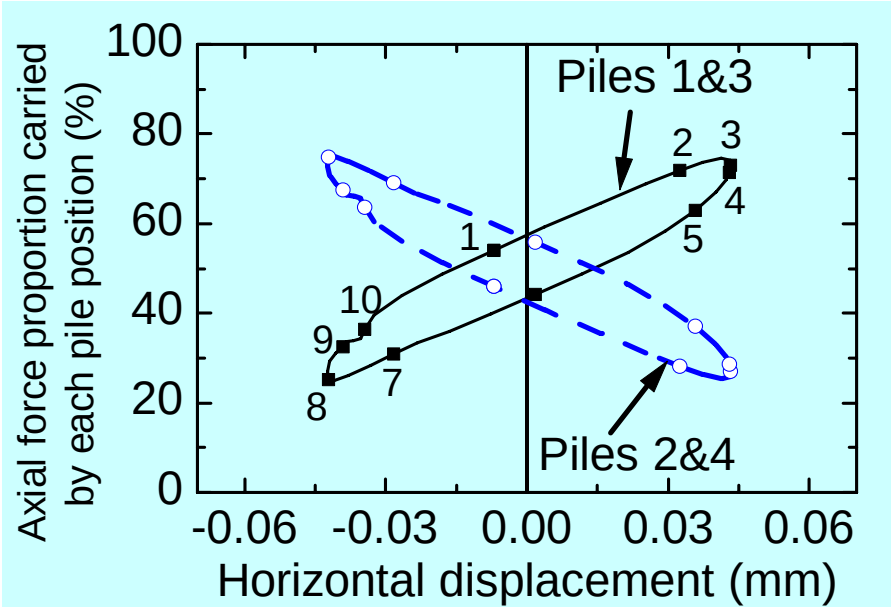

DRM (5Hz)

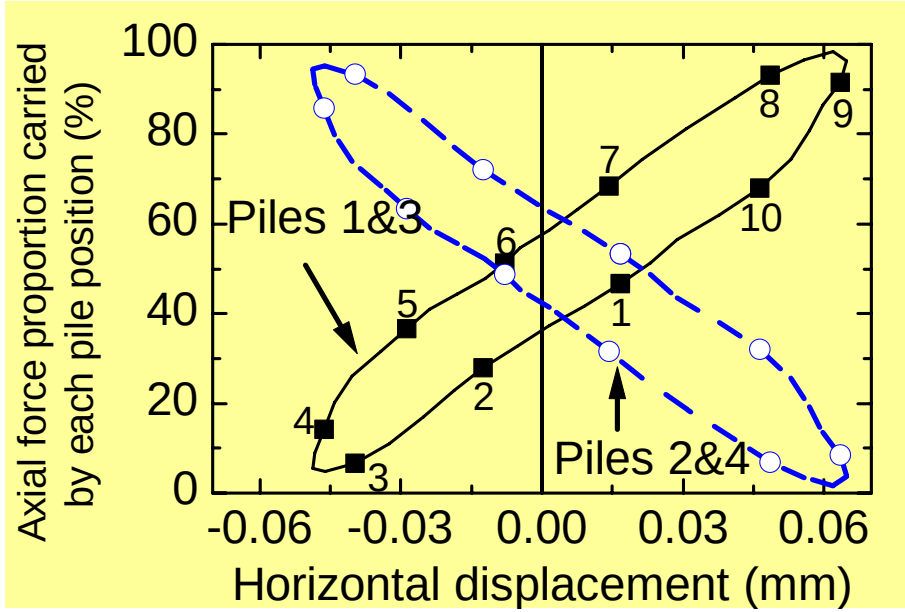

Proportion of vertical load carried by each pile during shaking test

A large part of the vertical load is carried by piles when the piles are the front piles at that moment.

This phenomenon is prominent in the middle gravity centre model.

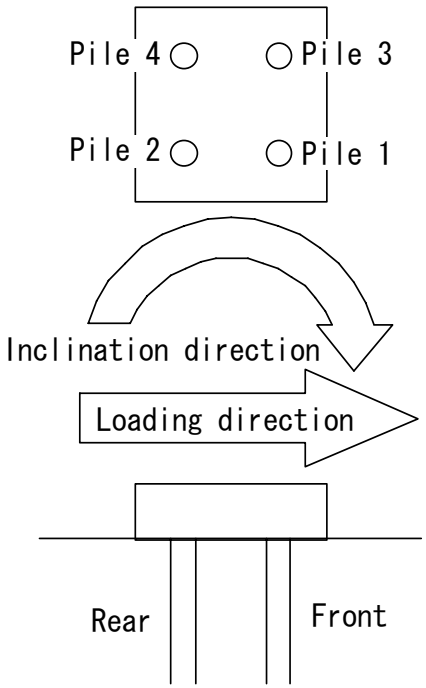

DRL (5Hz)

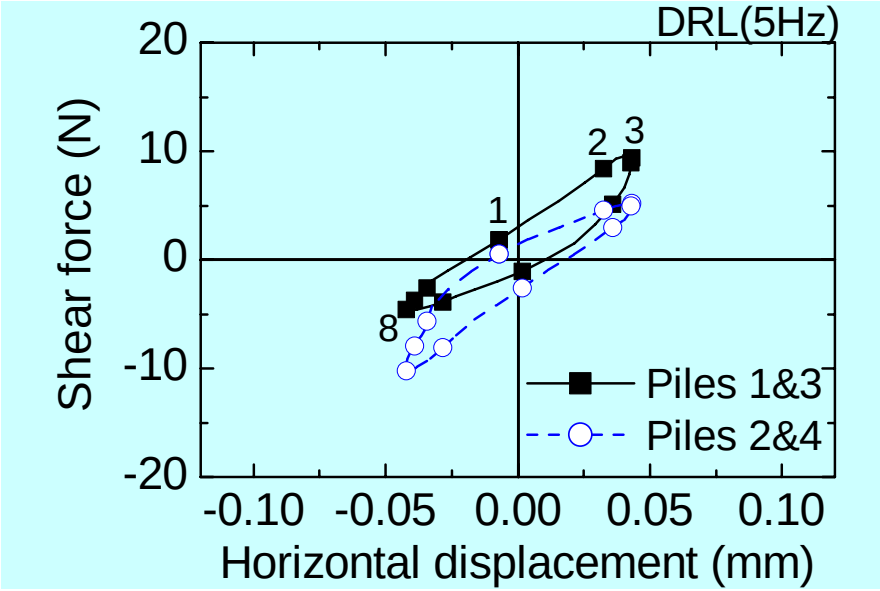

DRM (5Hz)

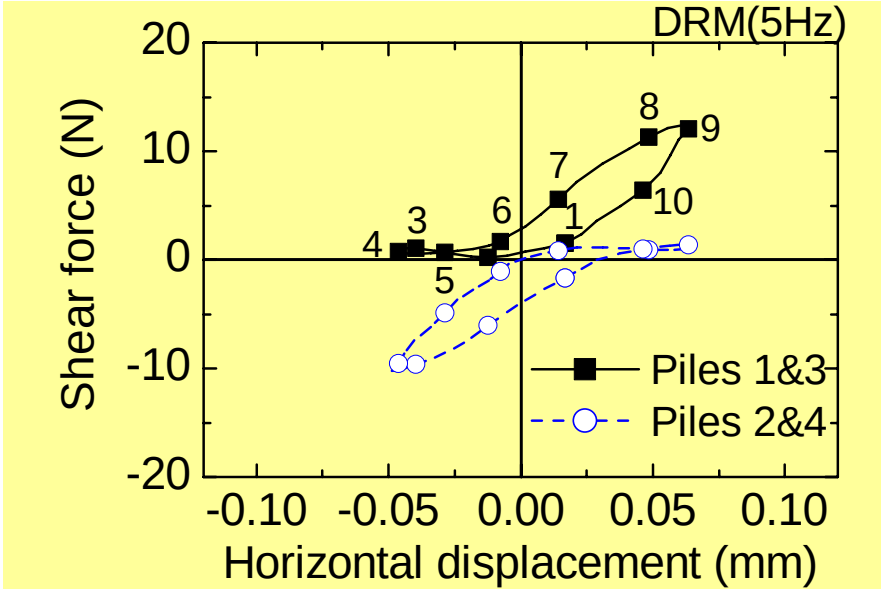

Shear forces carried by each pile head

A large part of the shear forces is carried by piles when the piles are the front piles at that moment.

This phenomenon is prominent in the middle gravity centre model.

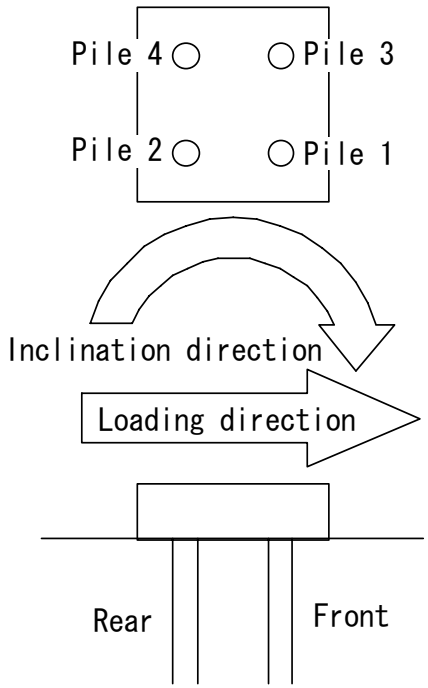

DRL (5 Hz) & SRL

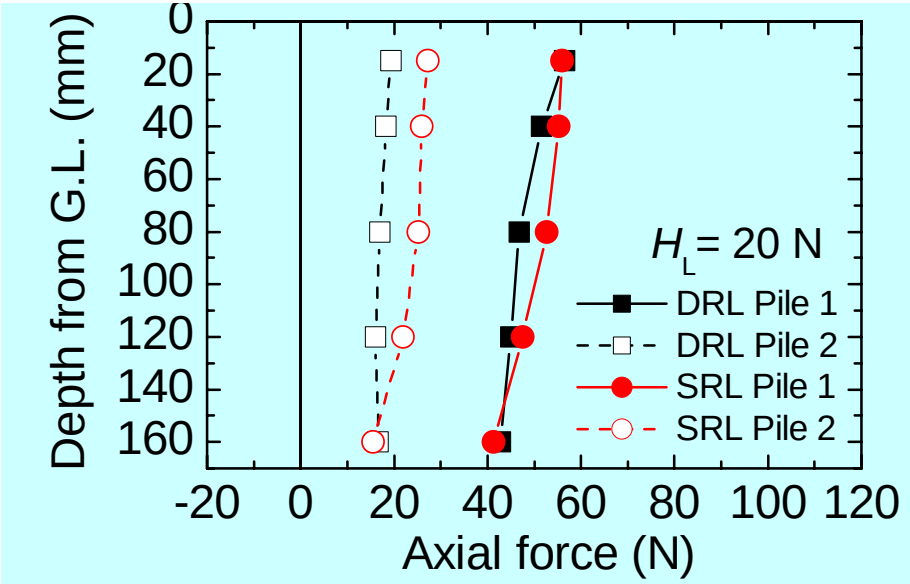

DRM (5 Hz) & SRM

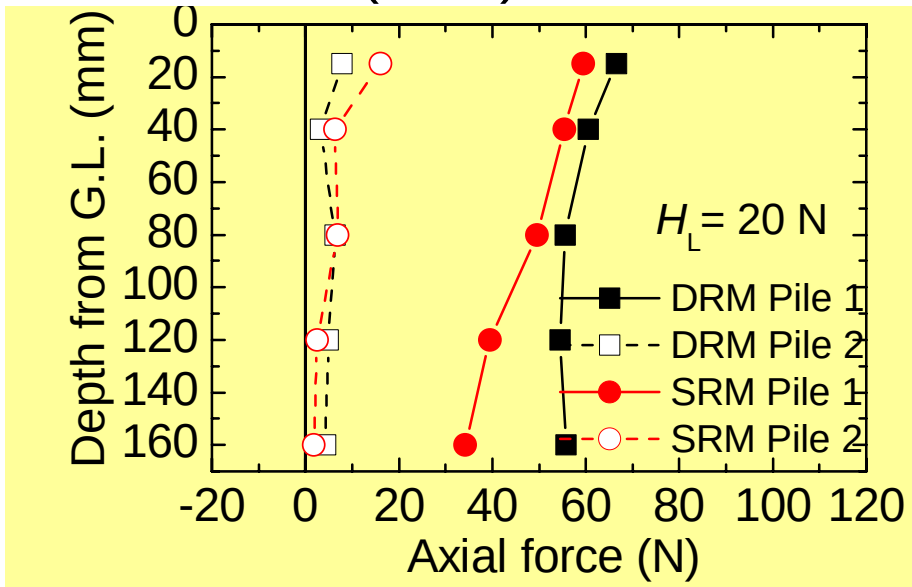

Axial forces in each pile

The results from the shaking table tests were comparable with those from the static horizontal load tests.

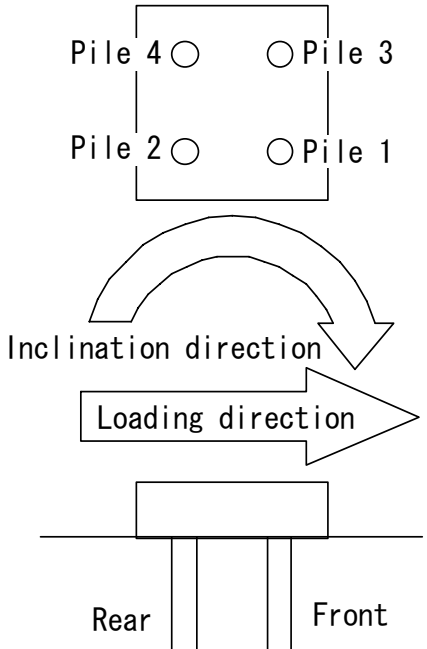

DRL (5 Hz) & SRL

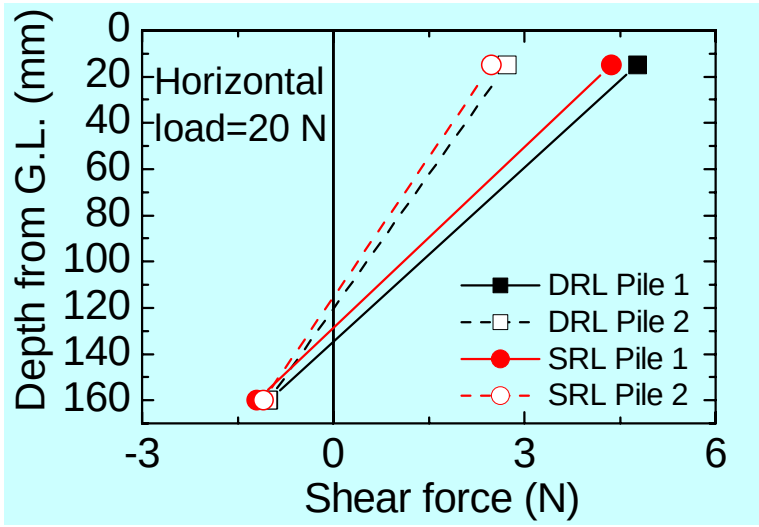

DRM (5 Hz) & SRM

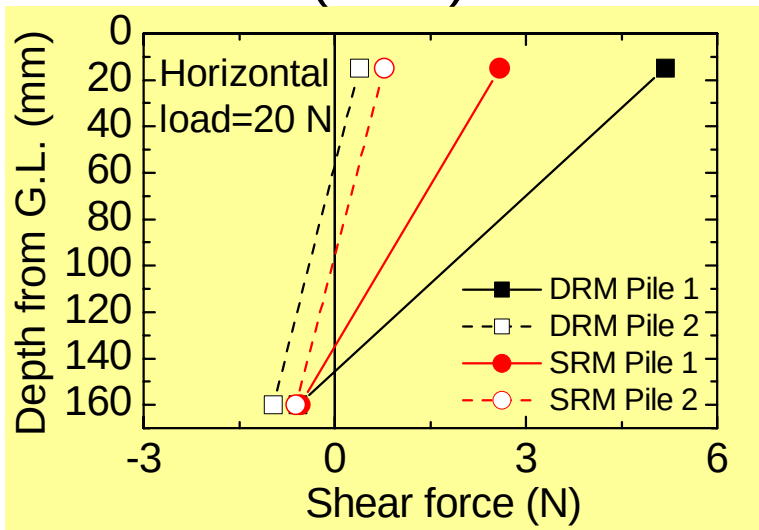

Distribution of shear forces in piles

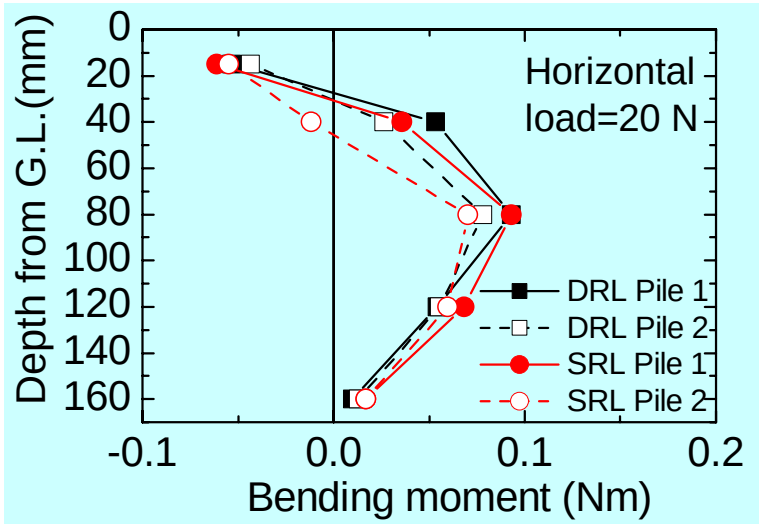

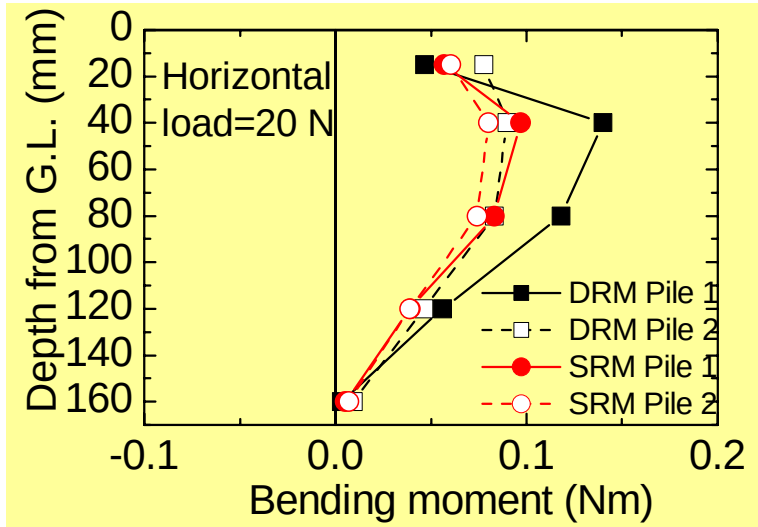

Distribution of bending moments in piles

Conclusions from shaking tests of piled raft models with rigid superstructures having different heights of gravity centre

- The resonant frequency is decreased as the height of the gravity centre of the superstructure is increased.
- At a low input frequency, the behaviour of the model piled raft having a superstructure of low gravity centre under seismic loading is similar to the behaviour of the model piled raft subjected to static horizontal loading.
- Even if the horizontal response accelerations of the gravity centres of the superstructures are the same, the inclination of the raft, the shear forces and the bending moments of the piles increase as the height of the gravity centre of the superstructure increases.
- Consideration of the height of the gravity centre of a superstructure in seismic design of piled raft foundation is important.

Influence of flexibility of superstructure on the behaviour of piled rafts in dry sand during shaking table test

Contents

A series of shaking tests of model piled rafts with flexible superstructures on them were carried out, in order to investigate the influence of the flexibility of superstructure on the whole structure consisted of the superstructure and the substructure.

Shaking table test of piled raft with flexible superstructure

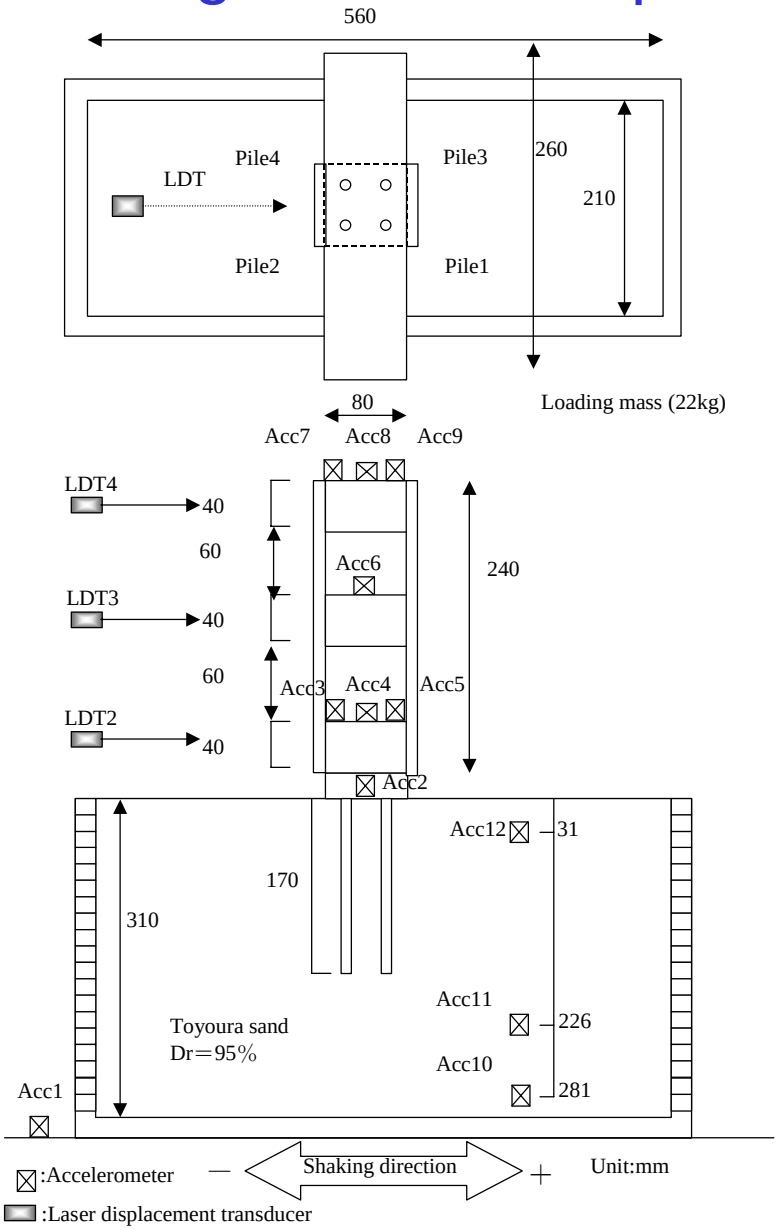

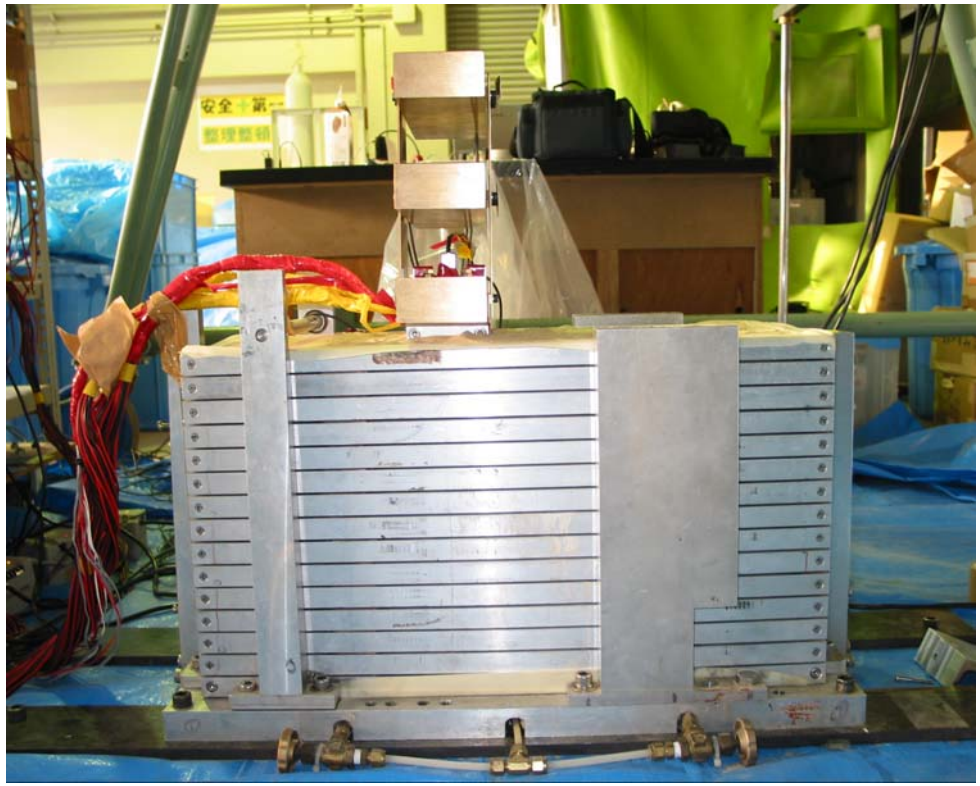

Model ground: dry Toyoura sand,

$D_r = 90\ \%$

Piled raft model

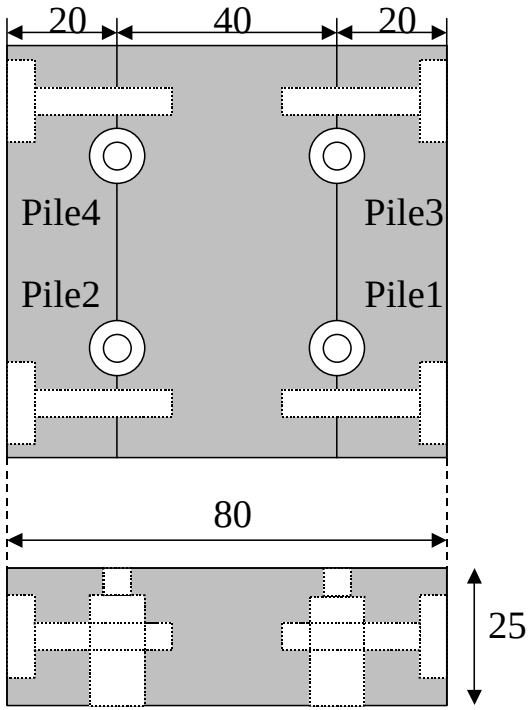

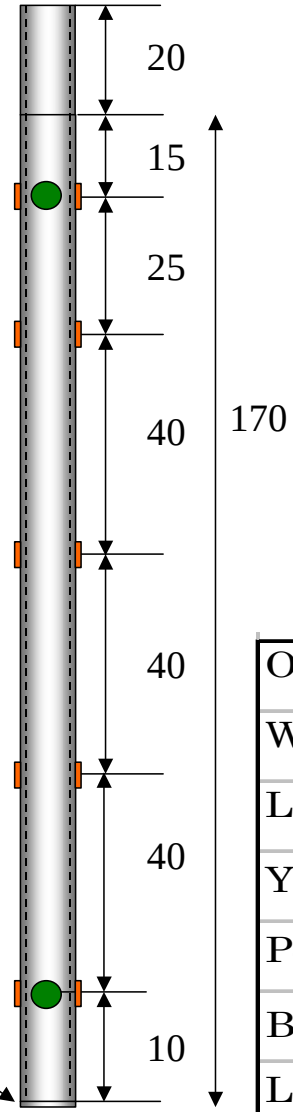

Axial strain

Shear strain

Aluminum pile
OD: 10mm
ID: 8mm

Outer diameter (mm)	10
Wall thickness (mm)	1
Length (mm)	170
Young's modulus, E_p (GPa)	67.1
Poisson's ratio, ν_p	0.345
Bending rigidity, E_pI (Nm^2)	19.4
Longitudinal rigidity, E_pA (N)	1.9×10^6

Flexible superstructure model

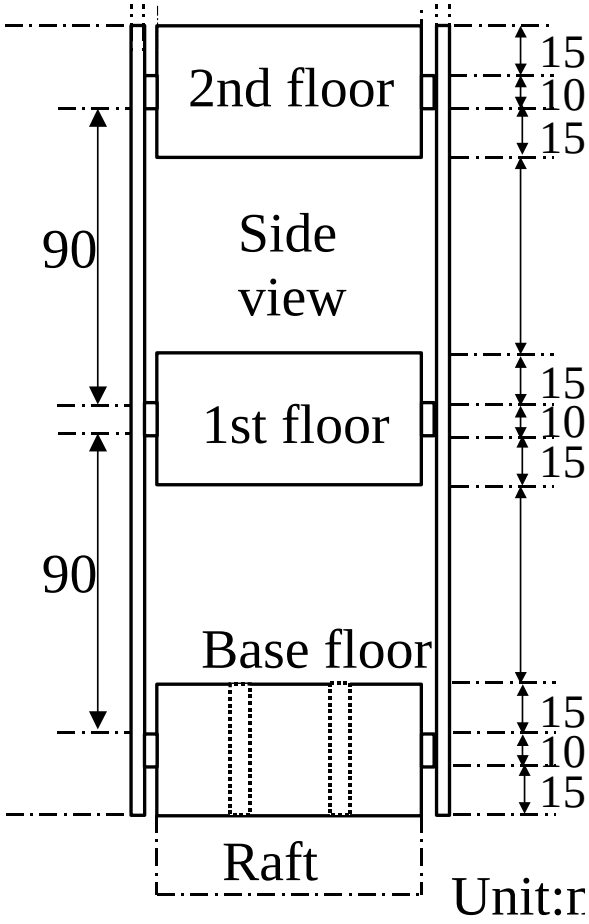

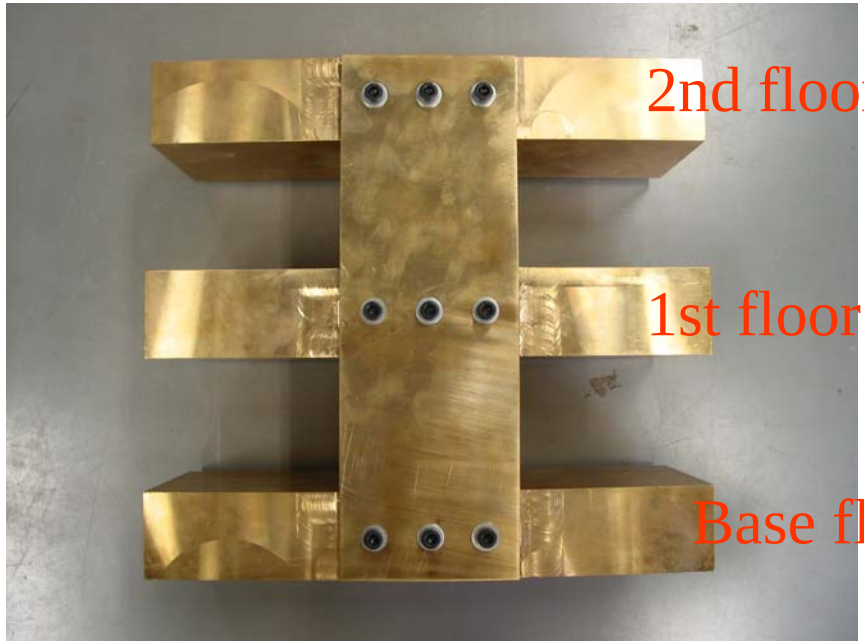

Wall thickness(mm)	1.0	2.0
Mass(kg)	21.2	21.6

Material: brass

Static horizontal load test of the superstructure alone

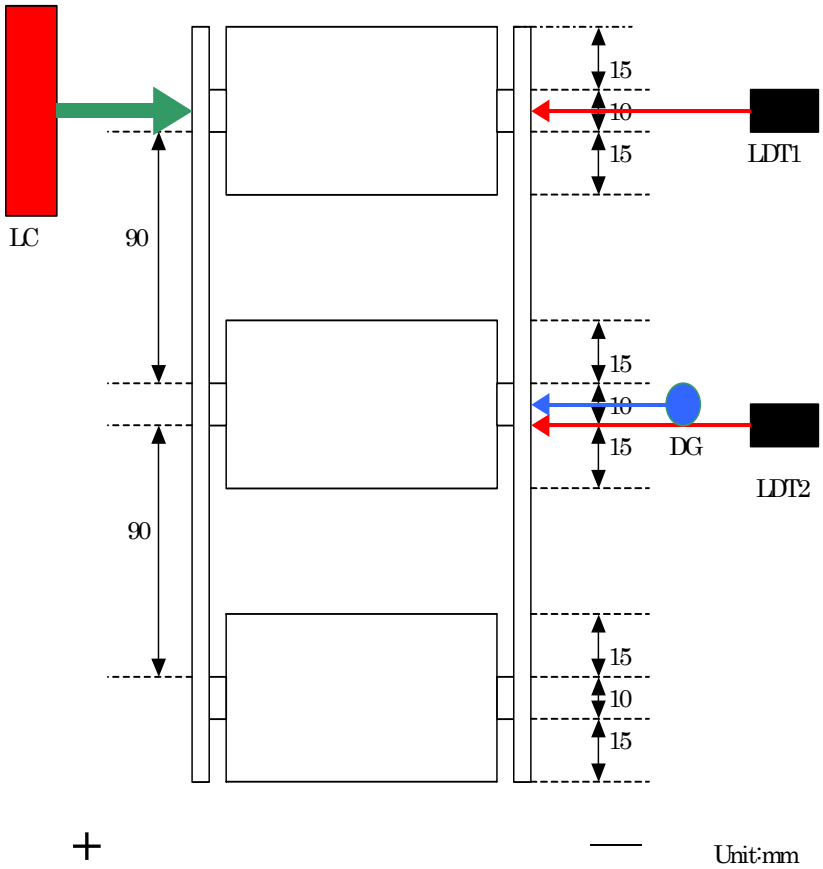

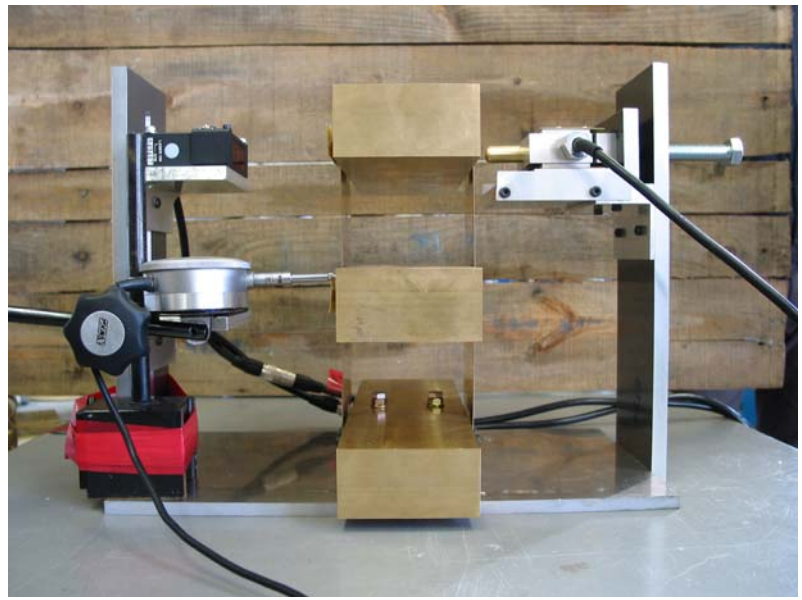

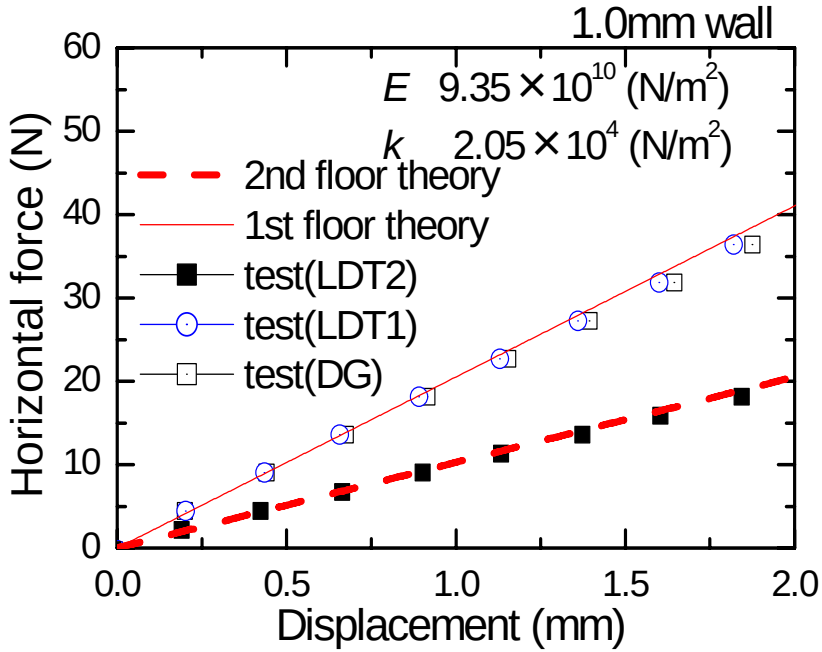

Shaking tests of the superstructure alone

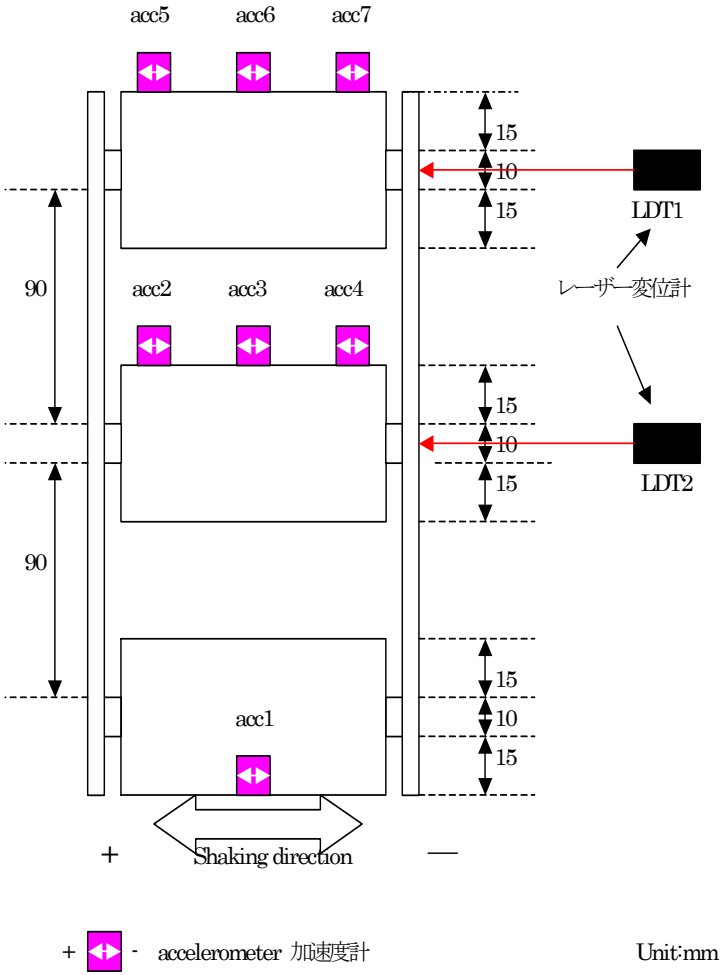

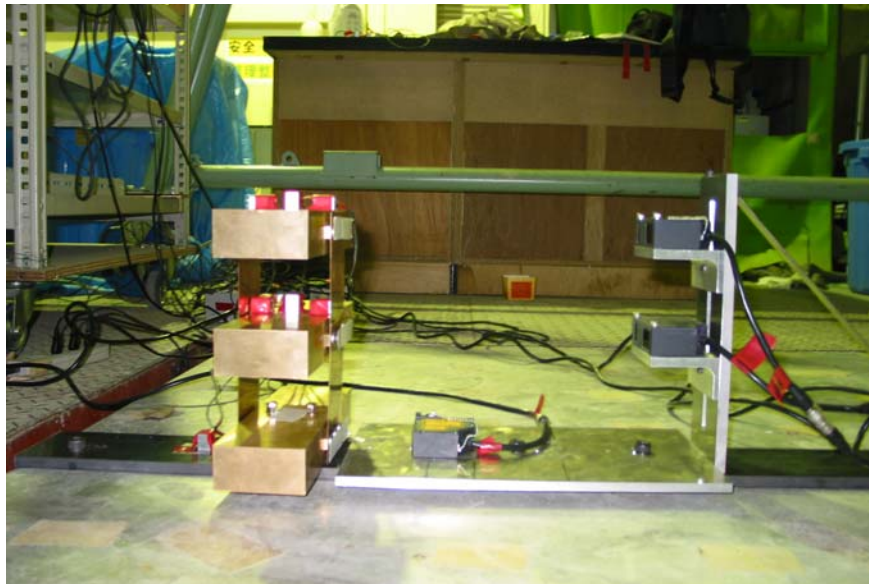

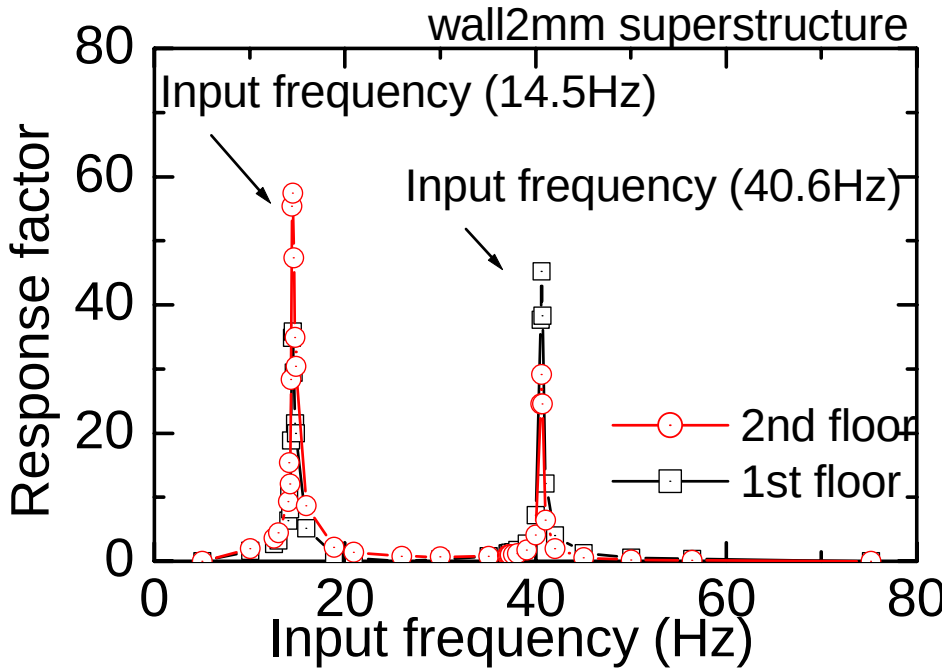

Properties of the model superstructures

	Thin wall model (W.T. = 1 mm)	Thick wall model (W.T. = 2 mm)
Wall thickness (mm)	1.0	2.0
Total mass (kg)	21.2	21.6
Horizontal stiffness of each layer (kN/m)	2.05×10	1.48×10^{2}
Young's modulus of wall material (kPa)	9.35×10^{7}	8.43×10^{7}
Primary resonant frequency (Hz)	5.3	14.2
Secondary resonant frequency (Hz)	13.9	40.6
Damping ratio	0.0032	0.0104

Test results

Frequency of input acceleration vs response factor

$$\text{Response factor} = \frac{\text{Peak of horizontal response acceleration}}{\text{Amplitude of input acceleration}}$$

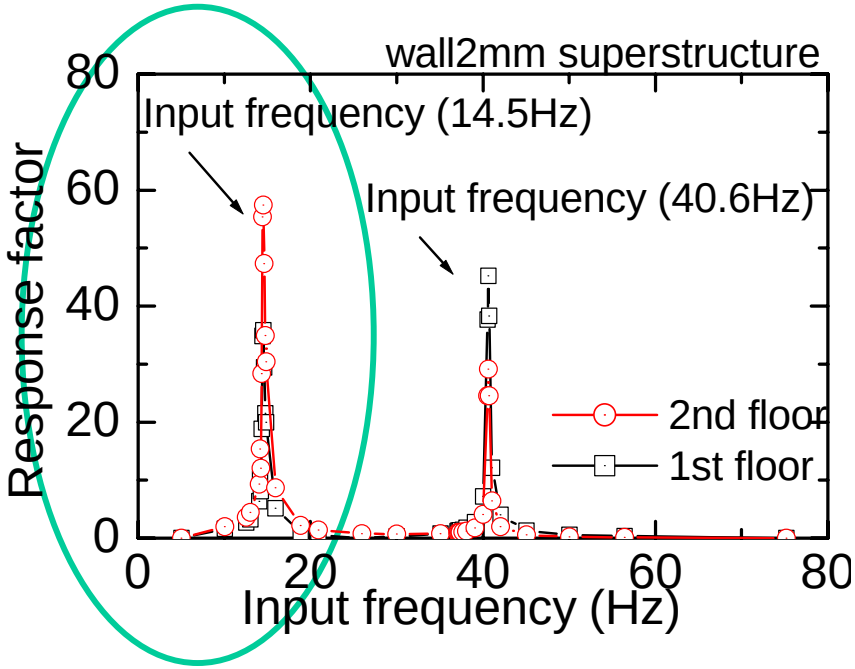

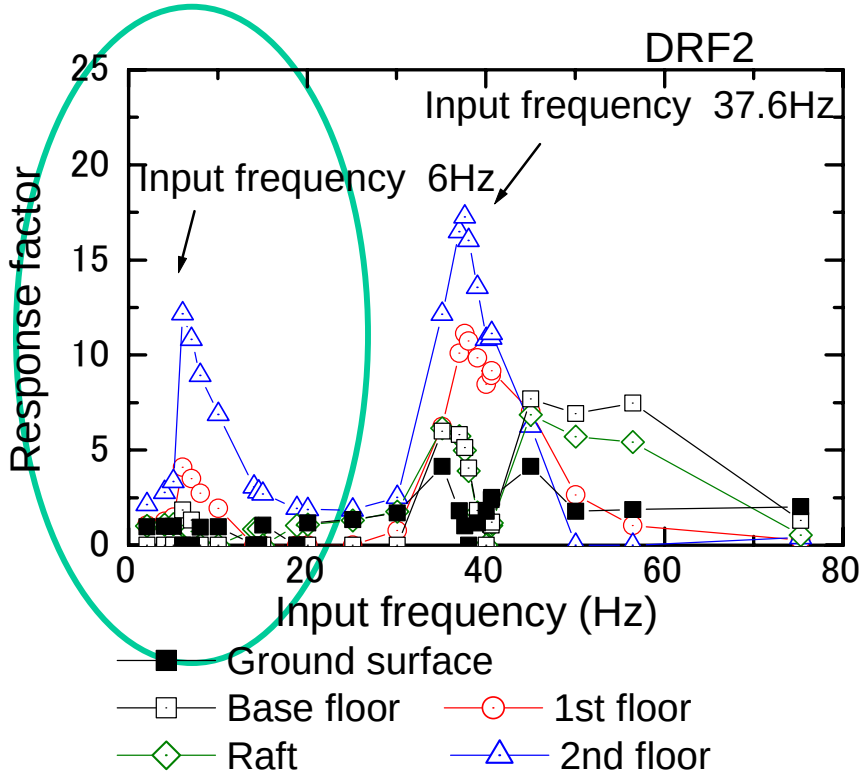

Primary natural frequency of the whole structure set in the ground was less than 4 Hz which was smaller than that of the superstructure alone.

Test results

Dynamic motions

at input frequency near the primary frequency of the superstructure

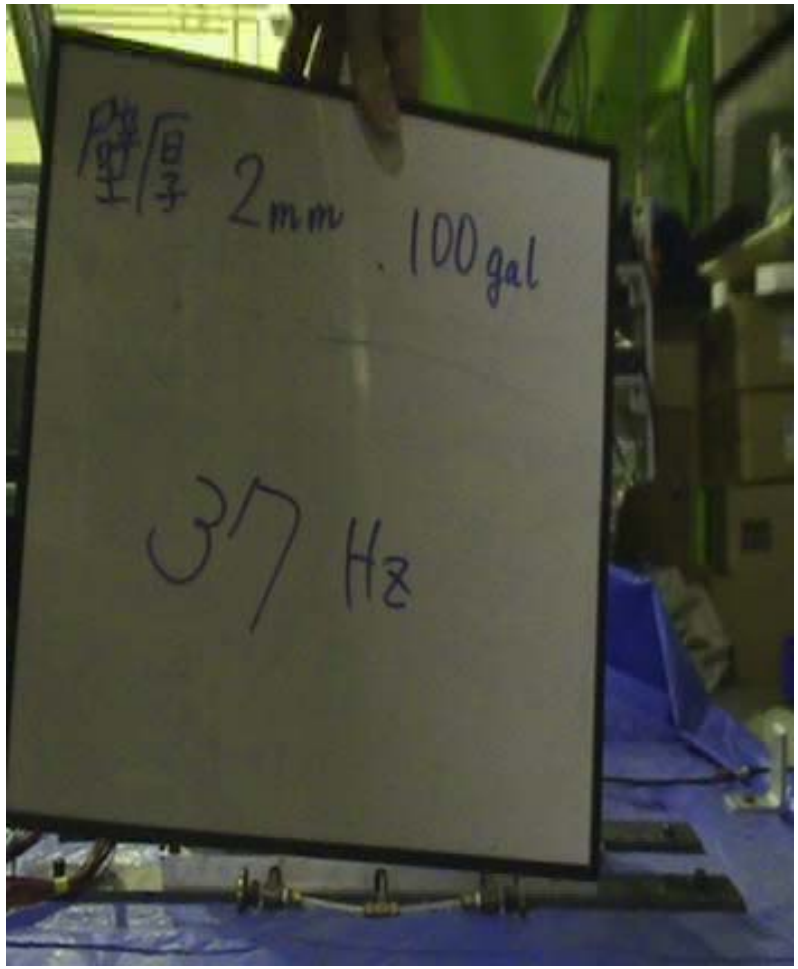

at input frequency near the secondary frequency of the superstructure

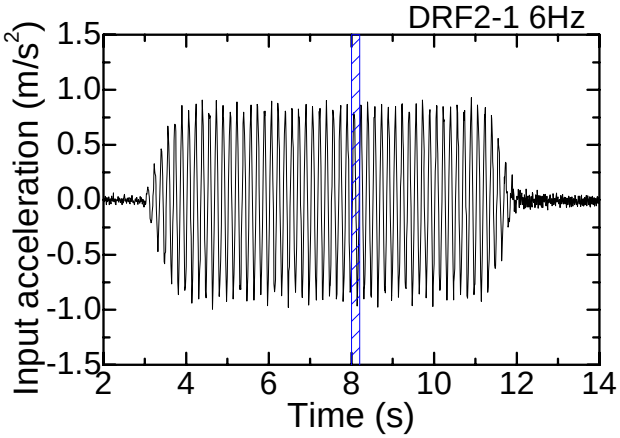

Input acceleration
(f = 6 Hz)

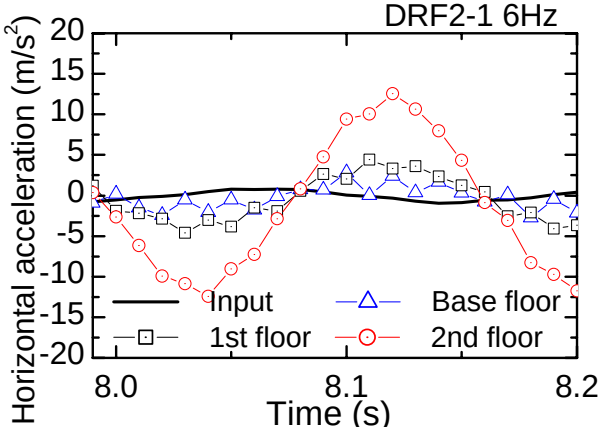

Horizontal accelerations
(f = 6 Hz)

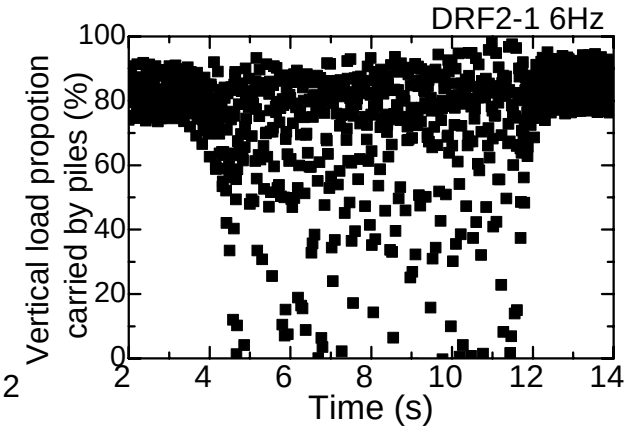

Proportion of vertical load carried by piles (f = 6 Hz)

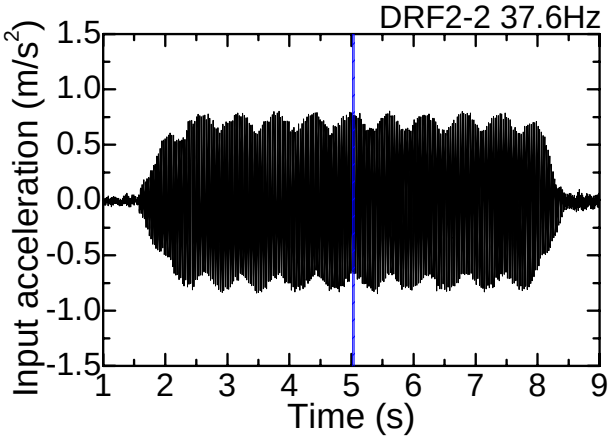

Input acceleration
(f = 37.6 Hz)

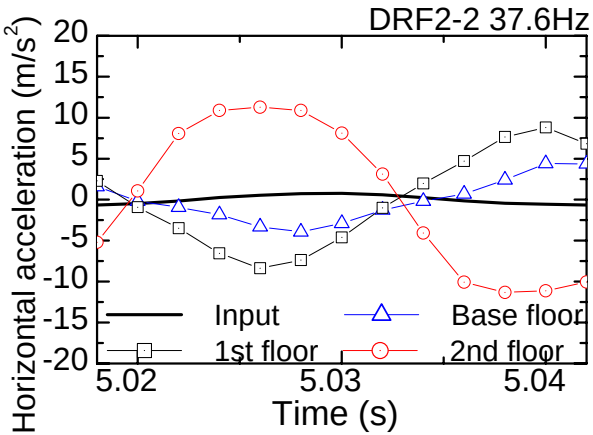

Horizontal accelerations
(f = 37.6 Hz)

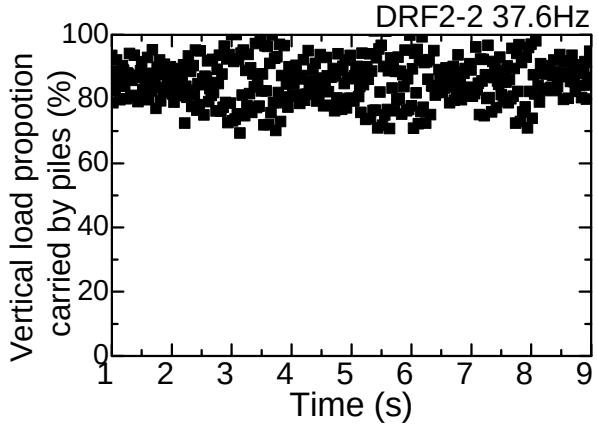

Proportion of vertical load carried by piles (f = 37.6 Hz)

At f = 6 Hz, there is no phase shift between each level of the superstructure (primary vibration mode occurs). In contrast at f = 37.6 Hz. phase shift occurs between each level of the superstructure (secondary vibration mode occurs).

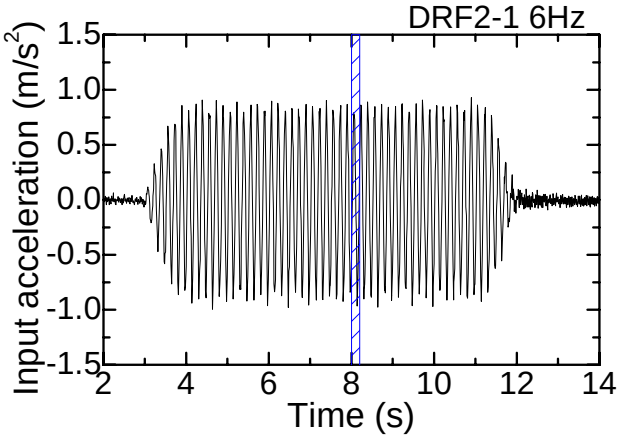

Input acceleration
(f = 6 Hz)

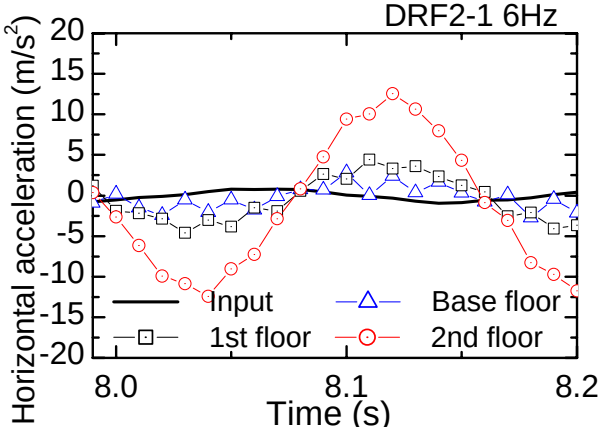

Horizontal accelerations
(f = 6 Hz)

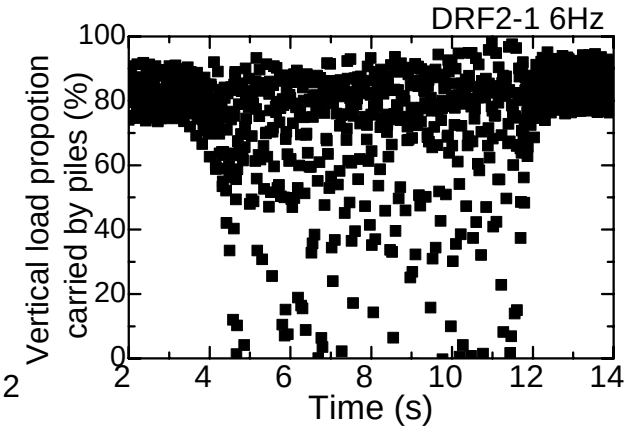

Proportion of vertical load carried by piles (f = 6 Hz)

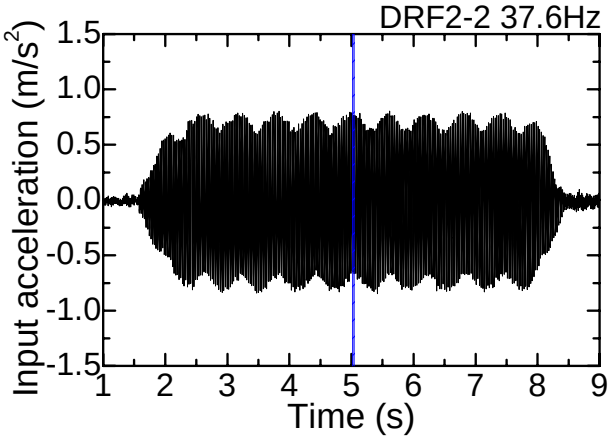

Input acceleration
(f = 37.6 Hz)

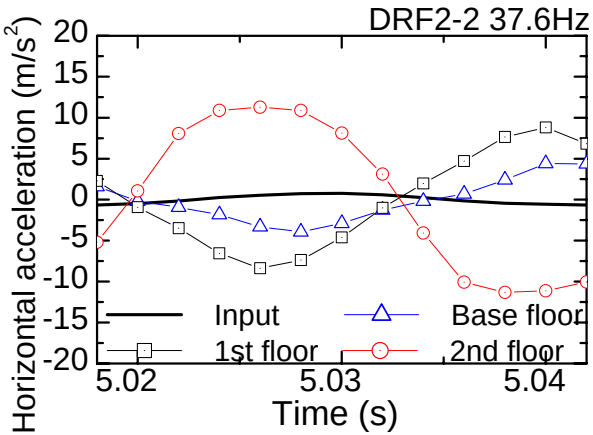

Horizontal accelerations
(f = 37.6 Hz)

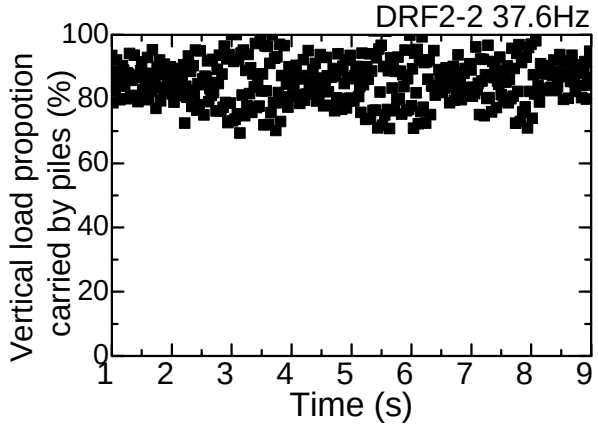

Proportion of vertical load carried by piles (f = 37.6 Hz)

Proportions of vertical load carried by the piles before and after shaking almost do no change, although the proportion oscillate largely for f = 6 Hz.

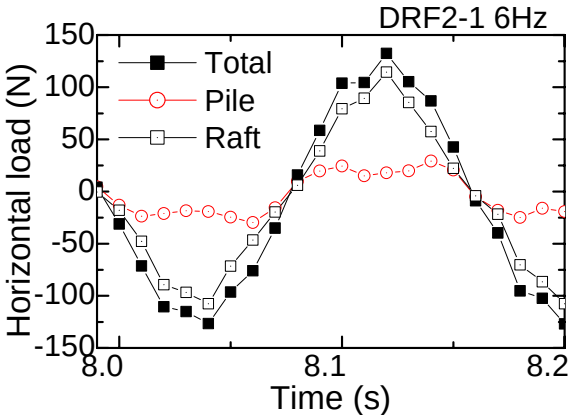

Horizontal loads
(f = 6 Hz)

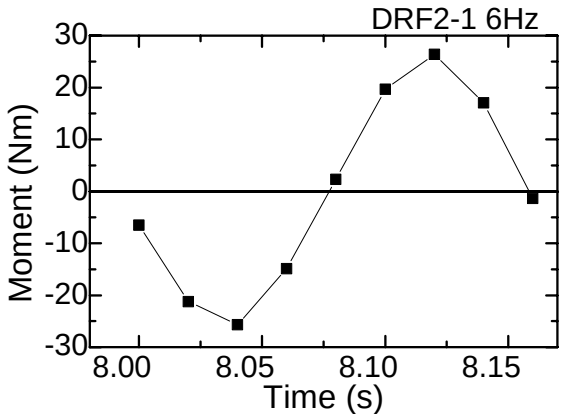

Overturning moment
(f = 6 Hz)

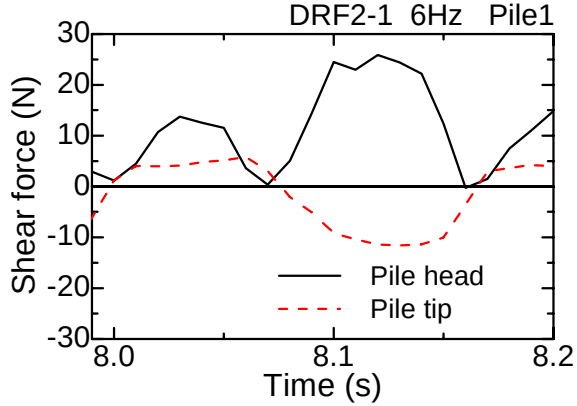

Shear forces at pile head and tip（f = 6 Hz)

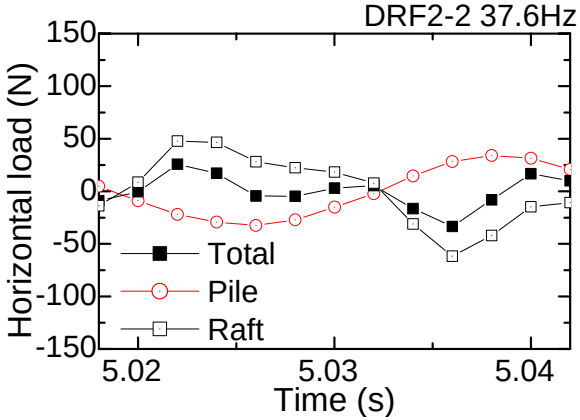

Horizontal loads
(f = 37.6 Hz)

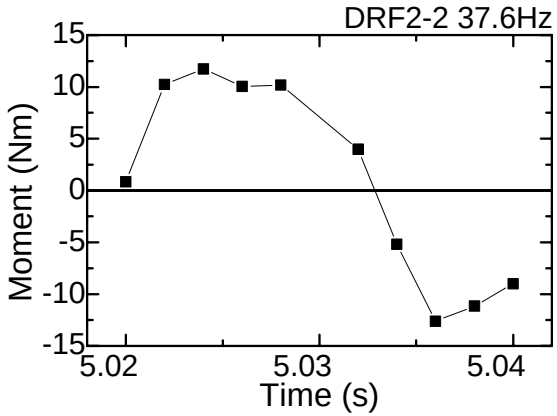

Overturning moment
(f = 6 Hz)

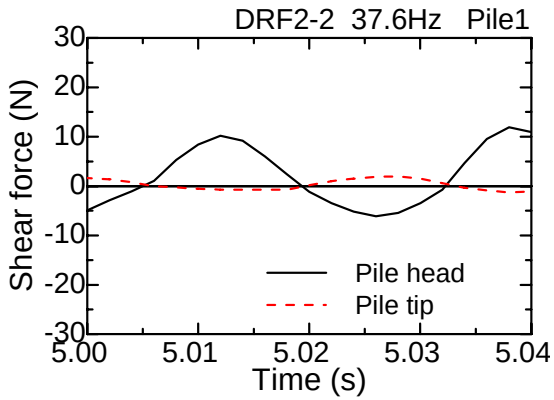

Shear forces at pile head and tip（f = 37.6 Hz)

Although the total load at f = 37.6 Hz reduces to 1/5 of that at f = 6 Hz, the overturning moment at f = 37.6 Hz is about half of that at f = 6 Hz.

Main findings

- Vibration mode of the superstructure has a great influence on behaviour of the foundation structure.
  - Responses of the superstructure such as horizontal accelerations and rocking motions become largest when input acceleration frequency is close to the primary resonant frequency of the superstructure.
  - Total horizontal load acting on the superstructure becomes small, even though relatively large horizontal accelerations are generated on each floor, due to secondary vibration mode of the superstructure.
- Within the test conditions, piled raft foundation is effective foundation system against earthquakes, because the shear resistance at the raft base is effectively mobilised during shaking.

Approximate analyses of the shaking test

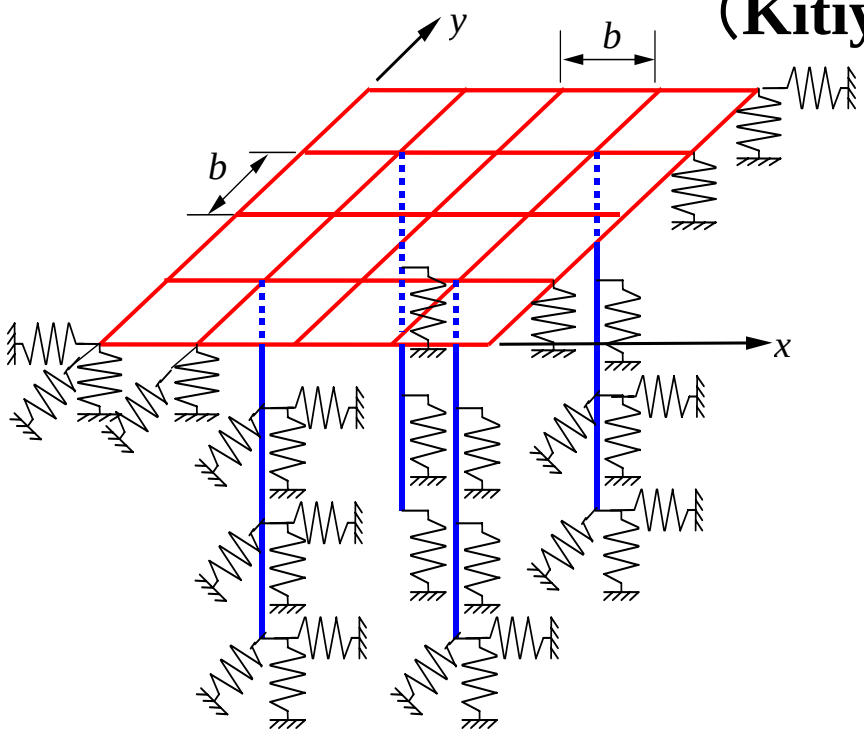

（Kitiyodom & Matsumoto; 2002, 2003）

$$K_z^{\mathrm{R}} = \frac{4Ga}{1-\nu_{\mathrm{s}}}$$

$$K_x^{\mathrm{R}} = K_y^{\mathrm{R}} = \frac{32(1-\nu_{\mathrm{s}})Ga}{7-8\nu_{\mathrm{s}}}$$

$$K_z^{\mathrm{P}} = 2\pi G\Delta L / \ln(r_{\mathrm{m}} / r_{\mathrm{o}})$$

$$K_x^{\mathrm{P}} = K_y^{\mathrm{P}} = \zeta E_{\mathrm{s}}\Delta L$$

Analytical conditions (Foundation structure)

Model was scaled up to prototype model with $\lambda = 50$ in the analysis.

Similitude for 1-g test（Iai, 1989）

Length	λ	Disp.	$\lambda^{3/2}$
Density	1	Velocity	$\lambda^{3/4}$
Stress	λ	Accel.	1
Strain	$\lambda^{1/2}$	Bending rigidity	$\lambda^{7/2}$
Time	$\lambda^{3/4}$	Longitudinal rigidity	$\lambda^{3/2}$
Frequency	$1/\lambda^{3/4}$		

All the results from now will be shown in prototype scale.

Analytical conditions (Foundation structure)

Model was scaled up to prototype model with $\lambda = 50$ in the analysis.

Pile	Length	8.5 m	Outer diameter	0.5 m
	Young's modulus	279.8 GN/m^2 (as solid pile compatible with E_pI)		
Raft	Width	4 m	Poisson's ratio	0.16
	Breadth	4 m	Young's modulus	70.6 GN/m^2
	Thickness	1 m (substantially rigid)		
Soil	Thickness	15 m	Poisson's ratio	0.3
	Friction angle	45 deg.	Density	1.63 t/m^3
	Multi-layer ground			

Analytical conditions (Ground)

Ground: 20 layer ground with the shear modulus, *G*, increasing with depth

The shear modulus, *G*, is estimated from

$$G = 29.2\left(p / 0.1 \right)^{0.5} \quad \text{(MPa)} \qquad p\text{: confining pressure}$$

based on the results of tri-axial test of the sand.

Analytical conditions (External loads)

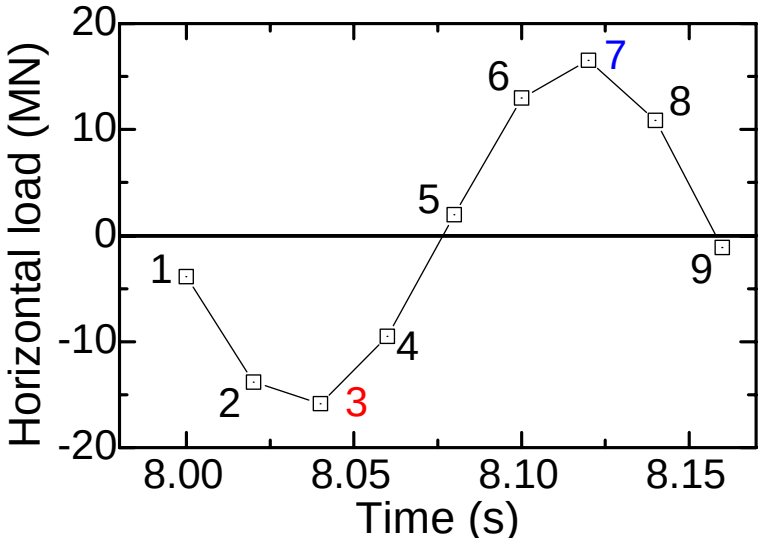

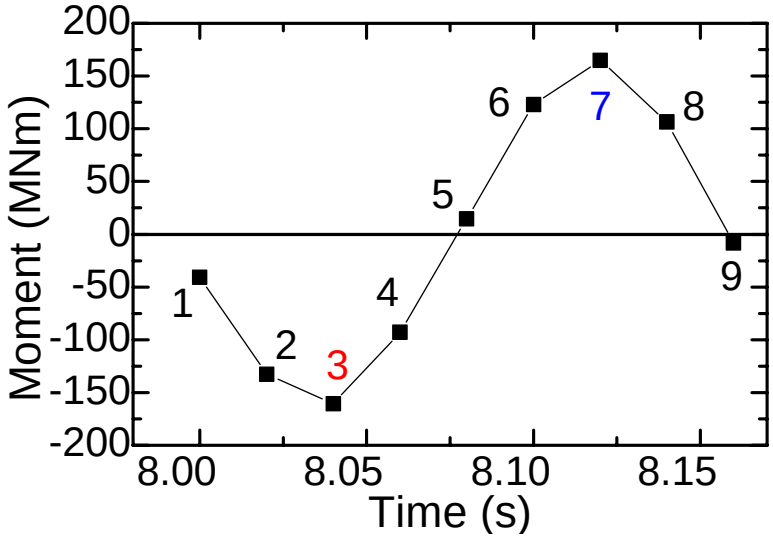

Horizontal load

Overturning moment

f = 6 Hz (primary vibration mode occurred)

Static analysis with external loads at time instants 3 and 7 acting on the raft simultaneously.

Analytical conditions (External loads)

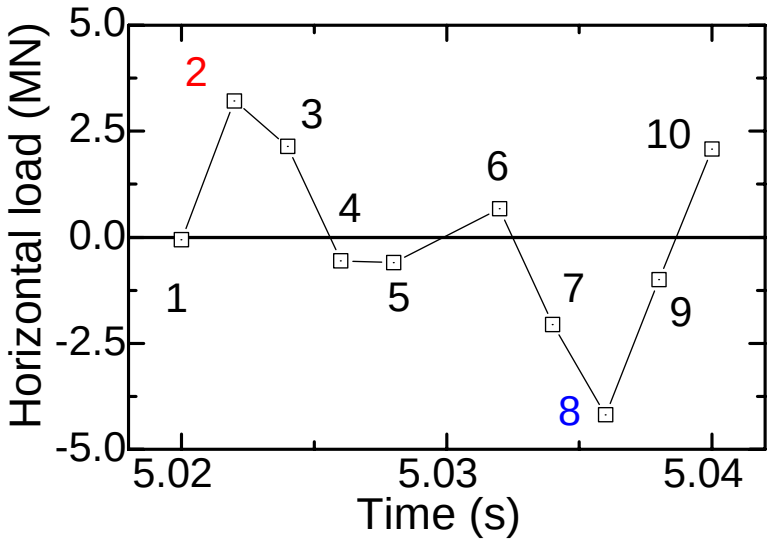

Horizontal load

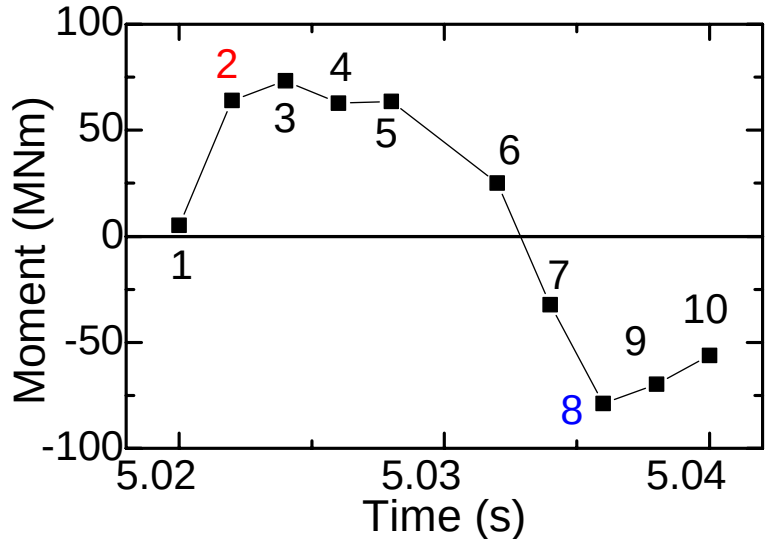

Overturning moment

f = 37.6 Hz (secondary vibration mode occurred)

Static analysis with external loads at time instants 2 and 8 acting on the raft simultaneously.

Analysis results

f = 6 Hz (primary vibration mode)

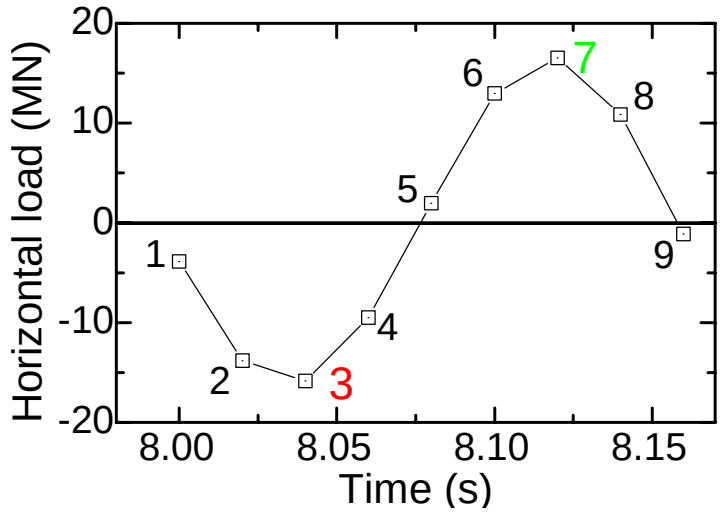

At time instant 7,
pile 1: leading (front pile)
pile 2: following (rear) pile

At time instant 3,
pile 1: following (rear) pile
pile 2: leading (front pile)

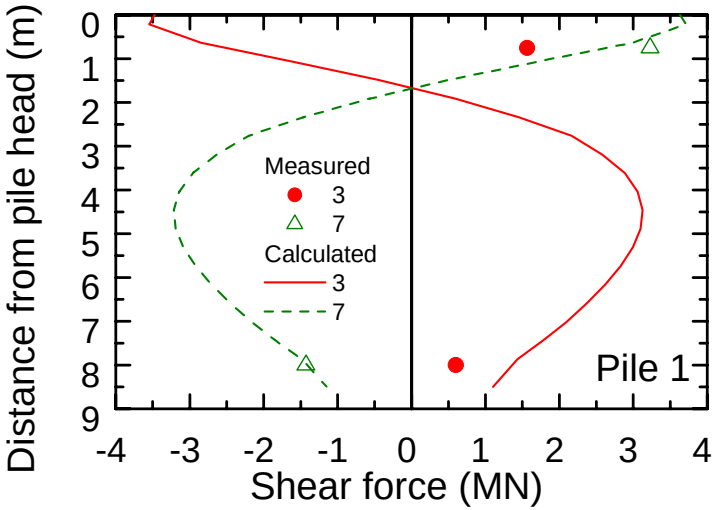

Shear force in pile 1

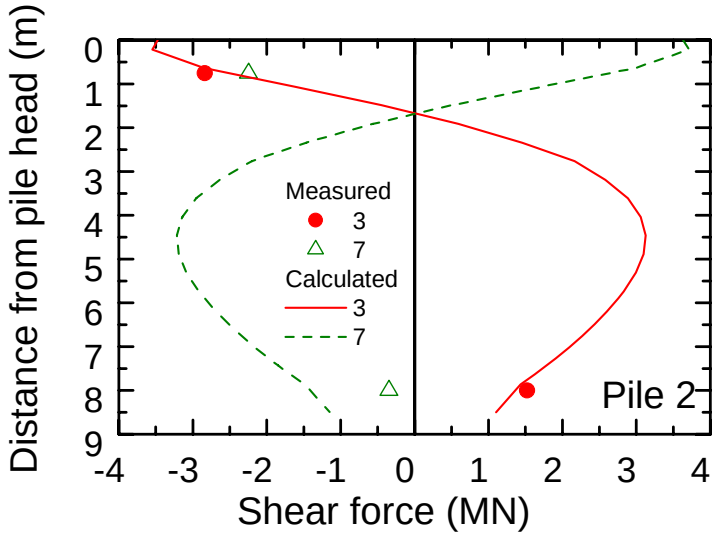

Shear force in pile 2

Analysis results

f = 6 Hz (primary vibration mode)

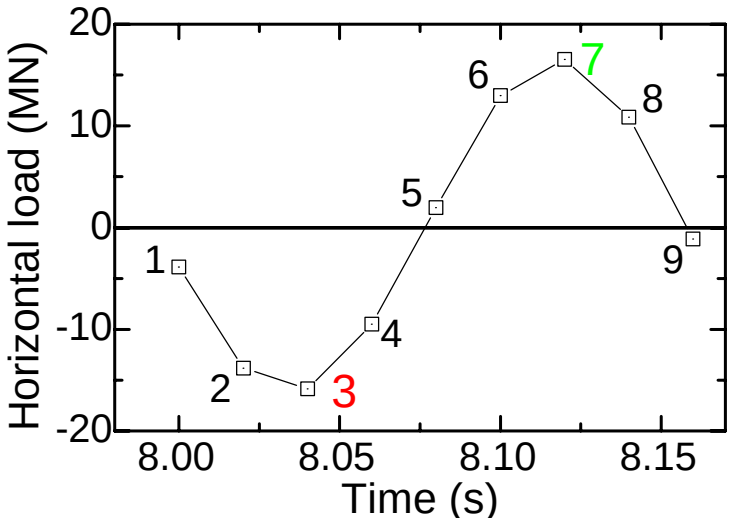

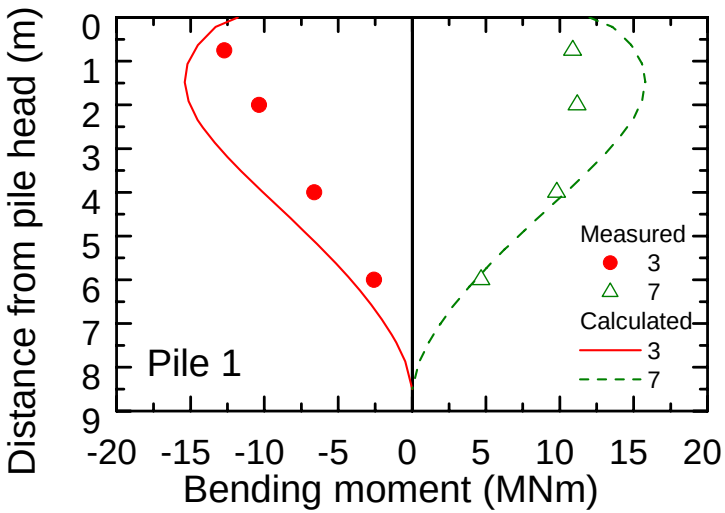

Bending moments in pile 1

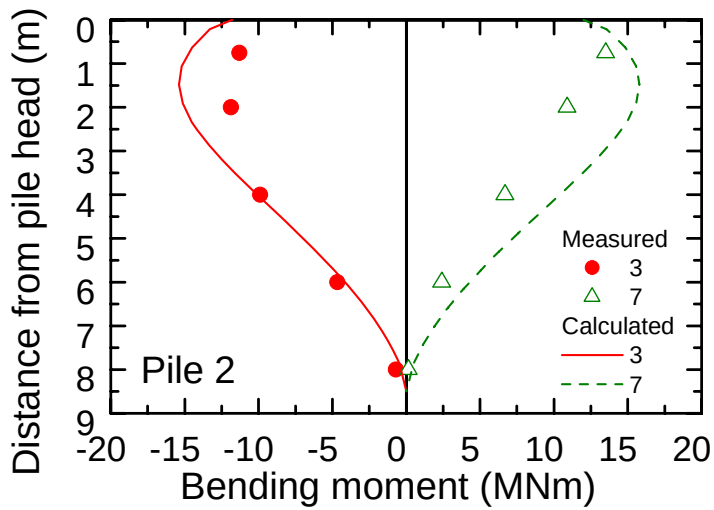

Bending moments in pile 2

Analysis results

f = 37.6 Hz (secondary vibration mode)

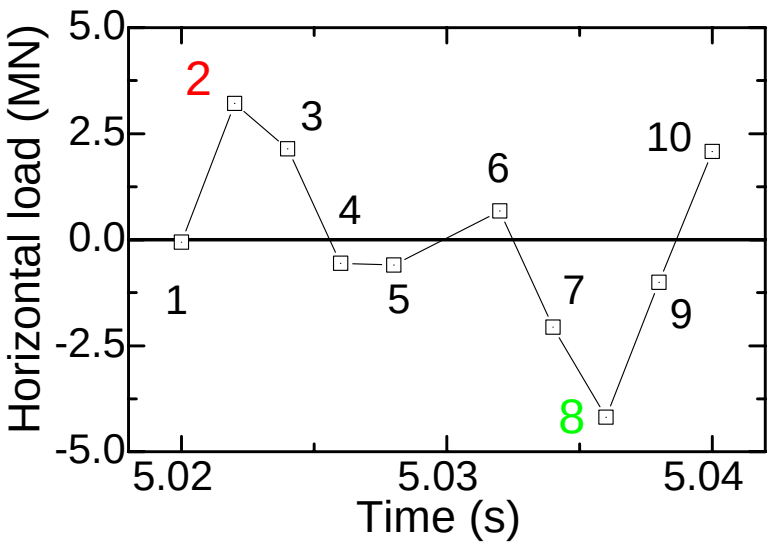

At time instant 2,
pile 1: leading (front pile)
pile 2: following (rear) pile

At time instant 8,
pile 1: following (rear) pile
pile 2: leading (front pile)

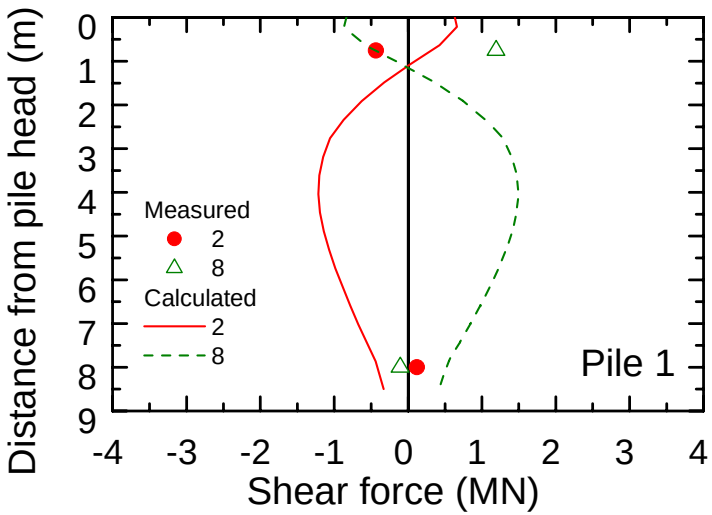

Shear force in pile 1

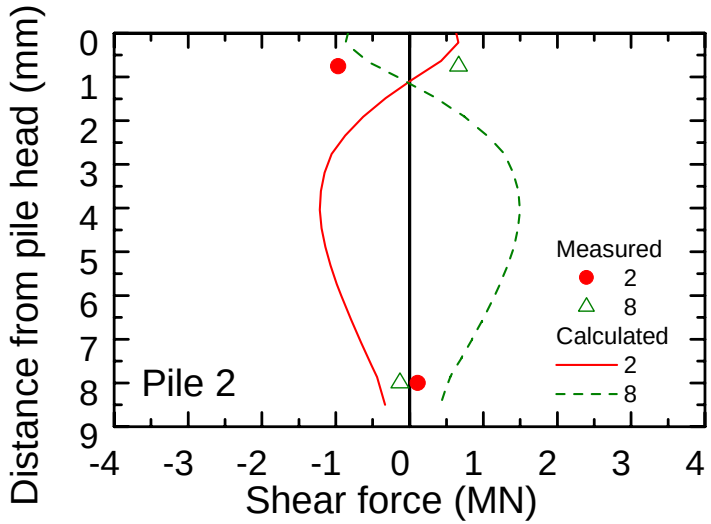

Shear force in pile 2

Analysis results

f = 37.6 Hz (secondary vibration mode)

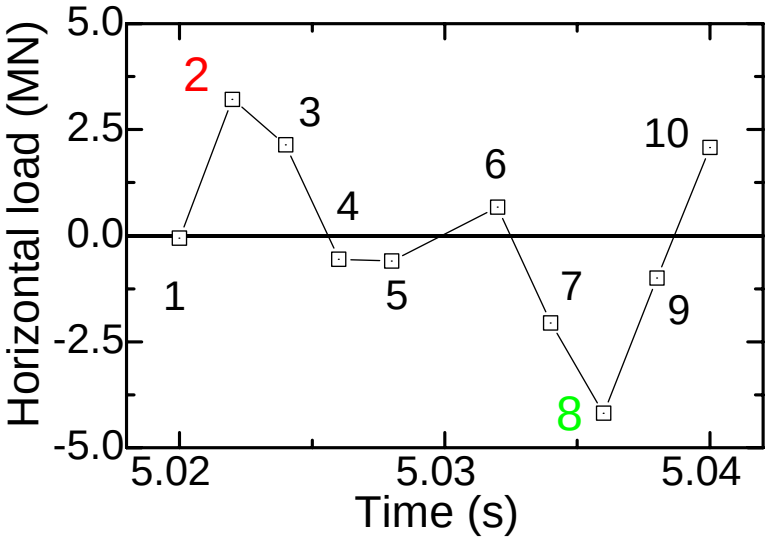

Analysis could not simulate the measurements well

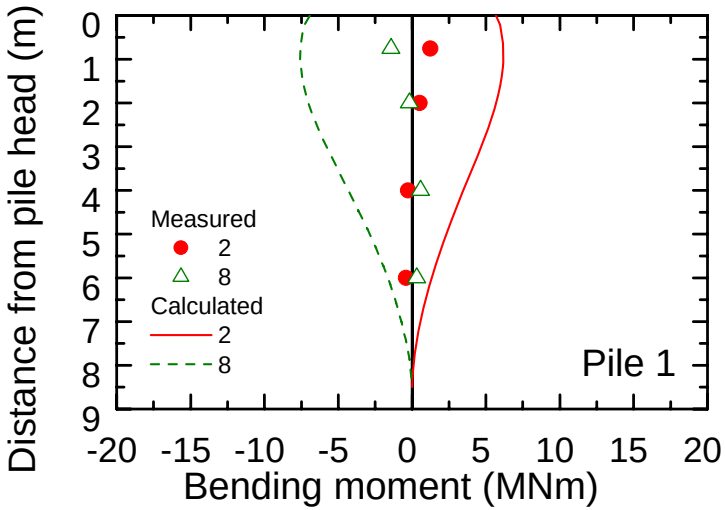

Shear force in pile 1

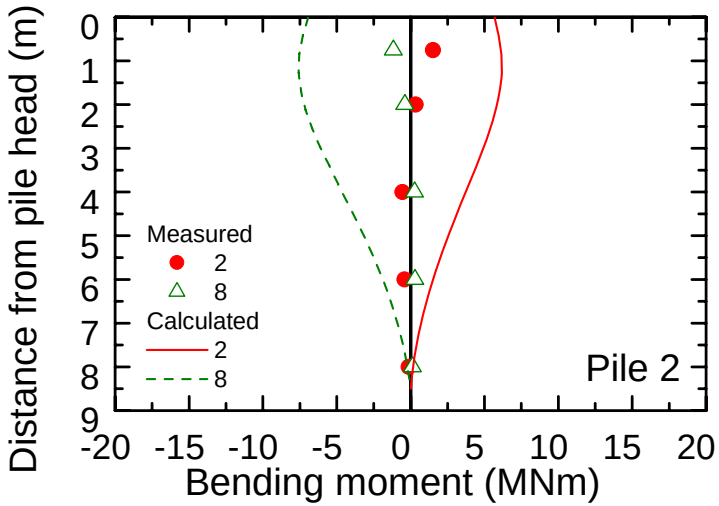

Shear force in pile 2

Analysis results

f = 37.6 Hz (secondary vibration mode)

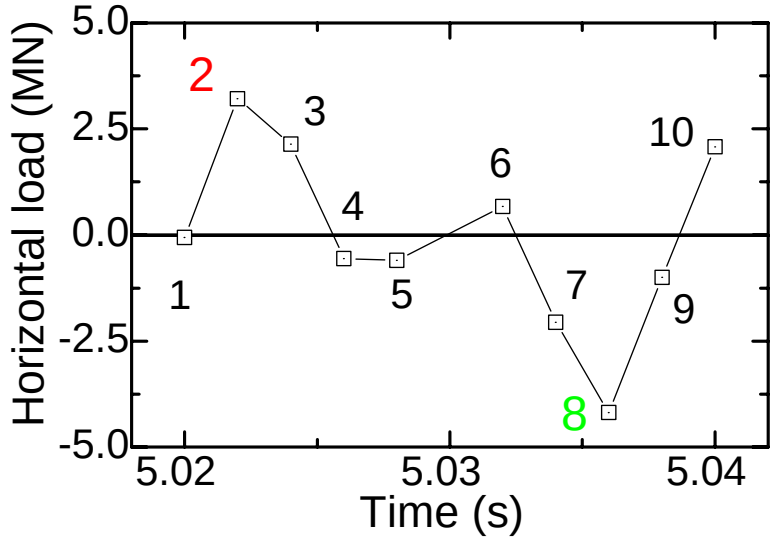

Analysis could not simulate the measurements

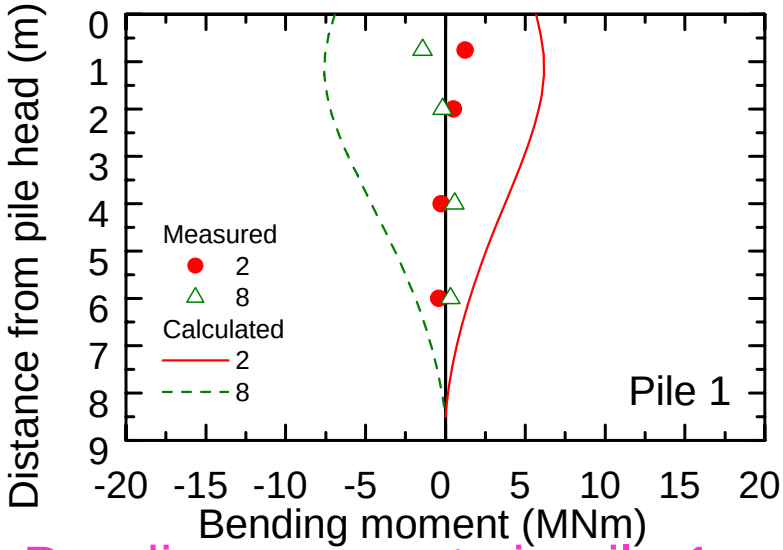

Bending moments in pile 1

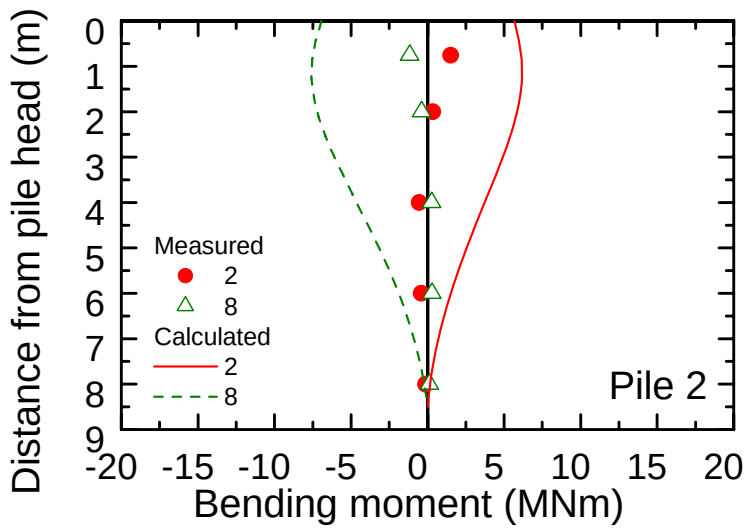

Bending moments in pile 2

Distribution of ground movements

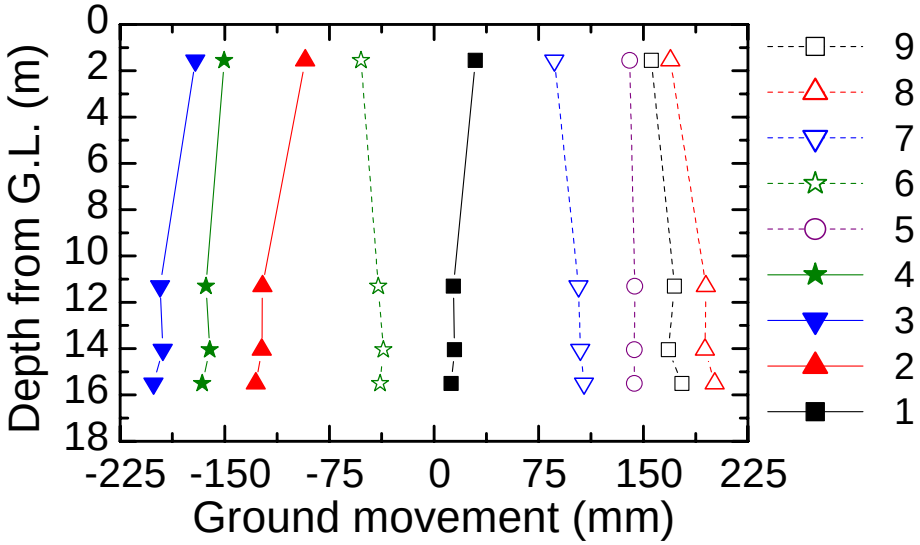

(*f* =6 Hz: primary vibration mode of the superstructure)

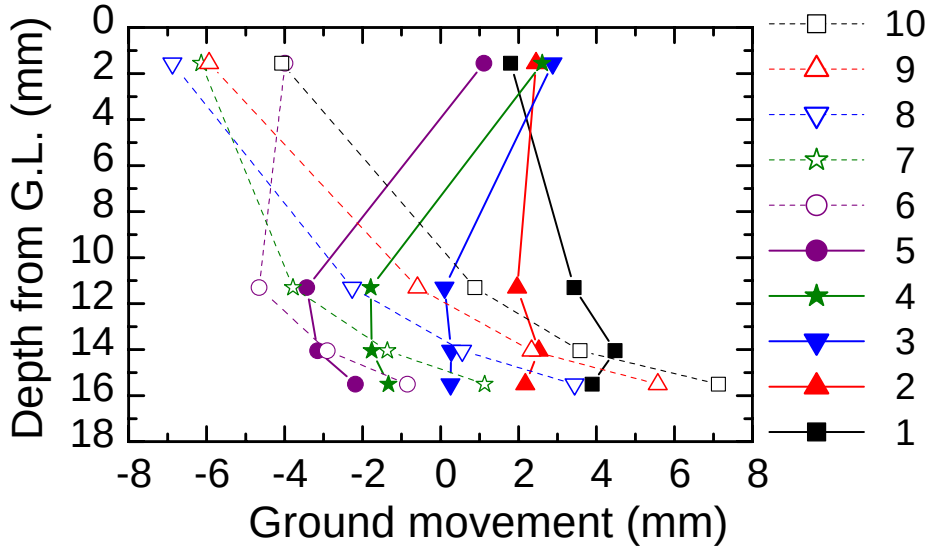

(*f* =37.6 Hz: secondary vibration mode of the superstructure)

When the superstructure exhibits the primary vibration mode, the ground also behaves in a primary vibration mode.

When the superstructure exhibits the secondary vibration mode, the ground also behaves in a secondary vibration mode.

Kinematic effect should be taken into account in the analysis.

Analysis results with kinematic effect

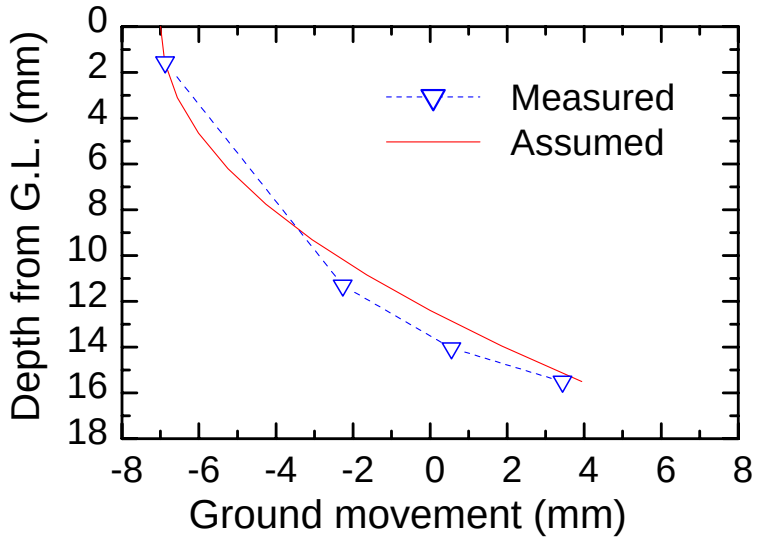

The calculated results with kinematic effect are closer to the measured values.

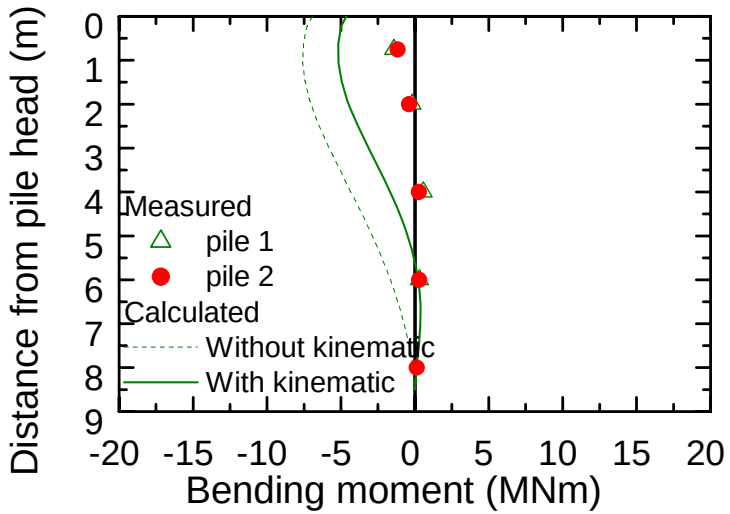

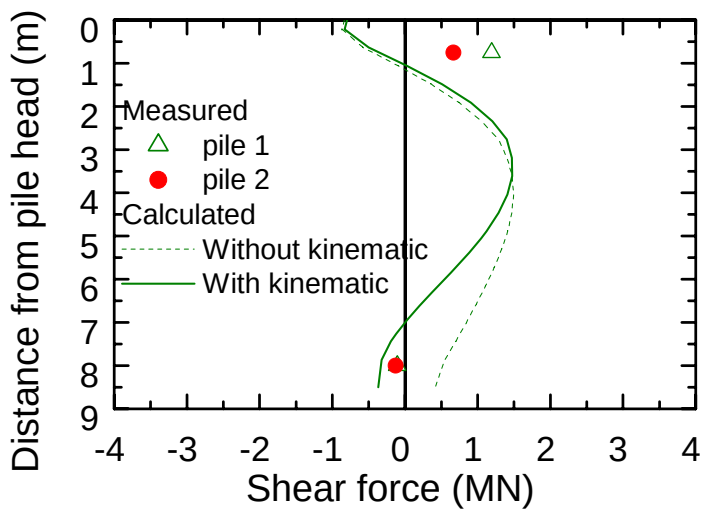

DYNAMIC ANALYSIS METHODS OF PILED RAFT

Comparative analyses of pile foundations subjected to earthquake

Analytical methods

- Simplified 3-dimensional dynamic analysis methods of piled raft
- Three dimensional FEM modelling of piled raft subjected to earthquake
  - Raft and piles are modelled by solid elements
  - Raft and piles are modelled by plate elements and beam elements

Foundation types analysed

Single pile, pile group and piled raft

DYNAMIC ANALYSIS METHODS OF PILED RAFT

Simplified 3-dimensional dynamic analysis method of piled raft
(Kitiyodom, Sonoda & Matsumoto 2005)

Raft : Plate elements with masses
Piles : Beam elements with masses
Soil : Springs at raft and pile nodes

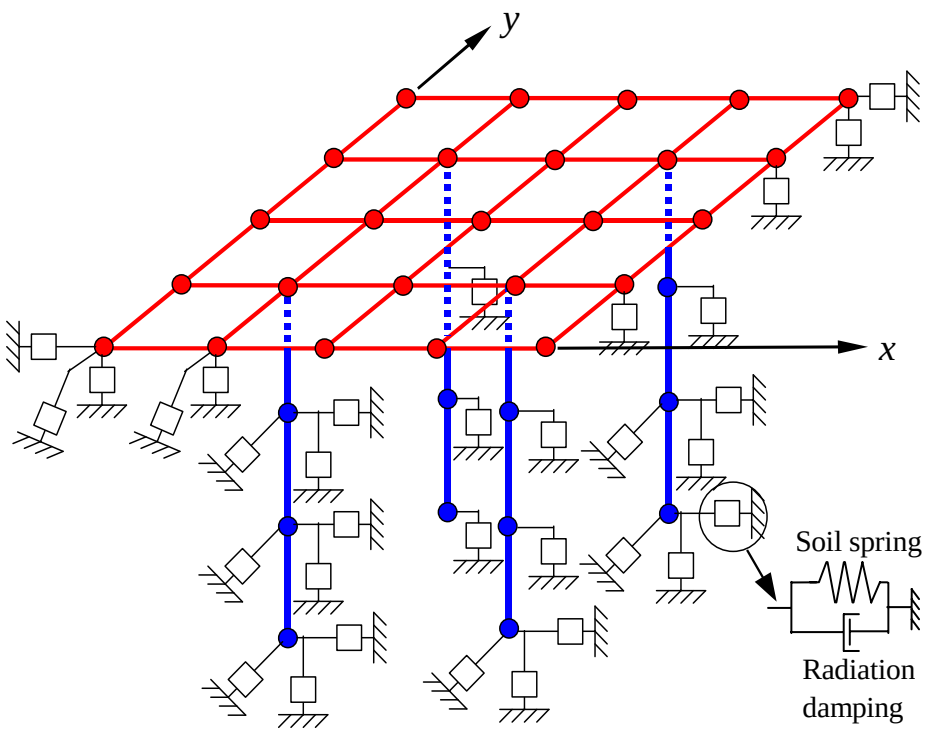

Plate-beam-spring-mass modelling of a piled raft

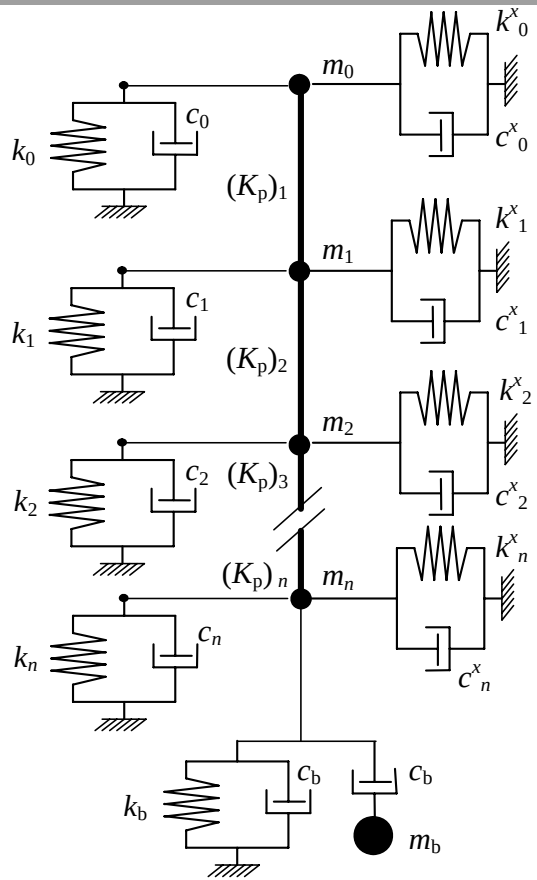

Hybrid modelling of the pile and the soil
(two horizontal soil resistance models)

DYNAMIC ANALYSIS METHODS OF PILED RAFT

Simplified 3-dimensional dynamic analysis method of piled raft
(Kitiyodom, Sonoda & Matsumoto 2005)

Raft : Plate elements with masses
Piles : Beam elements with masses
Soil : Springs at raft and pile nodes

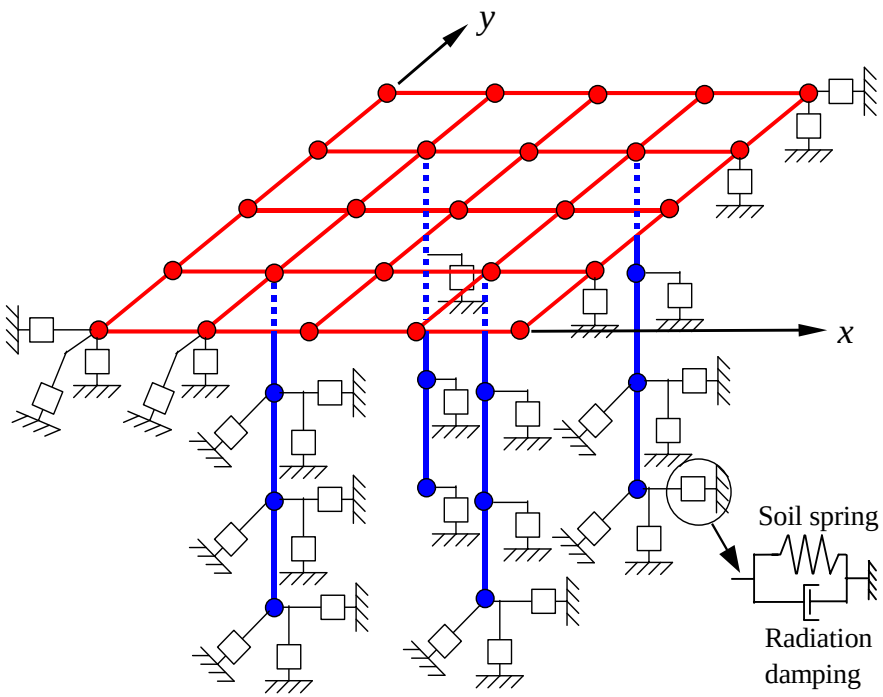

Plate-beam-spring-mass modelling of a piled raft

Equilibrium of forces for the piles and the raft:

$$\left[K_{\mathrm{p}}\right]\{w\}+\left[M_{\mathrm{p}}\right]\{\ddot{w}\}=\{F_{\mathrm{p}}\}+\{P\} \quad (1)$$

$$\left[K_{\mathrm{r}}\right]\{w\}+\left[M_{\mathrm{r}}\right]\{\ddot{w}\}=\{F_{\mathrm{r}}\}-\{P\} \quad (2)$$

$[K_{\mathrm{p}}]$ = Pile stiffness matrix
$[K_{\mathrm{r}}]$ = Raft stiffness matrix
$[M_{\mathrm{p}}]$ = Pile mass matrix
$[M_{\mathrm{r}}]$ = Raft mass matrix
$\{w\}$ = Displacement vector
$\{F_{\mathrm{p}}\}$ = External force vector acting on the piles,
$\{F_{\mathrm{r}}\}$ = External force vector acting on the raft
$\{P\}$ = Internal force vector.

DYNAMIC ANALYSIS METHODS OF PILED RAFT

Simplified 3-dimensional dynamic analysis method of piled raft
(Kitiyodom, Sonoda & Matsumoto 2005)

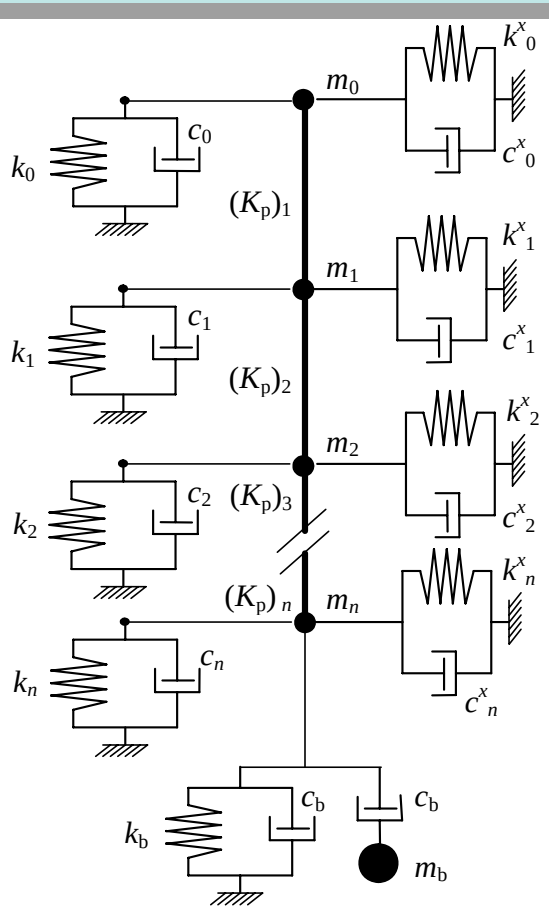

Hybrid modelling of the pile and the soil

(two horizontal soil resistance models)

Parameters of soil resistance at pile nodes

Shaft resistance

Spring $$k = \frac{2.75G_s}{\pi d},\ k^x = k^y = \frac{4G_s}{d} \quad (3)$$

Damping $$c = \frac{G_s}{V_s},\ c^x = c^y = \frac{4.5G_s}{V_s} \quad (4)$$

(Novak et al 1978)

Base resistance

Spring $$k_b = \frac{8G_s}{\pi d(1-\nu_s)} \quad (5)$$

Damping $$c_b = \frac{3.4}{\pi(1-\nu_s)}\frac{G_s}{V_s} \quad (6)$$

Soil mass $$m_b = 16 r_o \rho_s \frac{0.1-\nu_s^4}{\pi(1-\nu_s)} \quad (7)$$

(Deeks & Randolphl 1995)

DYNAMIC ANALYSIS METHODS OF PILED RAFT

Simplified 3-dimensional dynamic analysis method of piled raft
(Kitiyodom, Sonoda & Matsumoto 2005)

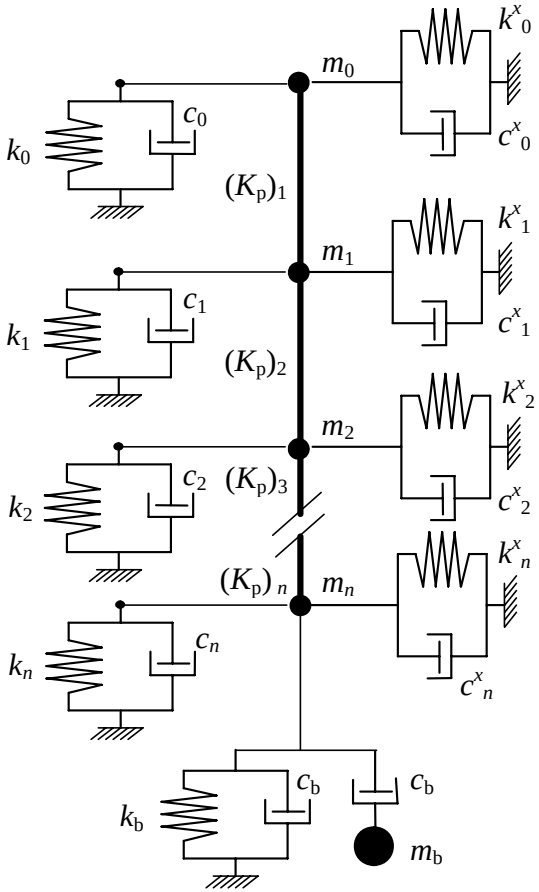

Hybrid modelling of the pile and the soil

(two horizontal soil resistance models)

Parameters of soil resistance at raft nodes

Shaft resistance

$$k_r = \frac{4G_s}{\pi a(1-\nu_s)},\quad k_r{}^x = k_r{}^y = \frac{32(1-\nu_s)G_s}{\pi a(7-8\nu_s)} \qquad (8)$$

$$c_r = \frac{3.4}{\pi(1-\nu_s)}\frac{G_s}{V_s},\quad c_r{}^x = c_r{}^y = \frac{18.4(1-\nu_s)}{\pi(7-8\nu_s)}\frac{G_s}{V_s} \qquad (9)$$

(Richart, Hall & Woods 1970)

Expression of soil resistance in matrix form:

$$[K_s]\{w\} + [C_s]\{\dot{w}\} + [M_s]\{\ddot{w}\} = \{P\} \qquad (10)$$

DYNAMIC ANALYSIS METHODS OF PILED RAFT

Simplified 3-dimensional dynamic analysis method of piled raft
(Kitiyodom, Sonoda & Matsumoto 2005)

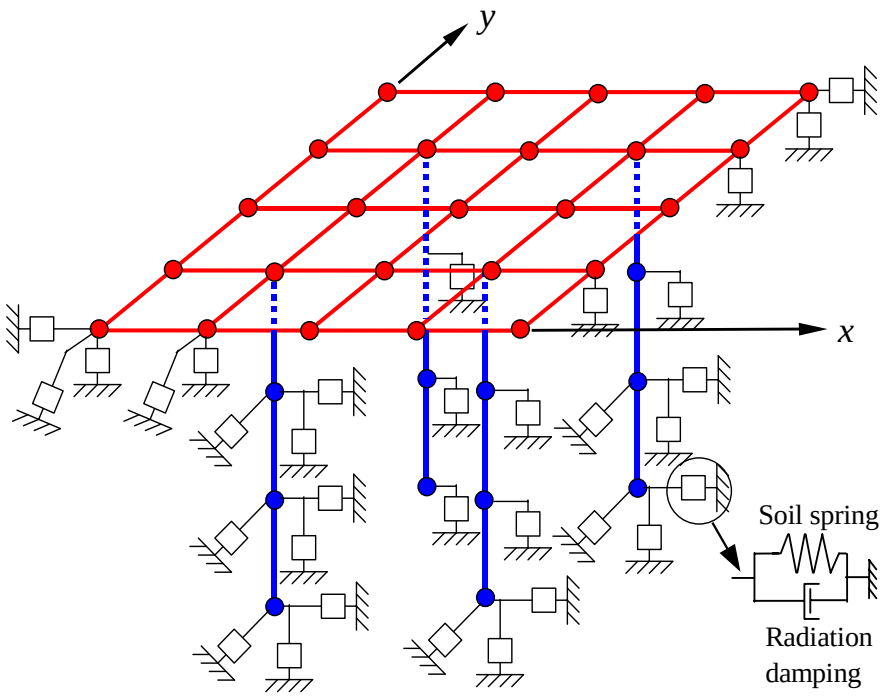

Plate-beam-spring-mass modelling of a piled raft

Equilibrium of forces for the piles and the raft:

$$\left[K_{\mathrm{p}}\right]\{w\}+\left[M_{\mathrm{p}}\right]\{\ddot{w}\}=\{F_{\mathrm{p}}\}+\{P\} \quad (1)$$

$$\left[K_{\mathrm{r}}\right]\{w\}+\left[M_{\mathrm{r}}\right]\{\ddot{w}\}=\{F_{\mathrm{r}}\}-\{P\} \quad (2)$$

Soil resistance:

$$\left[K_{\mathrm{s}}\right]\{w\}+\left[C_{\mathrm{s}}\right]\{\dot{w}\}+\left[M_{\mathrm{s}}\right]\{\ddot{w}\}=\{P\} \quad (10)$$

Governing equation for the whole system:

$$[K]\{w\}+[C]\{\dot{w}\}+[M]\{\ddot{w}\}=\{F\} \quad (11)$$

$$[K]=[K_{\mathrm{p}}]+[K_{\mathrm{r}}]+[K_{\mathrm{s}}]$$
$$[C]=[C_{\mathrm{s}}]$$
$$[M]=[M_{\mathrm{p}}]+[M_{\mathrm{r}}]+[M_{\mathrm{s}}]$$
$$\{F\}=\{F_{\mathrm{p}}\}+\{F_{\mathrm{r}}\}.$$

DYNAMIC ANALYSIS METHODS OF PILED RAFT

Simplified 3-dimensional dynamic analysis method of piled raft
(Kitiyodom, Sonoda & Matsumoto 2005)

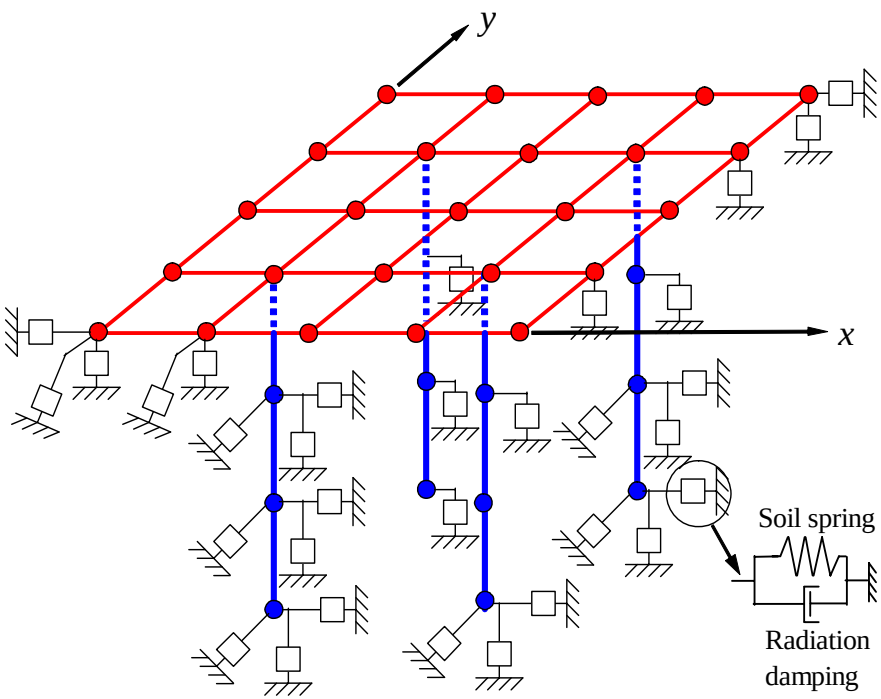

Plate-beam-spring-mass modelling of a piled raft

Governing equation for the whole system:

$$[K]\{w\}+[C]\{\dot{w}\}+[M]\{\ddot{w}\}=\{F\} \quad (11)$$

In the case of the pile foundation subjected to earthquake load, the induced external force vector {*F*} can be calculated by

$$\{F\}=[K_s]\{w_0\}+[C_s]\{\dot{w}_0\} \quad (12)$$

$\{w_0\}$ = the free field ground movements

$\{\dot{w}_0\}$ = the free filed velocities induced by an earthquake

DYNAMIC ANALYSIS METHODS OF PILED RAFT

Simplified 3-dimensional dynamic analysis method of piled raft
(Kitiyodom, Sonoda & Matsumoto 2005)

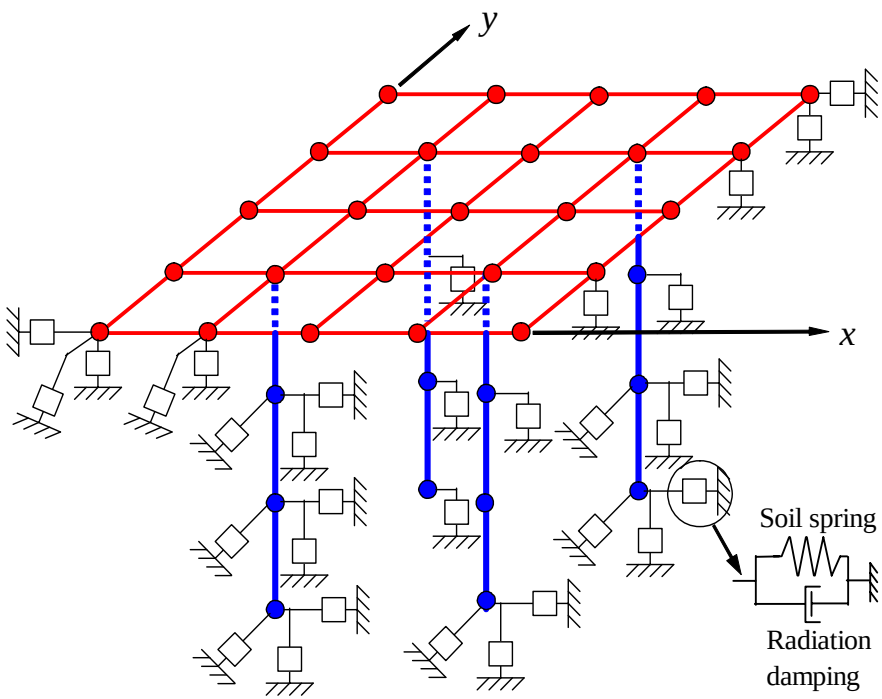

Plate-beam-spring-mass modelling of a piled raft

Governing equation for the whole system:

$$[K]\{w\}+[C]\{\dot{w}\}+[M]\{\ddot{w}\}=\{F\} \quad (11)$$

Forces at nodes induced by an earthquake:

$$\{F\}=[K_s]\{w_0\}+[C_s]\{\dot{w}_0\} \quad (12)$$

Equations (11) and (12) are converted to incremental forms.

Newmark β - method is used to solve these equations.

DYNAMIC ANALYSIS METHODS OF PILED RAFT

Simplified 3-dimensional dynamic analysis method of piled raft

Governing equation for the whole system:

$$[K]\{w\}+[C]\{\dot{w}\}+[M]\{\ddot{w}\}=\{F\}$$

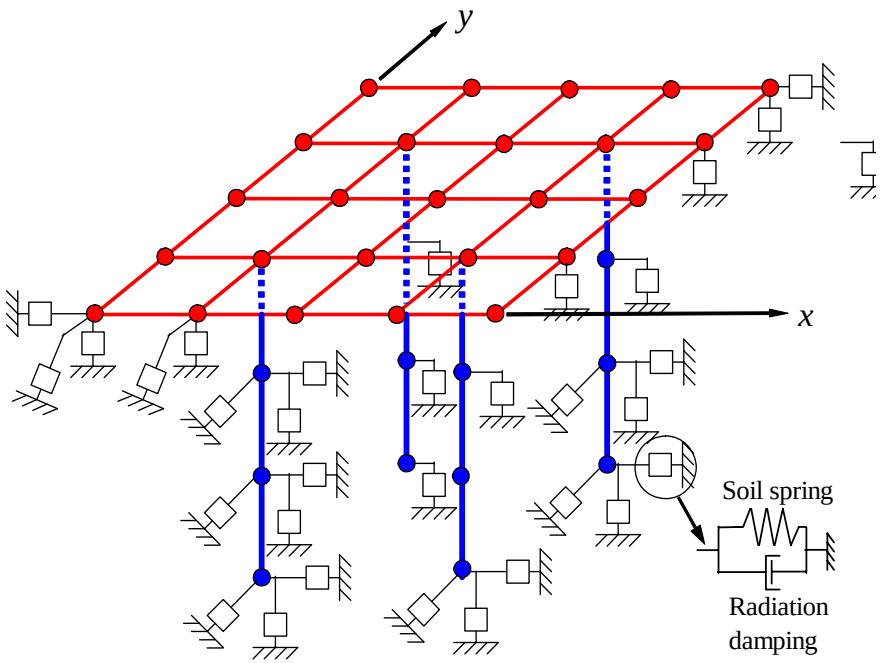

Plate-beam-spring-mass modelling of a piled raft

Note:

Dynamic interactions between the soil springs are not taken into account in the present DPRAB.

DYNAMIC ANALYSIS METHODS OF PILED RAFT

Simplified 3-dimensional dynamic analysis method of piled raft
(Kitiyodom, Sonoda & Matsumoto 2005)

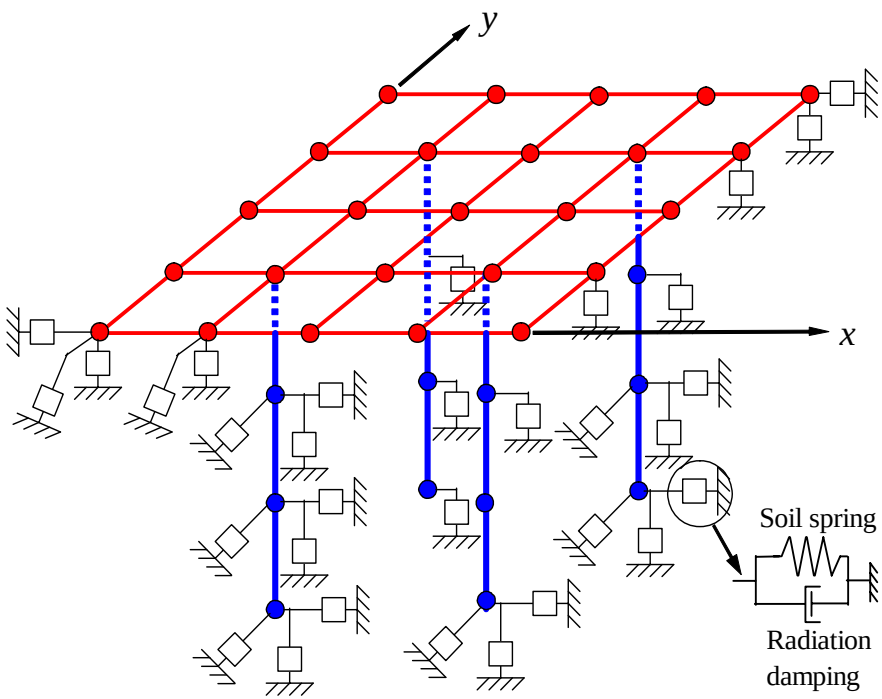

Plate-beam-spring-mass modelling of a piled raft

Governing equation for the whole system:

$$[K]\{w\}+[C]\{\dot{w}\}+[M]\{\ddot{w}\}=\{F\} \quad (11)$$

Forces at nodes induced by an earthquake:

$$\{F\}=[K_s]\{w_0\}+[C_s]\{\dot{w}_0\} \quad (12)$$

DYNAMIC ANALYSIS METHODS OF PILED RAFT

Simplified 3-dimensional dynamic analysis method of piled raft

(Kitiyodom, Sonoda & Matsumoto 2005)

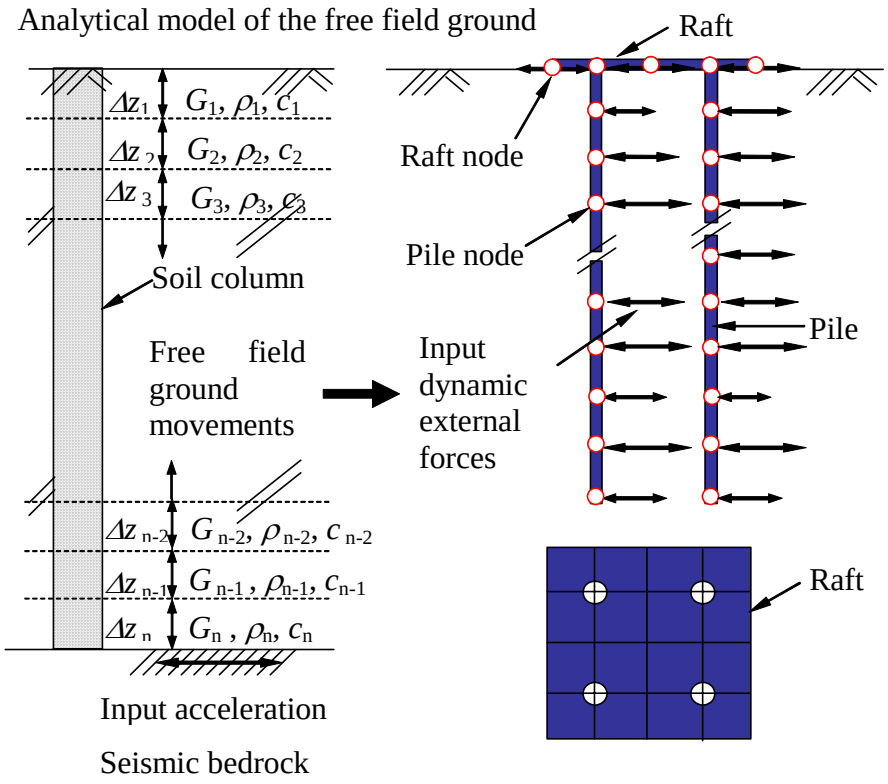

Analysis procedure used in D-PRAB

1. Calculate changes with time of free-field ground movements and velocities

2. Calculate changes with time of forces at nodes induced by an earthquake

$$\{F\} = [K_s]\{w_0\} + [C_s]\{\dot{w}_0\} \quad (12)$$

3. Solve the governing equation

$$[K]\{w\} + [C]\{\dot{w}\} + [M]\{\ddot{w}\} = \{F\} \quad (11)$$

- Displacements, velocities and accelerations at raft and pile nodes
- Bending moments of raft
- Axial forces, shear forces and bending moments of piles

DYNAMIC ANALYSIS METHODS OF PILED RAFT

D-PRAB

Calculation of free-field ground movements

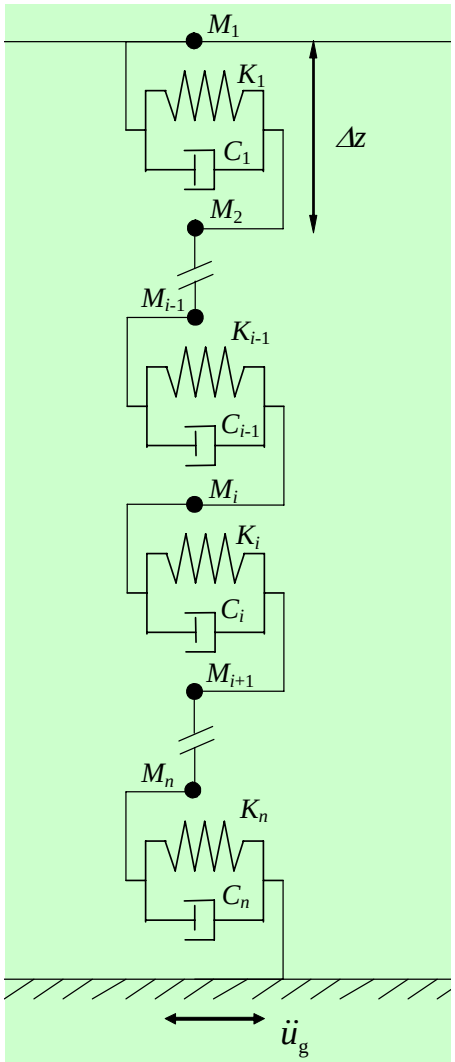

Lumped mass-spring-dashpot model

(after Idriss & Seed 1968)

Governing equation:

$$[K_m]\{u\}+[C_m]\{\dot{u}\}+[M_m]\{\ddot{u}\}=-[M_m]\{\ddot{u}_g\}$$

$[M_m]$ = the soil mass matrix

$[C_m]$ = soil damping matrix

$[K_m]$ = soil stiffness matrix

$\{u\}$ = vector of the relative displacements between each layer.

Horizontal free field ground movement vector $\{u_0\}$:

$$\{u_0\}=\{u\}+\{u_g\}$$

$\{u_g\}$ = the input seismic displacement.

DYNAMIC ANALYSIS METHODS OF PILED RAFT

COMPARATIVE ANALYSES

Analytical conditions

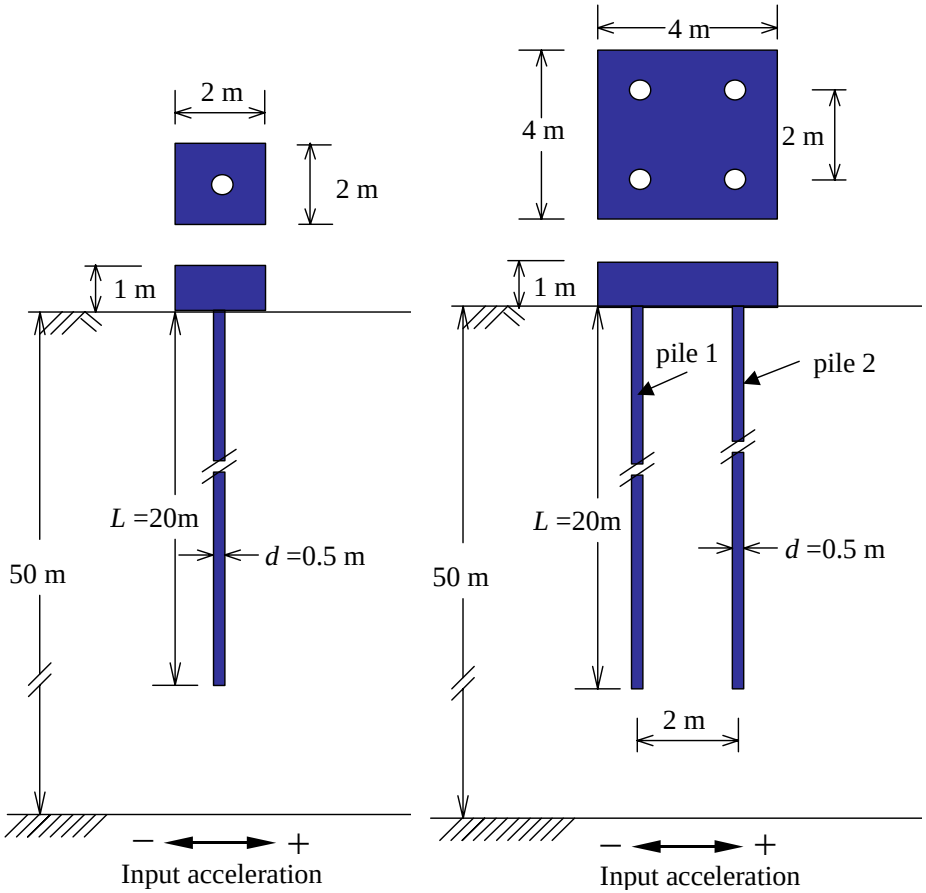

(a) Capped single pile

(b) Pile group & piled raft

Material properties used in analyses

Property	Value
Soil:	
Young's modulus	5.96×10^4 kPa
Poisson's ratio	0.49
Density	2 ton/m^3
Shear wave velocity	100 m/s
Pile:	
Young's modulus	3.84×10^7 kPa
Poisson's ratio	0.16
Density	2.4 ton/m^3
Longitudinal wave velocity	4000 m/s
Shear wave velocity	2626 m/s
Length	20 m
Diameter	0.5 m
Unit squared raft (pile cap):	
Young's modulus	3.84×10^7 kPa
Poisson's ratio	0.16
Density	2.4 ton/m^3
Width	2 m
Thickness	1 m

Problems analysed

DYNAMIC ANALYSIS METHODS OF PILED RAFT

COMPARATIVE ANALYSES

FEM modelling

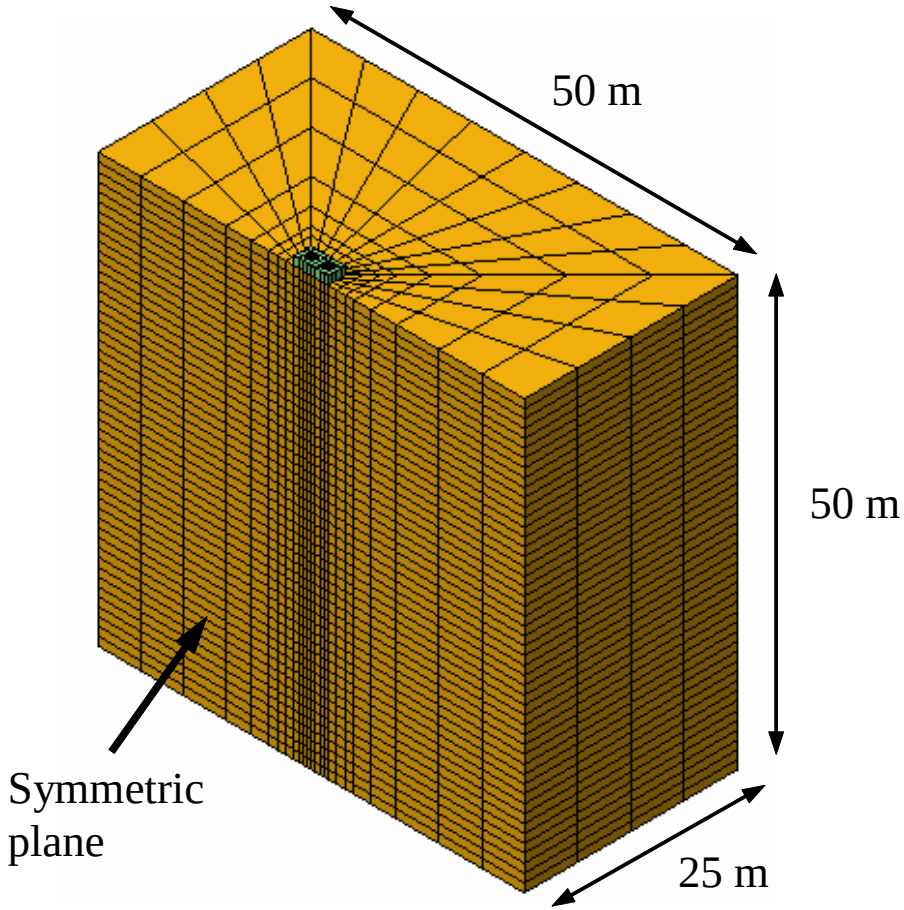

Whole model (Plane symmetric)

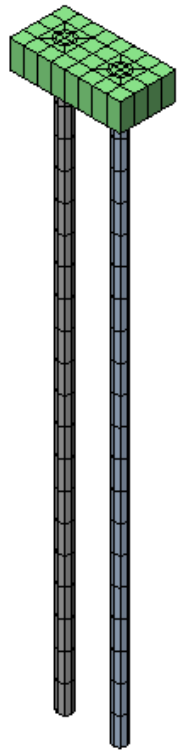

Solid elements

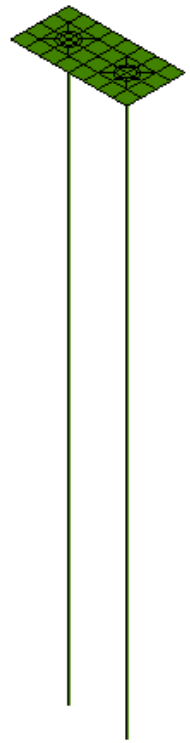

Plate and beam elements

Two types of modelling of raft and piles

DYNAMIC ANALYSIS METHODS OF PILED RAFT

COMPARATIVE ANALYSES

Input accelerations

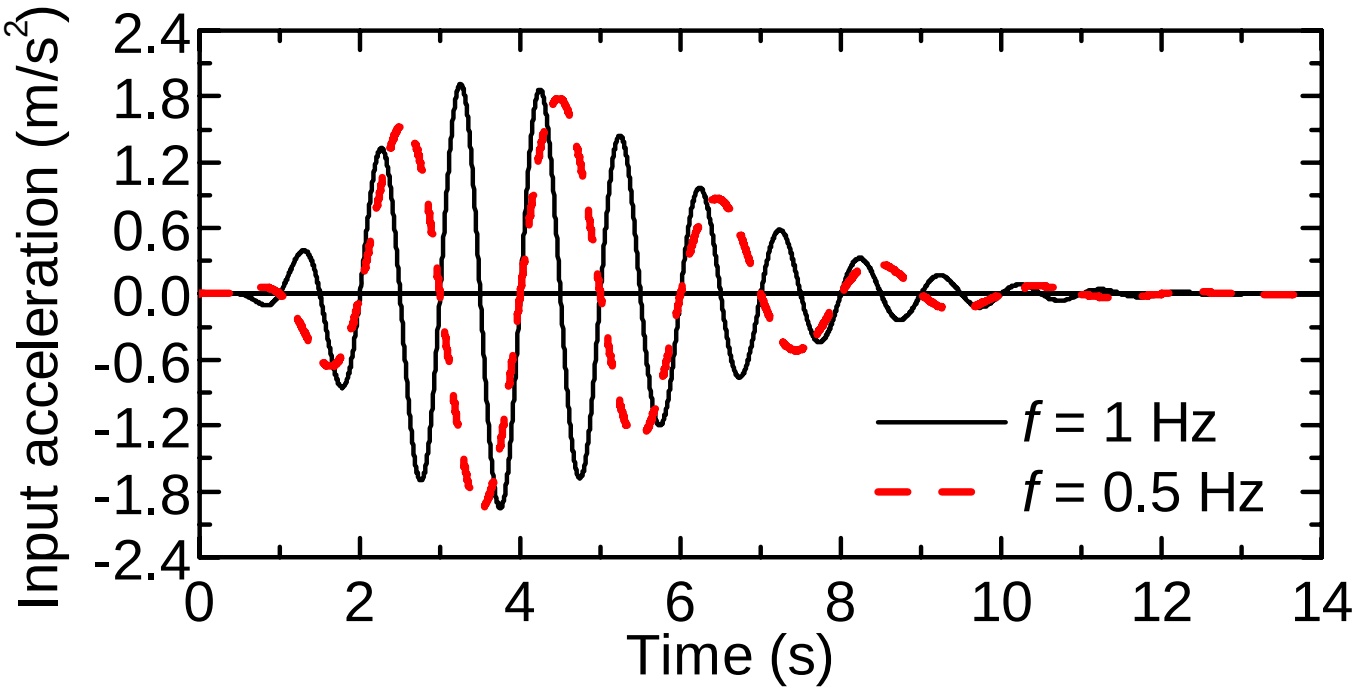

$$\ddot{u}(t) = \sqrt{\beta e^{-\alpha t} t^{\gamma}} \sin(2\pi f t)$$

$\alpha = 2.2$; $\beta = 0.375$; $\gamma = 8.0$; $f = 0.5$ and $f = 1.0$ Hz.

DYNAMIC ANALYSIS METHODS OF PILED RAFT

ANALYSIS RESULTS

Results of free field ground motion analysis

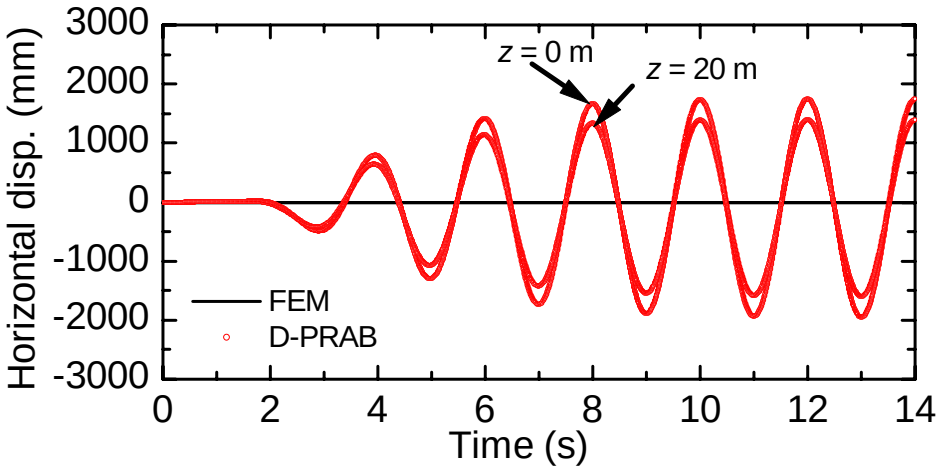

Free field ground movements (f = 0.5 Hz)

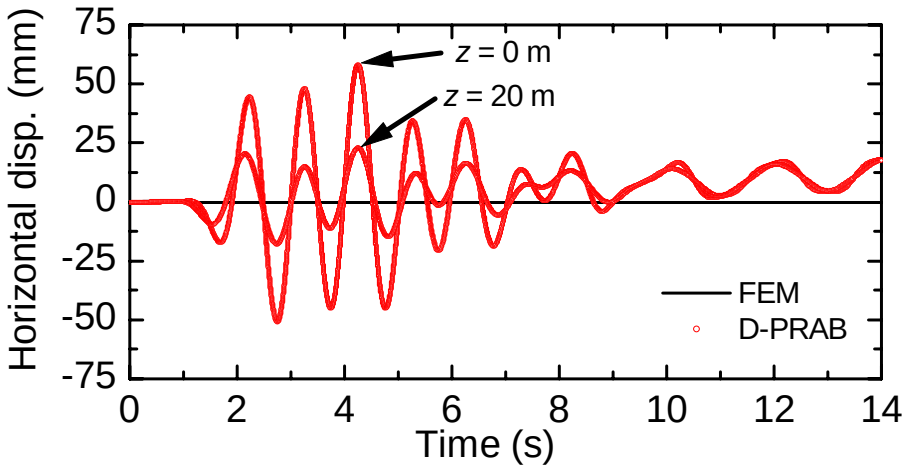

Free field ground movements (f = 1.0 Hz)

Natural frequency of the ground, f_n:

$$f_n = V_s / 4H$$

H = thickness of the ground
= 50 m

V_s = shear wave velocity
= 100 ms

DYNAMIC ANALYSIS METHODS OF PILED RAFT

ANALYSIS RESULTS

Analysis results of single pile

f = 0.5 Hz

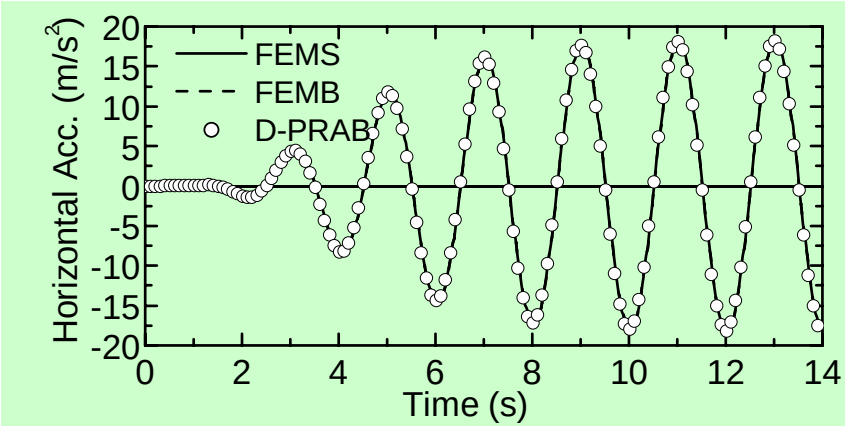

Horizontal acceleration at pile head

f = 1 Hz

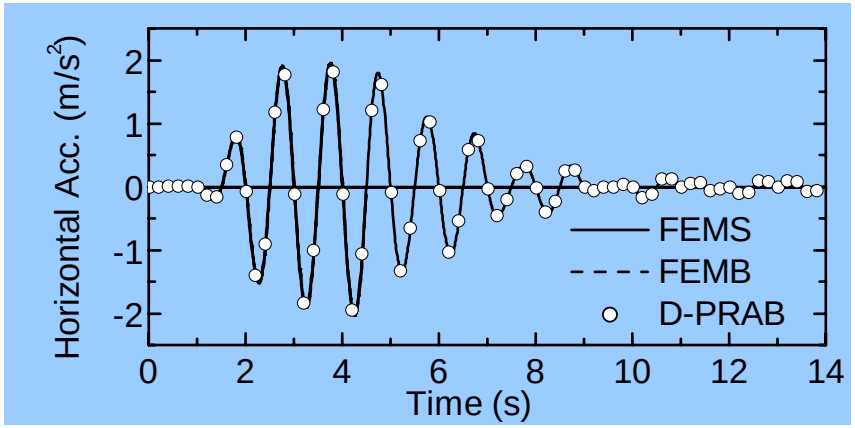

Horizontal acceleration at pile head

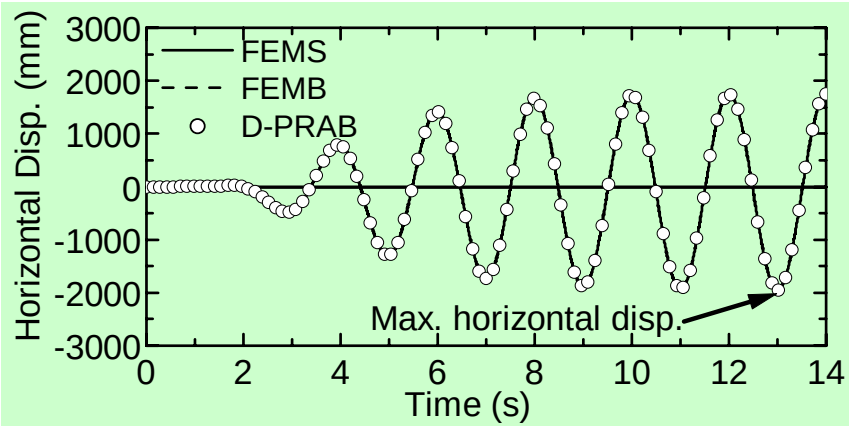

Horizontal displacement at pile head

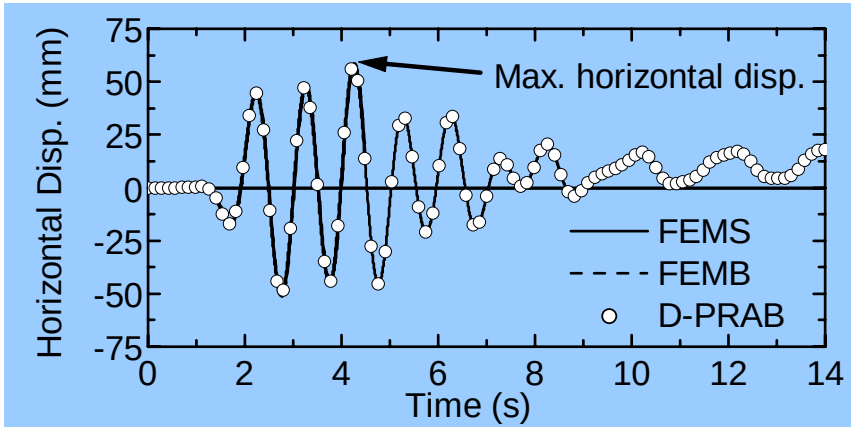

Horizontal displacement at pile head

DYNAMIC ANALYSIS METHODS OF PILED RAFT

ANALYSIS RESULTS

Analysis results of single pile

f = 0.5 Hz

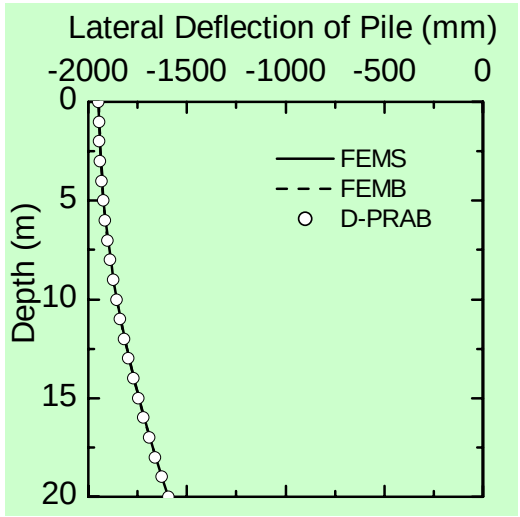

Lateral deflection

f = 1 Hz

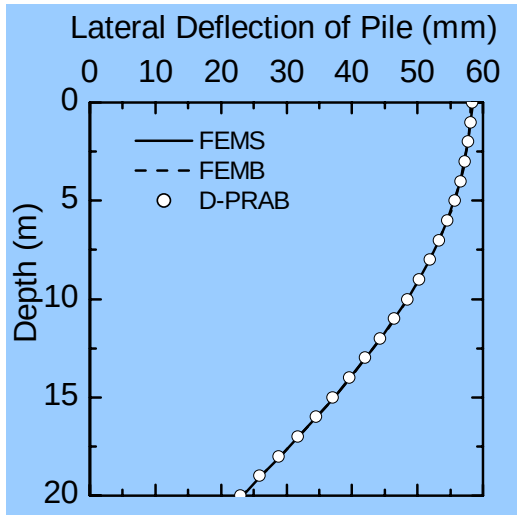

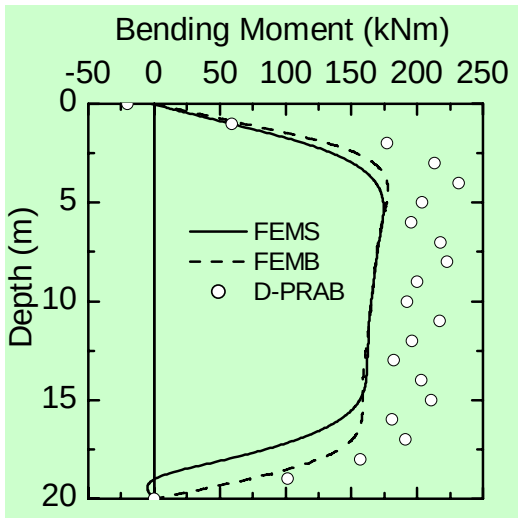

Bending moment

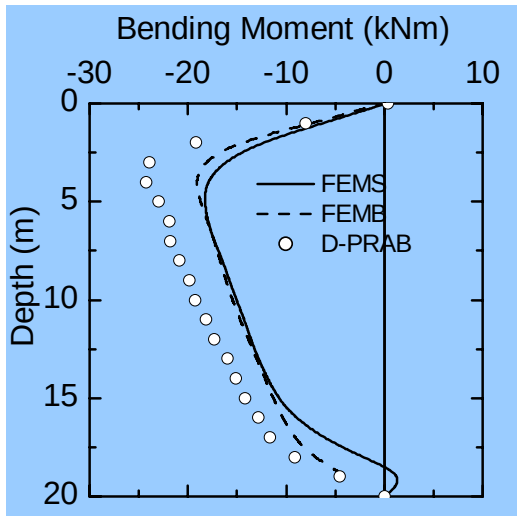

DYNAMIC ANALYSIS METHODS OF PILED RAFT

ANALYSIS RESULTS

Analysis results of pile group and piled raft for f = 1 Hz

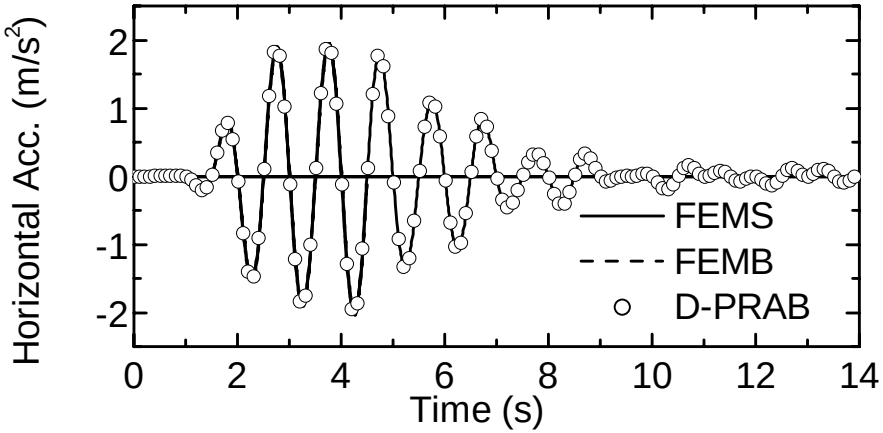

Horizontal acc. at pile head in pile group

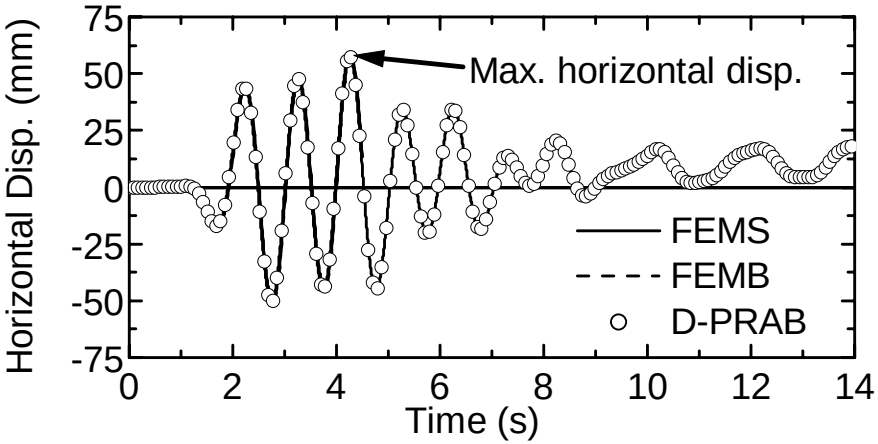

Horizontal disp. at pile head in pile group

Horizontal acceleration and displacement at pile head in the piled raft were very close to those in pile group.

DYNAMIC ANALYSIS METHODS OF PILED RAFT

ANALYSIS RESULTS

Responses of pile group for f = 1 Hz

Lateral deflection

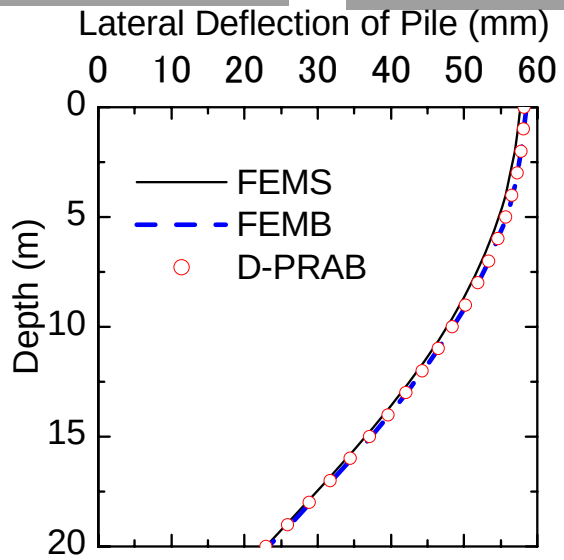

Bending moment

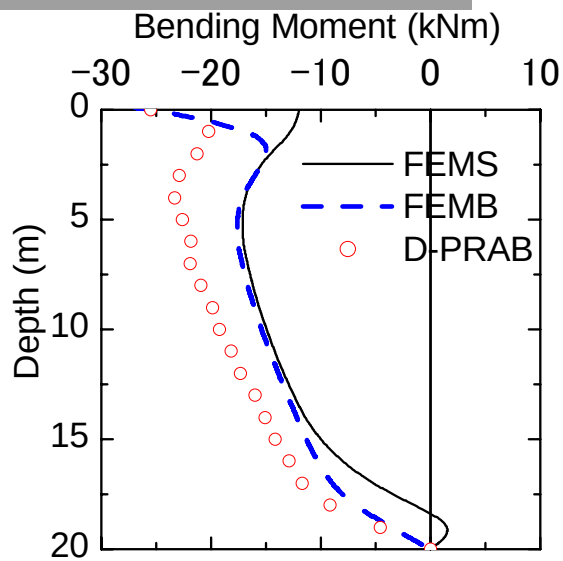

Vertical movement

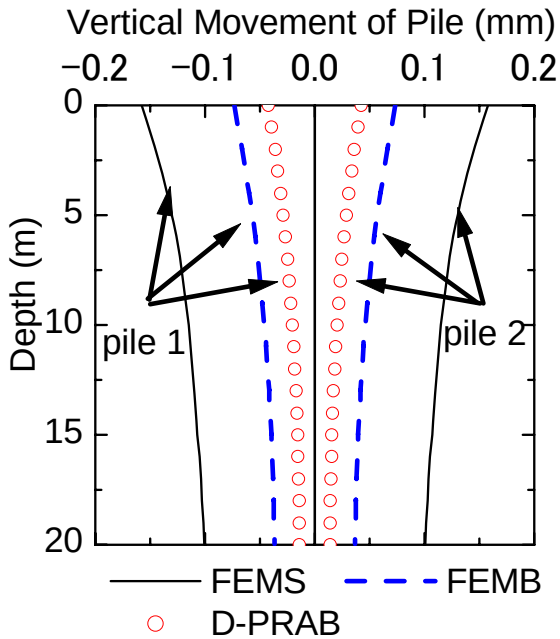

Axial force

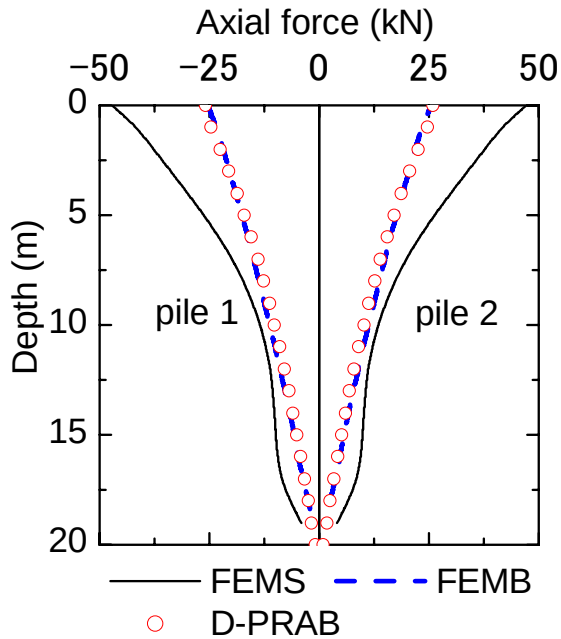

DYNAMIC ANALYSIS METHODS OF PILED RAFT

ANALYSIS RESULTS

Responses of piled raft for f = 1 Hz

Lateral deflection

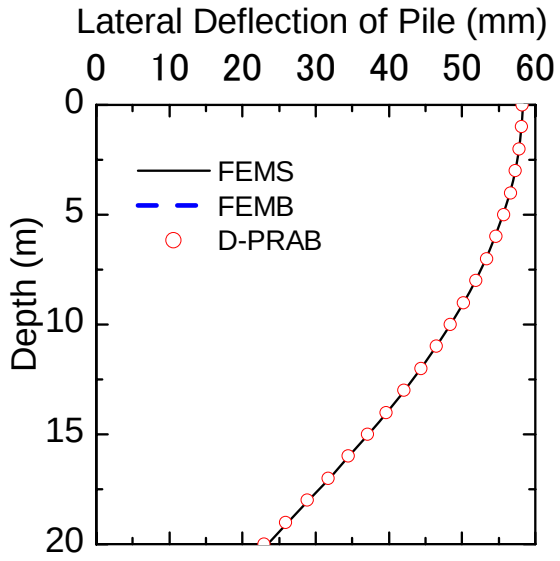

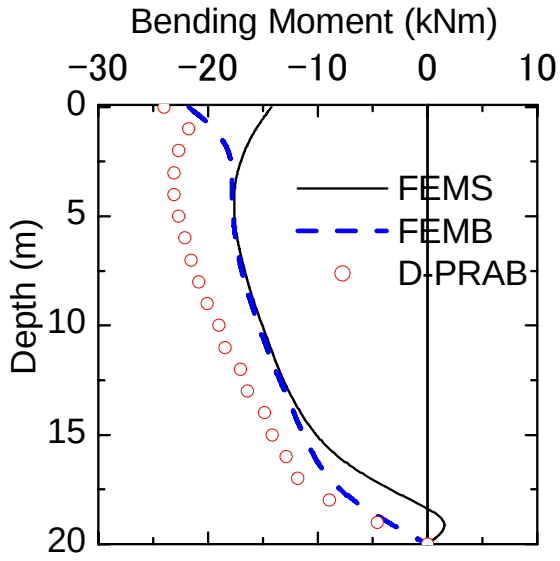

Bending moment

Vertical movement

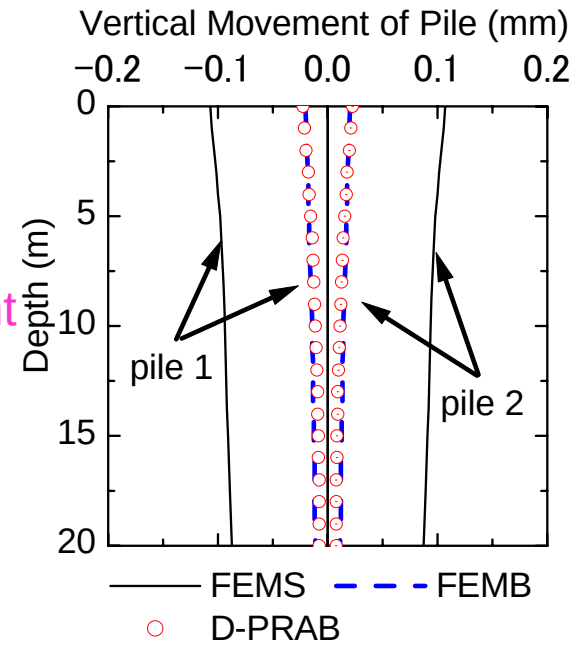

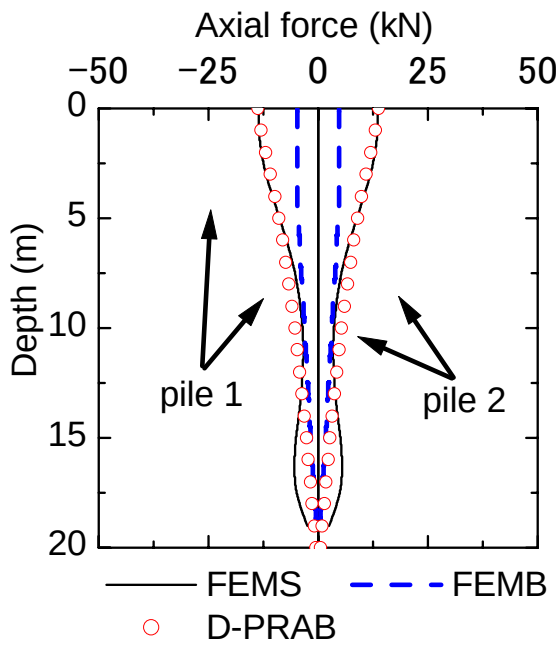

Axial force

DYNAMIC ANALYSIS METHODS OF PILED RAFT

ANALYSIS RESULTS

Comparison of single pile, pile group and piled raft (FEMS)

Lateral deflection

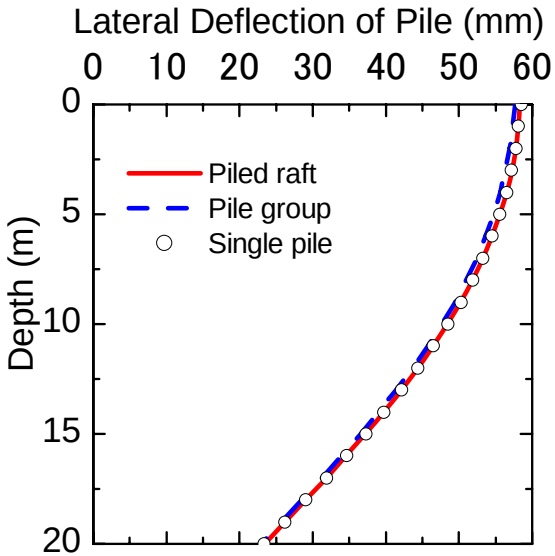

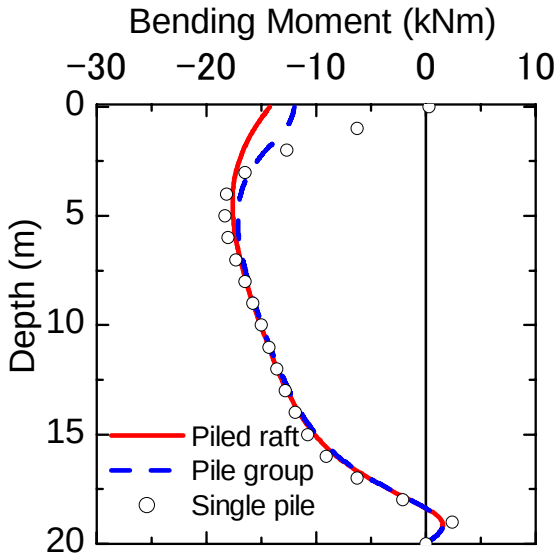

Bending moment

Vertical movement

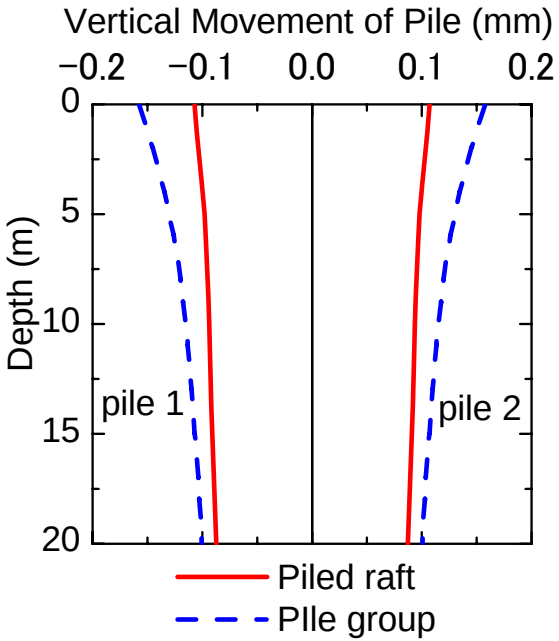

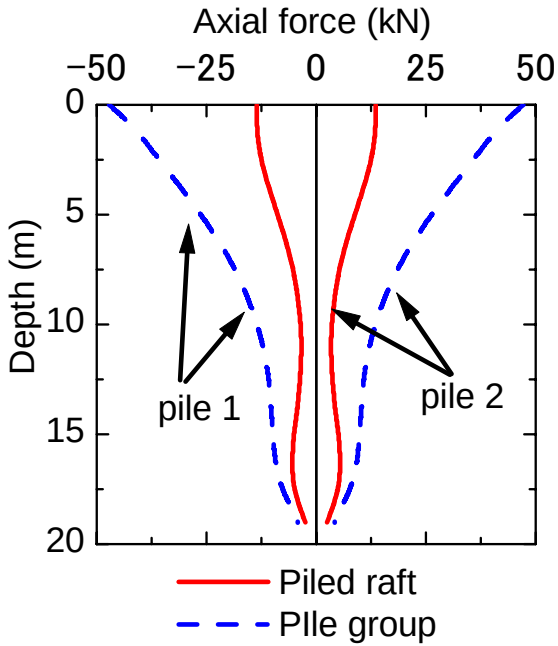

Axial force

DYNAMIC ANALYSIS METHODS OF PILED RAFT

SUMMARY

From the comparative analyses using the various solutions,

1) Horizontal accelerations and displacements of the single pile, the pile group and the piled raft calculated using the various methods are almost the same.

2) FEMB and D-PRAB tend to underestimate the vertical displacements of the pile compared to FEMS that is regarded as the most rigorous approach, although the vertical displacements are very small compared to the horizontal displacement.

SUMMARY (Cont'd)

From the comparison of the foundations calculated using FEMS,

3) Lateral displacements of the single pile, the pile group and the piled raft are almost the same for an earthquake.

4) Rocking motion of the piled raft is smaller than that of the pile group. The axial forces of the pile in the piled raft are much smaller than those in the pile group.

The above findings are valid for the cases that strains induced in the soil are small enough where the soil exhibits only elastic response and that effect of a superstructure does not exist

SUMMARY (Cont'd)

Following improvements are recommended for the simplified method D-PRAB:

1) Incorporation of dynamic interactions between the soil springs though the soil, in order to obtain more reliable vertical responses of the foundation.

2) Modelling of the superstructure for the analysis of a total structure composed of a superstructure and a substructure including piles.